ISSN 1645-6726

Instituto Nacional de Estatística
Statistics Portugal

REVSTAT
Statistical Journal

Special issue on “Business and Industrial Statistics"

Guest Editors:
Filipe Marques
Marco Reis
Carlos Coelho

**Volume 11, No.1
March 2013**

REVSTAT

Statistical Journal

Catalogação Recomendada

REVSTAT. Lisboa, 2003-
Revstat : statistical journal / ed. Instituto Nacional
de Estatística. - Vol. 1, 2003- . - Lisboa I.N.E.,
2003- . - 30 cm
Semestral. - Continuação de : Revista de Estatística =
ISSN 0873-4275. - edição exclusivamente em inglês
ISSN 1645-6726

CREDITS

- **PUBLISHER**
  - *Instituto Nacional de Estatística, I.P. (INE, I.P.)*
    Av. António José de Almeida, 2
    1000-043 LISBOA
    PORTUGAL
    Tel.: +351 218 426 100
    Fax: +351 218 454 084
    Web site: http://www.ine.pt
    Customer Support Service
    (National network): 808 201 808
    (Other networks): +351 218 440 695
- **COVER DESIGN**
  - *Mário Bouçadas, designed on the stain glass window at INE, I.P., by the painter Abel Manta*
- **LAYOUT AND GRAPHIC DESIGN**
  - *Carlos Perpétuo*
- **PRINTING**
  - *Instituto Nacional de Estatística, I.P.*
- **EDITION**
  - *190 copies*
- **LEGAL DEPOSIT REGISTRATION**
  - *N.º 191915/03*

PRICE

[VAT included]

- Single issue ………………………………………………………….. **€ 11**
- Annual subscription (No. 1 Special Issue, No. 2 and No.3)………. **€ 26**
- Annual subscription (No. 2, No. 3) ……………………………….. **€ 18**

INDEX

Abstracted/indexed in: *Current Index to Statistics, DOAJ, Google Scholar, Journal Citation Reports/Science Edition, Mathematical Reviews, Science Citation Index Expanded*®*, SCOPUS* and *Zentralblatt für Mathematic.*

REVSTAT – Statistical Journal
Volume 11, Number 1, March 2013, 1–16

NONPARAMETRIC ESTIMATION OF THE TAIL-DEPENDENCE COEFFICIENT

Author: Marta Ferreira
– Center of Mathematics of Minho University, Portugal
msferreira@math.uminho.pt

Abstract:

- A common measure of tail dependence is the so-called tail-dependence coefficient. We present a nonparametric estimator of the tail-dependence coefficient and prove its strong consistency and asymptotic normality in the case of known marginal distribution functions. The finite-sample behavior as well as robustness will be assessed through simulation. Although it has a good performance, it is sensitive to the extreme value dependence assumption. We shall see that a block maxima procedure might improve the estimation. This will be illustrated through simulation. An application to financial data shall be presented at the end.

Key-Words:

- *extreme value theory; stable tail dependence function; tail-dependence coefficient.*

AMS Subject Classification:

- 62G32.

1. INTRODUCTION

Modern risk management is highly interested in assessing the amount of tail dependence. Many minimum-variance portfolio models are based on correlation, but correlation itself is not enough to describe a tail dependence structure and often results in misleading interpretations (Embrechts *et al.*, [7]). Multivariate extreme value theory (EVT) is the natural tool to measure and model such extremal dependence. The importance of this issue has led to several developments and applications in literature, e.g., Sibuya ([25]), Tiago de Oliveira ([27]), Joe ([16]), Coles *et al.* ([5]), Embrechts *et al.* ([8]), Frahm *et al.* ([11]), Schmidt and Stadtmüller ([23]), Ferreira and Ferreira ([9]); see de Carvalho and Ramos ([6]) for a recent survey.

The *tail-dependence coefficient* (TDC) measures the probability of occurring extreme values for one random variable (r.v.) given that another assumes an extreme value too. More precisely, it is defined as

$$\lambda = \lim_{t\to\infty} P\Big(F_1(X_1) > 1-1/t \mid F_2(X_2) > 1-1/t\Big)\,, \tag{1.1}$$

where F_1 and F_2 are the distribution functions (d.f.'s) of r.v.'s X_1 and X_2, respectively. Observe that it can be formulated as

$$\lambda = \lim_{\alpha\to 0} P\Big(X_1 > VaR_{1-\alpha}(X_1) \mid X_2 > VaR_{1-\alpha}(X_2)\Big)\,,$$

where $VaR_{1-\alpha}(X_i)$ $(i=1,2)$ is the Value-at-Risk of X_i at probability level $1-\alpha$ given by the quantile function evaluated at $1-\alpha$, $F_i^{-1}(1-\alpha) = \inf\{x : F_i(x) \geq 1-\alpha\}$ (see e.g., Schmidt and Stadtmüller, [23]). The TDC can also be defined via the notion of copula, introduced by Sklar ([26]). A copula C is a cumulative distribution function whose margins are uniformly distributed on $[0,1]$. If C is the copula of (X_1,X_2) having joint d.f. F, i.e., $F(x_1,x_2) = C\big(F_1(x_1),F_2(x_2)\big)$, observe that

$$\begin{aligned}\lambda &= 2 - \lim_{t\to\infty} t\,P\Big(F_1(X_1) > 1-1/t \;\text{ or }\; F_2(X_2) > 1-1/t\Big)\\ &= 2 - \lim_{t\to\infty} t\Big\{1 - C\big(1-1/t,\, 1-1/t\big)\Big\}\,.\end{aligned} \tag{1.2}$$

The TDC was the first tail dependence concept appearing in literature in a Sibuya's paper, where it was shown that, no matter how high we choose the correlation of normal random pairs, if we go far enough into the tail, extreme events tend to occur independently in each margin (Sibuya, [25]). It characterizes the dependence in the tail of a random pair (X_1,X_2), in the sense that, $\lambda > 0$ corresponds to tail dependence whose degree is measured by the value of λ, whereas $\lambda = 0$ means tail independence. The well-known bivariate t-distribution presents tail dependence, whereas the above mentioned bivariate normal is an example of tail independent model.

The conventional multivariate extreme value theory has emphasized the asymptotically dependent class resulting in its wide use. However, if the series are truly asymptotically independent, i.e., $\lambda = 0$, an overestimation of extreme value dependence, and consequently of the risk, will take place (see, e.g., Poon *et al.*, [21]; for further details about asymptotically independent class and respective models and coefficients, see also Ledford and Tawn, [19, 20]). Therefore, it is important to conclude whether (X_1, X_2) is tail dependent or not. In practice, this is not an easy task and one must be careful by inferring tail dependence from a finite random sample. Tests for tail independence can be seen in, e.g., Zhang ([28]), Hüsler and Li ([15]) and references therein. Frahm *et al.* ([11]) presents illustrations of misidentifications of the dependence structure. The bad performance of several nonparametric TDC estimators under tail independence was also shown in this latter paper through simulation. We remark that the examples that were used only concern models whose dependence function is not of the extreme value type. Here we present a nonparametric estimator for the TDC derived from Ferreira and Ferreira ([10]) and thus under an extreme value dependence, which we denote $\widehat{\lambda}^{(\mathrm{FF})}$. Strong consistency and asymptotic normality are proved (this latter in the case of known marginal d.f.'s). The finite-sample behavior and robustness are analyzed through simulation. We also compare with other existing methods. The simulation studies reveal some sensitivity to an extreme value dependence assumption and a large bias problem in the particular case of tail independence. In practice this may be overcome by taking block maxima, but one must be careful with a bias-variance trade-off arising from the number of block maxima to be considered: the larger this number the smaller the variance but the larger the bias (Frahm *et al.*, [11]). The simulation studies present improvements in estimates in some cases and allow to conclude the best block length choice. We end with an application to financial data.

2. EVT AND TAIL DEPENDENCE

Let $\{(X_1^{(n)}, X_2^{(n)})\}_{n\geq 1}$ be i.i.d. copies of 2-dimensional random vector, (X_1, X_2), with common d.f. $\mathbf{F}$, and let $M_j^{(n)} = \max_{1\leq i\leq n} X_j^{(i)}$, $j = 1, 2$, be the partial maxima for each marginal. If there exist sequences of constants $a_j^{(n)} > 0$, $b_j^{(n)} \in \mathbb{R}$, for $j = 1, 2$, and a distribution function G with non-degenerate margins, such that

$$\begin{aligned} P\Big(M_1^{(n)} \leq a_1^{(n)} x_1 + b_1^{(n)},\ M_2^{(n)} \leq a_2^{(n)} x_2 + b_2^{(n)}\Big) \;=& \\ =\; \mathbf{F}^n\Big(a_1^{(n)} x_1 + b_1^{(n)},\ a_2^{(n)} x_2 + b_2^{(n)}\Big) \underset{n\to\infty}{\longrightarrow} \mathbf{G}(x_1, x_2)\ ,& \end{aligned} \tag{2.1}$$

for all continuity points of $\mathbf{G}(x_1, x_2)$, then it must be a bivariate extreme value distribution, given by

$$\mathbf{G}(x_1, x_2) \;=\; \exp\Big[-l\big\{-\log G_1(x_1),\, -\log G_2(x_2)\big\}\Big]\,, \tag{2.2}$$

for some bivariate function l, where G_j, $j = 1, 2$, is the marginal d.f. of $\mathbf{G}$. We also say that $\mathbf{F}$ belongs to the max-domain of attraction of $\mathbf{G}$, in short, $\mathbf{F} \in \mathcal{D}(\mathbf{G})$. The function l in (2.2) is called *stable tail dependence function*, sometimes denoted extreme value dependence. It can be verified that l is convex, is homogeneous of order 1, and that $\max(x_1, x_2) \le l(x_1, x_2) \le x_1 + x_2$ for all $(x_1, x_2) \in [0, \infty)^2$, where the upper bound is due to the positive dependence of extreme value models and corresponds to independence whilst the lower bound means complete dependence (see, e.g. Beirlant *et al.* [1], Section 8.2.2). These properties also hold in the d-variate case, with $d > 2$. The statement in (2.1) has a similar formulation for the respective copulas, say $C_{\mathbf{X}}$ and C:

$$C^n_{\mathbf{X}}(u_1^{1/n}, u_2^{1/n}) \underset{n\to\infty}{\longrightarrow} C(u_1, u_2)\ , \tag{2.3}$$

where

$$C(u_1, u_2) \;=\; \exp\Big\{-l\big(-\log u_1,\, -\log u_2\big)\Big\} \tag{2.4}$$

is called a bivariate extreme value copula. In the sequel it will be denoted BEV copula and we will also refer the extreme value dependence context as a BEV dependence. The defining feature of a BEV copula is the max-stability property, i.e., $C(u_1, u_2) = C(u_1^{1/m}, u_2^{1/m})^m$ for every integer $m \ge 1$, $\forall\,(u_1, u_2) \in [0, 1]^2$. The max-domain of attraction condition (2.1) implies (2.3) but the reciprocal is not true since it must also be imposed that each marginal belongs to some max-domain of attraction. Since we have

$$\begin{aligned}
&\lim_{t\to\infty} t\,P\Big(F_1(X_1) > 1 - 1/t,\ F_2(X_2) > 1 - 1/t\Big) = \\
&\qquad = \; 2 \,-\, \lim_{t\to\infty} t\Big\{1 - C\big(1 - 1/t,\, 1 - 1/t\big)\Big\} \\
&\qquad = \; 2 \,-\, \lim_{t\to\infty} \log C^t\big(1 - 1/t,\, 1 - 1/t\big) \\
&\qquad = \; 2 \,-\, \lim_{t\to\infty} \log C\big((1 - 1/t)^t,\, (1 - 1/t)^t\big) \\
&\qquad = \; 2 \,-\, l(1, 1)\ ,
\end{aligned} \tag{2.5}$$

the TDC of a BEV copula can be obtained through the function l as

$$\lambda \;=\; 2 - l(1, 1)\ . \tag{2.6}$$

In the following we list some examples of stable tail dependence functions of BEV copulas and respective tail dependence:

- *Logistic:* $l(v_1, v_2) = (v_1^{1/r} + v_2^{1/r})^r$, with $v_j \ge 0$ and parameter $0 < r \le 1$; complete dependence is obtained in the limit as $r \to 0$ and independence when $r = 1$.

- *Asymmetric Logistic:* $l(v_1,v_2) = (1-t_1)\,v_1 + (1-t_2)\,v_2 + \big\{(t_1v_1)^{1/r} + (t_2v_2)^{1/r}\big\}^r$, with $v_j \geq 0$ and parameters $0 < r \leq 1$ and $0 \leq t_j \leq 1$, $j=1,2$; when $t_1 = t_2 = 1$ the asymmetric logistic model is equivalent to the logistic model; independence is obtained when either $r=1$, $t_1=0$ or $t_2=0$. Complete dependence is obtained in the limit when $t_1=t_2=1$ and r approaches zero.
- *Hüsler–Reiss:* $l(v_1,v_2) = v_1\Phi\big(r^{-1} + \frac{1}{2}\,r\log(v_1/v_2)\big) + v_2\,\Phi\big(r^{-1} + \frac{1}{2}\,r \cdot \log(v_2/v_1)\big)$, with parameter $r>0$ and where Φ is the standard normal d.f.; complete dependence is obtained as $r\to\infty$ and independence as $r\to 0$.

Non-BEV copulas cannot be obtained in the limit in (2.3), i.e., do not satisfy max-stability and cannot be expressed through formulation (2.4) based on the extreme value dependence function l with the given properties.

Examples of non-BEV copulas correspond, for instance, to the class of elliptical ones. The bivariate normal and the symmetric generalized hyperbolic distributions are tail independent models within this class. On the other hand, the bivariate t-distribution presents tail dependence with TDC,

$$\lambda \;=\; 2\,F_{t_{\nu+1}}\Big\{-\sqrt{(\nu+1)\,(1-\rho)/(1+\rho)}\Big\}\;,$$

where $\rho > -1$ and $F_{t_{\nu+1}}$ is the d.f. of the one dimensional $t_{\nu+1}$ distribution. See, e.g., Schmidt ([22]) and Frahm *et al.* ([11]).

Bivariate Archimedean copulas are another wide class that includes some tail independent non-BEV copulas such as Clayton, $C(u_1,u_2) = (u_1^{-\theta} + u_2^{-\theta} - 1)^{-1/\theta}$ with $\theta \geq 0$. Another special type which do not belong to either one of the three classes above is the tail independent Plackett-copula

$$C(u_1,u_2) \;=\; \frac{1+(\theta-1)\,(u_1+u_2) - \Big[\big\{1+(\theta-1)\,(u_1+u_2)\big\}^2 - 4u_1u_2\,\theta(\theta-1)\Big]^{1/2}}{2\,(\theta-1)}\;,$$

with parameter $\theta \in \mathbb{R}^+\backslash\{1\}$, and $C(u_1,u_2) = u_1u_2$, if $\theta=1$. For more details, see Joe ([16]).

3. ESTIMATION

The use of (semi)parametric estimators bears a model risk and may lead to wrong interpretations of the dependence structure. Nonparametric procedures avoid this type of misspecification but usually come along with a larger variance. Frahm *et al.* ([11]) confirms this assertion and shows that (semi)parametric estimators may have disastrous performances under wrong model assumptions.

So, in practice, if we are not sure about the type of model underlying data, nonparametric approach can be an alternative. Here we focus on nonparametric methods.

Huang ([14]), considered an estimator derived from the definition in (1.2) by plugging-in the respective empirical counterparts:

$$\widehat{\lambda}^{(\mathrm{H})} \;=\; 2 - \frac{1}{k_n}\sum_{i=1}^{n} \mathbf{1}_{\left\{\widehat{F}_1(X_1^{(i)})>1-\frac{k_n}{n} \text{ or } \widehat{F}_2(X_2^{(i)})>1-\frac{k_n}{n}\right\}}\,, \tag{3.1}$$

where $\widehat{F}_j$ is the empirical d.f. of F_j, $j = 1, 2$. Concerning estimation accuracy, some modifications of this latter may be used, like replacing the denominator n by $n + 1$, i.e., considering

$$\widehat{F}_j(u) \;=\; \frac{1}{n+1}\sum_{i=1}^{n} \mathbf{1}_{\left\{X_j^{(i)}\le u\right\}}$$

(Beirlant *et al.* [1], Section 9.4.1). A similar procedure was considered in Schimdt and Stadtmüler ([23]). For asymptotic properties, see the more recent results in Bücher and Dette ([2]). The consistency and asymptotic normality of the estimator $\widehat{\lambda}^{(\mathrm{H})}$ are derived with the asymptotics holding for an intermediate sequence $\{k_n\}$, $k_n \to \infty$ and $k_n/n \to 0$, as $n \to \infty$. The choice of $k \equiv k_n$ that allows for the 'best' bias–variance tradeoff is of major difficulty, since small values of k come along with a large variance whenever an increasing k results in a strong bias. A similar problem exists for univariate tail index estimations of heavy tailed distributions, for estimators of the stable tail dependence function l (Krajina, [18]) and other TDC estimators (e.g., Frahm *et al.* [11] and Schmidt and Stadtmüller [23]).

Under a BEV copula assumption, i.e., a copula with formulation (2.4), and given (2.6), estimators for the TDC can be obtained through the ones of the stable tail dependence function l. Within this context and motivated in Capéraà *et al.* ([4]), Frahm *et al.* ([11]) presented the estimator

$$2 - 2\,\exp\left[\frac{1}{n}\sum_{i=1}^{n}\log\left(\sqrt{\log\frac{1}{\widehat{F}_1(X_1^{(i)})}\,\log\frac{1}{\widehat{F}_2(X_2^{(i)})}}\Bigg/\log\frac{1}{\max\{\widehat{F}_1(X_1^{(i)}),\widehat{F}_2(X_2^{(i)})\}^2}\right)\right].$$

This rank-based estimator was shown to have the best performance among all nonparametric estimators considered in Frahm *et al.* ([11]). Optimally corrected versions can be seen in Genest and Segers ([12]) and alternative estimators are presented in Bücher *et al.* ([3]). In the sequel, we shall use a corrected version satisfying the boundary condition $l(1, 0) = l(0, 1) = 1$ considered in Genest and Segers ([12]), and here denoted $\widehat{\lambda}^{(\mathrm{CFG\text{-}C})}$.

Our approach is motivated by Ferreira and Ferreira ([10]) and has the same assumption of a BEV copula dependence structure. More precisely, it is based on the following representation of the stable tail dependence function:

$$l(x_1,x_2) = \frac{E\Big[\max\big\{F_1(X_1)^{1/x_1},\, F_2(X_2)^{1/x_2}\big\}\Big]}{1-E\Big[\max\big\{F_1(X_1)^{1/x_1},\, F_2(X_2)^{1/x_2}\big\}\Big]}\ , \tag{3.2}$$

where the expected values are estimated using sample means. Observe that the d.f. of $\max\big(F_1(X_1)^{1/x_1}, F_2(X_2)^{1/x_2}\big)$ is given by

$$\begin{aligned} P\Big(\max\big\{F_1(X_1)^{1/x_1}, F_2(X_2)^{1/x_2}\big\} \le u\Big) &= C\big(u^{x_1}, u^{x_2}\big) \\ &= \exp\Big(-l\big(-\log u^{x_1}, -\log u^{x_2}\big)\Big) \\ &= \exp\Big(-\big(-\log u\big)\, l\big(x_1,x_2\big)\Big) \\ &= u^{l(x_1,x_2)}\ , \end{aligned} \tag{3.3}$$

where the penultimate step is due to the first order homogeneity property of function l. Hence

$$E\Big[\max\big\{F_1(X_1)^{1/x_1}, F_2(X_2)^{1/x_2}\big\}\Big] = \frac{l(x_1,x_2)}{1+l(x_1,x_2)}\ .$$

Therefore, based on (2.6) and (3.2), we propose the estimator

$$\widehat{\lambda}^{(\mathrm{FF})} = 3 - \Big[1 - \overline{\max\big\{\widehat{F}_1(X_1), \widehat{F}_2(X_2)\big\}}\Big]^{-1}\ , \tag{3.4}$$

where $\overline{\max\big\{\widehat{F}_1(X_1), \widehat{F}_2(X_2)\big\}}$ is the sample mean of $\max\big\{\widehat{F}_1(X_1), \widehat{F}_2(X_2)\big\}$, i.e.,

$$\overline{\max\big\{\widehat{F}_1(X_1), \widehat{F}_2(X_2)\big\}} = \frac{1}{n}\sum_{i=1}^{n} \max\big\{\widehat{F}_1(X_1^{(i)}), \widehat{F}_2(X_2^{(i)})\big\}\ .$$

Proposition 3.1. *The estimator $\widehat{\lambda}^{(FF)}$ in (3.4) is strongly consistent.*

Proof: Observe that

$$\begin{aligned} &\left|\frac{1}{n}\sum_{i=1}^{n} \max_{j\in\{1,2\}}\Big\{\widehat{F_j}\big(X_j^{(i)}\big)\Big\} - E\Big[\max_{j\in\{1,2\}}\Big\{F_j\big(X_j\big)\Big\}\Big]\right| \le \\ &\qquad \le \left|\frac{1}{n}\sum_{i=1}^{n} \max_{j\in\{1,2\}}\Big\{\widehat{F_j}\big(X_j^{(i)}\big)\Big\} - \frac{1}{n}\sum_{i=1}^{n} \max_{j\in\{1,2\}}\Big\{F_j\big(X_j^{(i)}\big)\Big\}\right| \\ &\qquad\quad + \left|\frac{1}{n}\sum_{i=1}^{n} \max_{j\in\{1,2\}}\Big\{F_j\big(X_j^{(i)}\big)\Big\} - E\Big[\max_{j\in\{1,2\}}\Big\{F_j\big(X_j\big)\Big\}\Big]\right|\ , \end{aligned} \tag{3.5}$$

where the second term converges *almost surely* to zero by the *Strong Law of Large Numbers* (by (3.3), $\max_{j\in\{1,2\}}\big\{F_j(X_j)\big\} \sim \mathrm{Beta}\big(l(1,1),1\big)$, $1 \le l(1,1) \le 2$, and all the moments exist).

The first term in (3.5) is upper bounded by

$$\frac{1}{n}\sum_{i=1}^{n}\sum_{j\in\{1,2\}}\left|\widehat{F}_j\big(X_j^{(i)}\big)-F_j\big(X_j^{(i)}\big)\right| ,$$

which converges *almost surely* to zero according to Gilat and Hill ([13]; Theorem 1.1). See also Ferreira and Ferreira ([10], Proposition 3.7). □

The asymptotic normality in case the marginal d.f.'s are known is derived from Ferreira and Ferreira ([10], Proposition 3.3) and the delta method. More precisely, denoting this version as $\widehat{\lambda}_*^{(\mathrm{FF})}$, we have

$$\sqrt{n}\,\big(\widehat{\lambda}_*^{(\mathrm{FF})}-\lambda\big) \;\to\; N(0,\sigma^2) ,$$

where

$$\sigma^2 \;=\; \frac{l(1,1)\,\big(1+l(1,1)\big)^2}{2+l(1,1)} .$$

In the case of unknown marginals, we believe that the asymptotic normality of $\sqrt{n}\,\big(\widehat{\lambda}^{(\mathrm{FF})}-\lambda\big)$ may be derived from the weak convergence of the empirical copula process (Segers, [24]). This will be addressed in a future work.

Observe that estimators $\widehat{\lambda}^{(\mathrm{FF})}$ and $\widehat{\lambda}^{(\mathrm{CFG\text{-}C})}$ are obtained under the more restrictive assumption of an extreme value dependence but have a convergence rate of $\sqrt{n}$. On the other hand, estimator $\widehat{\lambda}^{(\mathrm{H})}$ has no restrictive assumptions but has to pay the price of a slower convergence rate $\sqrt{k_n}$, since only the largest $k_n = o(n)$ observations can be taken into account.

4. SIMULATION STUDY

In this section we analyze the finite-sample behavior of our estimator. We simulate 1000 independent random samples of sizes $n = 50, 100, 500, 1000$ from three BEV copulas with stable tail dependence functions: logistic, asymmetric logistic and Hüsler–Reiss. We consider the two types of dependence: tail dependence (Table 1) and tail independence (Table 2). The results obtained from the logistic and asymmetric logistic under tail independence are quite similar and thus we omit the latter case. In order to assess robustness we also analyze the case of non-BEV copulas, by considering, for tail dependence, a bivariate t-distribution with $\nu = 1.5$ degrees of freedom and, for tail independence, a BSGH distribution (Table 3). In both cases we take a correlation parameter of $\rho = 0.5$. Since the t-distribution is somewhat 'close' to being an extreme value copula (see Bücher, Dette and Volgushev [3], Section 2), we also consider a convex combination of a rotated Clayton copula (corresponding to negative dependence) and a t-distribution, more precisely, $C_\alpha(u_1,u_2) = \alpha\big(u_2 - C_{\mathrm{Clayton}}(1-u_1,u_2)\big) + (1-\alpha)\,C_{t_\nu}(u_1,u_2)$. For comparison, we compute estimator $\widehat{\lambda}^{(\mathrm{CFG\text{-}C})}$ which works under the same assumptions (i.e, an extreme value dependence) and the more general estimator $\widehat{\lambda}^{(\mathrm{H})}$ which has no model restrictions (the required choice of k to balance the variance-bias problem is based on an heuristic procedure in Frahm *et al.* [11]). Absolute empirical bias and the root mean-squared error (rmse) for all implemented TDC estimations are in Tables 1, 2 and 3.

Table 1: Tail dependent ($\lambda > 0$) BEV copulas with stable tail dependence functions: Logistic and Asym. Logistic with $r = 0.4$ and Hüsler–Reiss with $r = 3$.

	$\widehat{\lambda}^{(\mathrm{FF})}$ bias (rmse)	$\widehat{\lambda}^{(\mathrm{CFG\text{-}C})}$ bias (rmse)	$\widehat{\lambda}^{(\mathrm{H})}$ bias (rmse)
$\lambda = 0.6805$		Logistic	
$(n = 50)$	0.0019 (0.0994)	0.0050 (0.0556)	0.0395 (0.1962)
$(n = 100)$	0.0052 (0.0711)	0.0044 (0.0395)	0.0389 (0.1412)
$(n = 500)$	0.0006 (0.0330)	0.0005 (0.0180)	0.0216 (0.0883)
$(n = 1000)$	0.0002 (0.0232)	0.0004 (0.0122)	0.0099 (0.1379)
$\lambda = 0.3402$		Asym. Logistic	
$(n = 50)$	0.0085 (0.1147)	0.0332 (0.1122)	0.0527 (0.1836)
$(n = 100)$	0.0053 (0.0824)	0.0203 (0.0754)	0.0635 (0.1363)
$(n = 500)$	0.0020 (0.0389)	0.0045 (0.0355)	0.0335 (0.0847)
$(n = 1000)$	0.0014 (0.0287)	0.0031 (0.0245)	0.0038 (0.1193)
$\lambda = 0.7389$		Hüsler–Reiss	
$(n = 50)$	0.0040 (0.0484)	0.0057 (0.0462)	0.0202 (0.1697)
$(n = 100)$	0.0003 (0.0331)	0.0020 (0.0323)	0.0075 (0.1094)
$(n = 500)$	0.0002 (0.0152)	0.0007 (0.0140)	0.0011 (0.0655)
$(n = 1000)$	0.0002 (0.0292)	0.0005 (0.0097)	0.0103 (0.0342)

Table 2: Tail independent ($\lambda = 0$) BEV copulas with stable tail dependence functions: Logistic with $r = 1$ and Hüsler–Reiss with $r = 0.03$.

	$\widehat{\lambda}^{(\mathrm{FF})}$ bias (rmse)	$\widehat{\lambda}^{(\mathrm{CFG\text{-}C})}$ bias (rmse)	$\widehat{\lambda}^{(\mathrm{H})}$ bias (rmse)
$\lambda = 0$		Logistic	
$(n = 50)$	0.0230 (0.1284)	0.0900 (0.1389)	0.1040 (0.1644)
$(n = 100)$	0.0062 (0.0956)	0.0467 (0.0952)	0.1004 (0.1348)
$(n = 500)$	0.0036 (0.0415)	0.0140 (0.0361)	0.0492 (0.0650)
$(n = 1000)$	0.0017 (0.0296)	0.0077 (0.0257)	0.0502 (0.0578)
$\lambda \approx 0$		Hüsler–Reiss	
$(n = 50)$	0.0254 (0.1370)	0.0875 (0.1353)	0.1002 (0.1660)
$(n = 100)$	0.0084 (0.0966)	0.0412 (0.0883)	0.0991 (0.1336)
$(n = 500)$	0.0009 (0.0415)	0.0100 (0.0361)	0.0492 (0.0653)
$(n = 1000)$	0.0003 (0.0299)	0.0061 (0.0265)	0.0081 (0.0298)

Table 3: Non-BEV tail dependent case: t_ν with $\nu = 1.5$ and $\rho = 0.5$ and a convex combination of a rotated Clayton and t_ν (RC&T), $C_{0.5}(u_1, u_2) = 0.5\,\big(u_2 - C_{\text{Clayton}}(1 - u_1, u_2)\big) + 0.5\,C_{t_\nu}(u_1, u_2)$; non-BEV tail independent case: BSGH distribution with $\rho = 0.5$.

	$\widehat{\lambda}^{(\text{FF})}$ bias (rmse)	$\widehat{\lambda}^{(\text{CFG-C})}$ bias (rmse)	$\widehat{\lambda}^{(\text{H})}$ bias (rmse)
$\lambda = 0.4406$		t-distribution	
$(n = 50)$	0.0099 (0.1043)	0.0318 (0.1022)	0.0084 (0.1970)
$(n = 100)$	0.0087 (0.0711)	0.0213 (0.0743)	0.0094 (0.1393)
$(n = 500)$	0.0124 (0.0339)	0.0130 (0.0348)	0.0044 (0.0884)
$(n = 1000)$	0.0122 (0.0267)	0.0123 (0.0266)	0.0120 (0.1403)
$\lambda = 0.3669$		RC&T	
$(n = 50)$	0.4396 (0.6562)	0.2832 (0.4736)	0.2990 (0.3064)
$(n = 100)$	0.4052 (0.6440)	0.2879 (0.4282)	0.1371 (0.2779)
$(n = 500)$	0.3800 (0.6411)	0.2793 (0.4681)	0.1350 (0.2772)
$(n = 1000)$	0.3791 (0.6342)	0.2650 (0.4571)	0.1314 (0.2743)
$\lambda = 0$		BSGH	
$(n = 50)$	0.4288 (0.4396)	0.4305 (0.4544)	0.3730 (0.4238)
$(n = 100)$	0.4287 (0.4346)	0.4239 (0.4294)	0.3704 (0.3926)
$(n = 500)$	0.4248 (0.4259)	0.4030 (0.4052)	0.3130 (0.3232)
$(n = 1000)$	0.4238 (0.4243)	0.4001 (0.4008)	0.2188 (0.2489)

Estimators $\widehat{\lambda}^{(\text{FF})}$ and $\widehat{\lambda}^{(\text{CFG-C})}$ behave well within BEV copulas (or 'close' of being BEV as t-distribution). Yet, they performed poorly on a non-BEV dependence context (see Table 3). Estimator $\widehat{\lambda}^{(\text{H})}$ tends to present a slight larger bias but performs better under non extreme value dependence. This is consistent with a slower rate of convergence and the fact that it holds in a general framework, as discussed in the previous section. All estimators also performed poorly on tail independent non-BEV copulas. Our results do not contradict however the ones in Frahm *et al.* ([11]), where the misbehavior of nonparametric estimation concerned tail independence within non-BEV copulas. By considering a block maxima procedure, i.e., divide n-length data into m blocks of size $b = \lfloor n/m \rfloor$ ($\lfloor x \rfloor$ denotes the largest integer not exceeding x) and take only the maximum observation within each block, we obtain a sample of maximum, which is more consistent with an extreme values model and thus a BEV copula. This methodology involves a bias–variance tradeoff arising from the number of block maxima (block length) to be considered: the larger (smaller) this number the smaller the variance but the larger the bias (Frahm *et al.*, [11]). It requires not too small sample sizes to also provide not too small maxima samples. A simulation study to find the value(s) of b that better accommodates this compromise will be implemented in the next section.

4.1. Block maxima procedure for non-BEV dependence

We consider 1000 independent random samples of sizes $n = 500, 1000, 1500, 2000, 5000$ generated from the tail independent and non-BEV copulas: bivariate normal (BN), BSGH and Plackett-copula (BPC). We estimate the TDC through a block maxima procedure for block lengths $b = 15, 30, 60, 90$. The absolute empirical bias and the rmse of all implemented TDC estimations are presented in Tables 4 and 5, for BN and BPC, respectively. The results obtained for the BSGH case (omitted here) were not good in all the three estimators and, in practice,

Table 4: Block maxima samples with given length b of BN model with $\rho = 0.5$ (the case $b = 1$ correspond to the whole sample).

BN	$\widehat{\lambda}^{(\text{FF})}$	$\widehat{\lambda}^{(\text{CFG-C})}$	$\widehat{\lambda}^{(\text{H})}$
$(n = 500)$	bias (rmse)	bias (rmse)	bias (rmse)
$(b = 1)$	0.4025 (0.4036)	0.3702 (0.3733)	0.3244 (0.3294)
$(b = 15)$	0.2319 (0.2578)	0.2520 (0.2966)	0.1986 (0.2594)
$(b = 30)$	0.2081 (0.2924)	0.2958 (0.3351)	0.2241 (0.3825)
$(b = 60)$	0.2798 (0.4187)	0.3703 (0.4486)	0.1900 (0.4594)
$(b = 90)$	0.2887 (0.4275)	0.3734 (0.4937)	0.3816 (0.7975)
$(n = 1000)$	bias (rmse)	bias (rmse)	bias (rmse)
$(b = 1)$	0.4023 (0.4029)	0.3587 (0.3692)	0.3238 (0.3262)
$(b = 15)$	0.2046 (0.2297)	0.2201 (0.2438)	0.2037 (0.2498)
$(b = 30)$	0.1941 (0.2428)	0.2251 (0.2720)	0.2185 (0.3012)
$(b = 60)$	0.1724 (0.2695)	0.2625 (0.3234)	0.2000 (0.3578)
$(b = 90)$	0.2888 (0.3582)	0.3692 (0.4259)	0.3625 (0.5874)
$(n = 1500)$	bias (rmse)	bias (rmse)	bias (rmse)
$(b = 1)$	0.4024 (0.4028)	0.3562 (0.3663)	0.3236 (0.3253)
$(b = 15)$	0.2011 (0.2180)	0.2114 (0.2242)	0.1848 (0.2165)
$(b = 30)$	0.1612 (0.2015)	0.2001 (0.2328)	0.1682 (0.2309)
$(b = 60)$	0.1546 (0.2311)	0.2310 (0.2760)	0.2064 (0.3200)
$(b = 90)$	0.1708 (0.2696)	0.2674 (0.3093)	0.1964 (0.3480)
$(n = 2000)$	bias (rmse)	bias (rmse)	bias (rmse)
$(b = 1)$	0.3230 (0.3243)	0.3559 (0.3661)	0.3230 (0.3243)
$(b = 15)$	0.2012 (0.2141)	0.2013 (0.2155)	0.2054 (0.2312)
$(b = 30)$	0.1601 (0.1912)	0.1628 (0.2116)	0.1810 (0.2293)
$(b = 60)$	0.1600 (0.2172)	0.1600 (0.2111)	0.2047 (0.2887)
$(b = 90)$	0.1829 (0.2535)	0.2029 (0.2986)	0.2269 (0.3489)
$(n = 5000)$	bias (rmse)	bias (rmse)	bias (rmse)
$(b = 1)$	0.4024 (0.4025)	0.3603 (0.3644)	0.3234 (0.3240)
$(b = 15)$	0.1936 (0.1988)	0.1801 (0.1884)	0.1973 (0.2068)
$(b = 30)$	0.1595 (0.1730)	0.1519 (0.1717)	0.1762 (0.1952)
$(b = 60)$	0.1348 (0.1648)	0.1550 (0.1846)	0.1701 (0.2093)
$(b = 90)$	0.1283 (0.1744)	0.1677 (0.1948)	0.1742 (0.2288)

Table 5: Block maxima samples with given length b of BPC (Plackett-copula) with $\theta = 2$ (the case $b = 1$ correspond to the whole sample).

BPC	$\widehat{\lambda}^{(\mathrm{FF})}$	$\widehat{\lambda}^{(\mathrm{CFG\text{-}C})}$	$\widehat{\lambda}^{(\mathrm{H})}$
$(n = 500)$	bias (rmse)	bias (rmse)	bias (rmse)
$(b = 1)$	0.2028 (0.2062)	0.1766 (0.1805)	0.1676 (0.1741)
$(b = 15)$	0.0894 (0.1779)	0.1592 (0.2026)	0.1555 (0.2462)
$(b = 30)$	0.0801 (0.2341)	0.1954 (0.2565)	0.1329 (0.2833)
$(b = 60)$	0.1981 (0.3407)	0.3397 (0.3913)	0.1244 (0.3718)
$(b = 90)$	0.2189 (0.3892)	0.2695 (0.4624)	0.3942 (0.4507)
$(n = 1000)$	bias (rmse)	bias (rmse)	bias (rmse)
$(b = 1)$	0.2012 (0.2030)	0.1708 (0.1733)	0.1684 (0.1720)
$(b = 15)$	0.0538 (0.1249)	0.0906 (0.1313)	0.1134 (0.1613)
$(b = 30)$	0.0701 (0.1668)	0.1457 (0.1880)	0.1579 (0.2459)
$(b = 60)$	0.0955 (0.2315)	0.2122 (0.2623)	0.1517 (0.3090)
$(b = 90)$	0.2262 (0.3168)	0.3295 (0.3714)	0.3000 (0.5177)
$(n = 1500)$	bias (rmse)	bias (rmse)	bias (rmse)
$(b = 1)$	0.2019 (0.2031)	0.1695 (0.1705)	0.1684 (0.1708)
$(b = 15)$	0.0547 (0.1081)	0.0798 (0.1089)	0.1053 (0.1408)
$(b = 30)$	0.0514 (0.1389)	0.1068 (0.1452)	0.1042 (0.1667)
$(b = 60)$	0.0545 (0.1943)	0.1504 (0.2077)	0.1480 (0.2647)
$(b = 90)$	0.1000 (0.2250)	0.2077 (0.2610)	0.1535 (0.3084)
$(n = 2000)$	bias (rmse)	bias (rmse)	bias (rmse)
$(b = 1)$	0.2012 (0.2021)	0.1684 (0.1692)	0.1695 (0.1712)
$(b = 15)$	0.0539 (0.0967)	0.0713 (0.0971)	0.1141 (0.1141)
$(b = 30)$	0.0384 (0.1175)	0.0887 (0.1252)	0.1135 (0.1613)
$(b = 60)$	0.0642 (0.1728)	0.1390 (0.1831)	0.1405 (0.2262)
$(b = 90)$	0.0953 (0.2072)	0.1819 (0.1861)	0.1678 (0.2942)
$(n = 5000)$	bias (rmse)	bias (rmse)	bias (rmse)
$(b = 1)$	0.2015 (0.2018)	0.1665 (0.1669)	0.1697 (0.1704)
$(b = 15)$	0.0430 (0.0671)	0.0404 (0.0641)	0.1108 (0.1215)
$(b = 30)$	0.0345 (0.0807)	0.0495 (0.0781)	0.1065 (0.1283)
$(b = 60)$	0.0366 (0.1079)	0.0729 (0.1065)	0.1210 (0.1629)
$(b = 90)$	0.0397 (0.1376)	0.0895 (0.1323)	0.0970 (0.1407)

may lead to wrongly infer tail dependence. If this is an adequate model for data, then (semi)parametric estimators considered in Frahm [11]) are a more sensible choice. We have also implemented a block maxima procedure for the non-BEV case of the convex combination copula considered in Table 3 with similar results of the BPC and thus omitted. Observe that block maxima procedure improves estimates in some cases, in particular for estimators $\widehat{\lambda}^{(\mathrm{FF})}$ and $\widehat{\lambda}^{(\mathrm{CFG\text{-}C})}$. The adequate choices for block-length b in sample sizes ranging from, approximately, 500 and 1000, are $b = 15, 30$, while for sample sizes between 1000 and 2000 we can choose $b = 30, 60$, and for larger sample sizes (ranging from 2000 to 5000) a block-length $b = 60, 90$ seems appropriate.

4.2. Application to financial data

We consider the negative log-returns of Dow Jones (USA) and FTSE100 (UK) indexes for the time period 1994–2004. The corresponding scatter plot and TDC estimate plot of $\widehat{\lambda}^{(\mathrm{H})}$ for various k (Figure 1) show the presence of tail dependence and the order of magnitude of the tail-dependence coefficient.

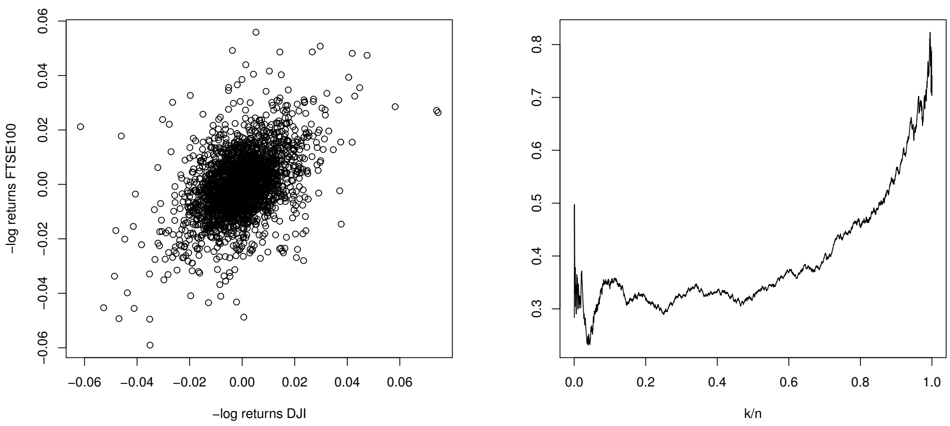

Figure 1: Scatter plot of Dow Jones versus FTSE100 negative log-returns ($n = 2529$ data points) and the corresponding TDC estimates $\widehat{\lambda}^H$ for various k/n.

Moreover, the typical variance-bias problem for various threshold values k can be observed, too. In particular, a small k induces a large variance, whereas an increasing k generates a strong bias of the TDC estimate. The threshold choosing procedure of k leads to a TDC estimate of $\widehat{\lambda}^{(\mathrm{H})} = 0.3397$ and from our estimator we derive $\widehat{\lambda}^{(\mathrm{FF})} = 0.3622$. In computing $\widehat{\lambda}^{(\mathrm{CFG\text{-}C})}$ we obtain 0.354. The results from the three considered estimators are quite close, leading to a tail-dependence estimate that should be approximately 0.35.

5. DISCUSSION

One must be careful by inferring tail dependence/independence from a finite random sample and (semi)parametric and nonparametric procedures have pros and cons. Thus, the message is that there is no perfect strategy and the best way to protect against errors is the application of several methods to the same data set. A test of tail independence is advised (see, e.g., Zhang [28], Hüsler and Li [15] and references therein). The proposed estimator has revealed good performance even in the independent case. However the simulation results showed sensitivity to the assumption of an extreme value dependence structure and we recommend to test in advance for this hypothesis. See Kojadinovic, Yan and Segers ([17]) or Bücher, Dette and Volgushev ([3]) and references therein. A block maxima procedure may improve the estimates. A study focused on the asymptotic properties will be addressed in a future work.

ACKNOWLEDGMENTS

This research was financed by FEDER Funds through "Programa Operacional Factores de Competitividade — COMPETE" and by Portuguese Funds through FCT — "Fundação para a Ciência e a Tecnologia", within the Project Est-C/MAT/UI0013/2011.

We also acknowledge the valuable suggestions from the referees.

REFERENCES

[1] Beirlant, J.; Goegebeur, Y.; Segers, J. and Teugels, J. (2004). *Statistics Of Extremes: Theory and Application*, John Wiley, England.

[2] Bücher, A. and Dette, H. (2012). Multiplier bootstrap of tail copulas with applications, *Bernoulli*, to appear.

[3] Bücher, A.; Dette, H. and Volgushev, S. (2011). New estimators of the Pickands dependence function and a test for extreme-value dependence, *The Annals of Statistics*, **39**(4), 1963–2006.

[4] Capéraà, P.; Fougères, A.L. and Genest, C. (1997). A nonparametric estimation procedure for bivariate extreme value copulas, *Biometrika*, **84**, 567–577.

[5] Coles, S.; Heffernan, J. and Tawn, J. (1999). Dependence measures for extreme value analysis, *Extremes*, **2**, 339–366.

[6] de Carvalho, M. and Ramos, A. (2012). Bivariate extreme statistics, II, *Revstat*, **10**, 83–107.

[7] Embrechts, P.; McNeil, A. and Straumann, D. (2002). *Correlation and dependence in risk management: properties and pitfalls.* In "Risk Management: Value at Risk and Beyond" (M.A.H. Dempster, Ed.), Cambridge University Press, Cambridge, 176–223.

[8] Embrechts, P.; Lindskog, F. and McNeil, A. (2003). *Modelling dependence with copulas and applications to risk management.* In "Handbook of Heavy Tailed Distributions in Finance" (S. Rachev, Ed.), Elsevier, 329–384.

[9] Ferreira, H. and Ferreira, M. (2012). Tail dependence between order statistics, *Journal of Multivariate Analysis*, **105**(1), 176–192.

[10] Ferreira, H. and Ferreira, M. (2012). On extremal dependence of block vectors, *Kybernetika*, **48**(5), 988–1006.

[11] Frahm, G.; Junker, M. and Schmidt, R. (2005). Estimating the tail-dependence coefficient: properties and pitfalls, *Insurance: Mathematics & Economics*, **37**(1), 80–100.

[12] Genest, C. and Segers, J. (2009). Rank-based inference for bivariate extreme-value copulas, *The Annals of Statistics*, **37**, 2990–3022.

[13] Gilat, D. and Hill, T. (1992). One-sided refinements of the strong law of large numbers and the Glivenko–Cantelli Theorem, *The Annals of Probability*, **20**, 1213–1221.

[14] Huang, X. (1992). *Statistics of Bivariate Extreme Values*, Ph. D. thesis, Tinbergen Institute Research Series 22, Erasmus University, Rotterdam.

[15] Hüsler, J. and Li, D. (2009). Testing asymptotic independence in bivariate extremes, *Journal of Statistical Planning and Inference*, **139**, 990–998.

[16] Joe, H. (1997). *Multivariate Models and Dependence Concepts*, Chapman & Hall, London.

[17] Kojadinovic, I.; Segers, J. and Yan, J. (2011). Large-sample tests of extreme-value dependence for multivariate copulas, *The Canadian Journal of Statistics*, **39**(4), 703–720.

[18] Krajina, A. (2010). *An M–Estimator of Multivariate Tail Dependence*, Tilburg University Press, Tilburg.

[19] Ledford, A. and Tawn, J.A. (1996). Statistics for near independence in multivariate extreme values, *Biometrika*, **83**, 169–187.

[20] Ledford, A. and Tawn, J.A. (1997). Modelling dependence within joint tail regions, *Journal of the Royal Statistical Society, Series B*, **59**, 475–499.

[21] Poon, S.-H.; Rockinger, M. and Tawn, J. (2004). Extreme value dependence in financial markets: diagnostics, models, and financial implications, *Review of Financial Studies*, **17**(2), 581–610.

[22] Schmidt, R. (2002). Tail dependence for elliptically contoured distributions, *Mathematical Methods of Operations Research*, **55**, 301–327.

[23] Schmidt, R. and Stadtmüller, U. (2006). Nonparametric estimation of tail dependence, *Scandinavian Journal of Statistics*, **33**, 307–335.

[24] Segers, J. (2012). Asymptotics of empirical copula processes under nonrestrictive smoothness assumptions, *Bernoulli*, **18**, 764–782.

[25] Sibuya, M. (1960). Bivariate extreme statistics, *Annals of the Institute of Statistical Mathematics*, **11**, 195–210.

[26] Sklar, A. (1959). Fonctions de répartition à n dimensions et leurs marges, *Publications de l'Institut de Statistique de l'Université de Paris*, **8**, 229–231.

[27] Tiago de Oliveira, J. (1962–1963). Structure theory of bivariate extremes: extensions, *Estudos de Matemática, Estatística e Econometria*, **7**, 165–195.

[28] Zhang, Z. (2008). Quotient correlation: a sample based alternative to Pearson's correlation, *The Annals of Statistics*, **36**(2), 1007–1030.

REVSTAT – Statistical Journal
Volume 11, Number 1, March 2013, 17–43

NONCENTRAL GENERALIZED MULTIVARIATE BETA TYPE II DISTRIBUTION

Authors: K. Adamski, S.W. Human, A. Bekker and J.J.J. Roux
– University of Pretoria, Pretoria, 0002, South Africa
karien.adamski@up.ac.za
schalk.human@up.ac.za
andriette.bekker@up.ac.za

Abstract:

- The distribution of the variables that originates from monitoring the variance when the mean encountered a sustained shift is considered — specifically for the case when measurements from each sample are independent and identically distributed normal random variables. It is shown that the solution to this problem involves a sequence of dependent random variables that are constructed from independent noncentral chi-squared random variables. This sequence of dependent random variables are the key to understanding the performance of the process used to monitor the variance and are the focus of this article. For simplicity, the marginal (i.e. the univariate and bivariate) distributions and the joint (i.e. the trivariate) distribution of only the first three random variables following a change in the variance is considered. A multivariate generalization is proposed which can be used to calculate the entire run-length (i.e. the waiting time until the first signal) distribution.

Key-Words:

- *confluent hypergeometric functions; hypergeometric functions; multivariate beta distribution; noncentral chi-squared; shift in process mean and variance.*

AMS Subject Classification:

- 62E15, 62H10.

1. INTRODUCTION

We propose a noncentral generalized multivariate beta type II distribution constructed from independent noncentral chi-squared random variables using the variables in common technique. This is a new contribution to the existing beta type II distributions considered in the literature. Tang (1938) studied the distribution of the ratios of noncentral chi-squared random variables defined on the positive domain. He considered the ratio, consisting of independent variates, where the numerator was a noncentral chi-squared random variable while the denominator was a central chi-squared random variable, as well as the ratio where both the numerator and denominator were noncentral chi-squared random variables — this was applied to study the properties of analysis of variance tests under nonstandard conditions. Patnaik (1949) coined the phrase noncentral F for the first ratio mentioned above. The second ratio is referred to as the doubly noncentral F distribution. An overview of these distributions is given by Johnson, Kotz & Balakrishnan (1995). More recently Pe and Drygas (2006) proposed an alternative presentation for the doubly noncentral F by using the results on the product of two hypergeometric functions. In a bivariate context Gupta *et al.* (2009) derived a noncentral bivariate beta type I distribution, using a ratio of noncentral gamma random variables, that is defined on the unit square; applying the appropriate transformation will yield a noncentral beta type II distribution defined on the positive domain. The noncentral Dirichlet type II distribution was derived by Troskie (1967) as the joint distribution of $V_i = \frac{Y_i}{Y_{r+1}}$, $i = 1, 2, ..., r$ where Y_i is chi-squared distributed and Y_{r+1} has a noncentral chi-squared distribution. Sánchez and Nagar (2003) derived the version where both Y_i and Y_{r+1} are noncentral gamma random variables.

Section 2 provides an overview of the practical problem which is the genesis of the random variables $U_0 = \frac{\lambda W_0}{X}$ and $U_j = \frac{\lambda W_j}{X+\lambda\sum_{k=0}^{j-1} W_k}$, $j = 1, 2, ..., p$ with $\lambda > 0$ where X and W_i, $i = 0, 1, ..., p$ are noncentral chi-squared distributed. In Section 3 the distribution of the first three random variables, i.e. U_0, U_1, U_2 is derived. Bivariate densities and univariate densities of (U_0, U_1, U_2) also receive attention. Section 4 proposes a multivariate extension, followed by shape analysis, an example and probability calculations in Sections 5 and 6, respectively.

2. PROBLEM STATEMENT

Adamski *et al.* (2012) proposed a generalized multivariate beta distribution; the dependence structure and construction of the random variables originate in a practical setting where the process mean is monitored, using a control chart (see e.g. Montgomery, 2009), when the measurements are independent and identically distributed having been collected from an $\text{Exp}(\theta)$ distribution, where θ was assumed to be unknown.

Monitoring the unknown process variance assuming that the observations from each independent sample are independent identically distributed (i.i.d.) normal random variables with the mean known was introduced by Quesenberry (1991). To gain insight into the performance of such a control chart, in other words, to determine the probability of detecting a shift immediately or after a number of samples, the joint distribution of the plotting statistics is needed. Exact expressions for the joint distribution of the plotting statistics for the chart proposed by Quesenberry (1991) can be obtained from the distribution derived by Adamski *et al.* (2012), the key difference is the fact that it is only the degrees of freedom of the chi-squared random variables that changes.

Monitoring of the unknown process variance when the known location parameter sustained a permanent shift leads to a noncentral version of the generalized multivariate beta distribution proposed by Adamski *et al.* (2012). To derive this new noncentral generalized multivariate beta type II distribution we proceed in two steps. First we describe the practical setting which motivates the derivation of the distribution, and secondly we derive the distributions in sections 3 and 4. To this end, let $(X_{i1}, X_{i2}, ..., X_{in_i})$, $i = 1, 2, ...$ represent successive, independent samples of size $n_i \geq 1$ measurements made on a sequence of items produced in time. Assume that these values are independent and identically distributed having been collected from a $N(\mu_0, \sigma^2)$ distribution where the parameters μ_0 and σ^2 denotes the known process mean and unknown process variance, respectively. Take note that a sample can even consist of an individual observation because the process mean is assumed to be known and the variance of the sample can still be calculated as $S_i^2 = (X_{i1} - \mu_0)^2$. Suppose that from sample (time period) $\kappa > 1$ the unknown process variance parameter has changed from σ^2 to $\sigma_1^2 = \lambda\sigma^2$ (also unknown) where $\lambda \neq 1$ and $\lambda > 0$, but the known process mean also encountered an unknown sustained shift from sample (time period) $h > 1$ onwards, i.e. it changed from μ_0 to μ_1 where μ_1 is also known. To clarify, the mean of the process at start-up is assumed to be known and denoted μ_0 but the time and the size of the shift in the mean will be unknown in a practical situation. In order to incorporate and/or evaluate the influence of these changes in the parameters on the performance of the control chart for the variance, we assume fixed/deterministic values for these parameters — essentially this implies then that the mean is known following the shift, i.e. denoted by μ_1. Therefore, the main interest is monitoring the process variance when the process mean is known, although this mean can suffer at some time an unknown shift. In practice it is important to note that even though the mean and the variance of the normal distribution can change independently, the performance of a Shewhart type control chart for the mean depends on the process variance and vice versa.

This dependency is due to the plotting statistics and the control limits used. The proposed control chart could thus be useful in practice when the control chart for monitoring the mean fails to detect the shift in the mean. For example, in case a small shift in the mean occurs and a Shewhart-type chart for the mean is used (which is known for the inefficiency in detecting small shifts compared to the EWMA (exponentially weighted moving average) and CUSUM (cumulative sum) charts for the mean which are better in detecting small shifts (Montgomery, 2009)) the shift might go undetected.

Based on the time of the shift in the process mean, this problem can be viewed in three ways, as illustrated in Figure 1.

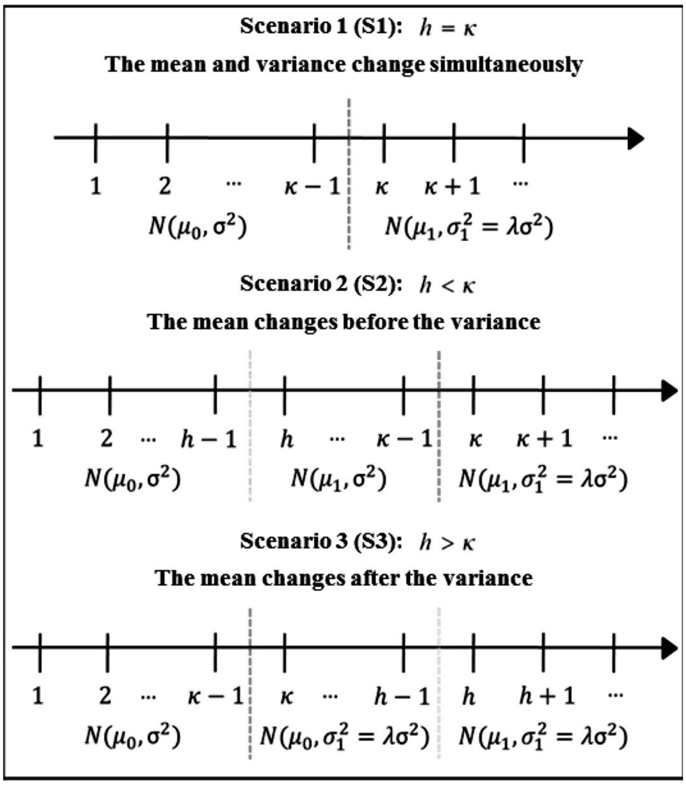
Scenario 1 (S1): $h = \kappa$
The mean and variance change simultaneously
1
2
⋯
$\kappa - 1$
κ
$\kappa + 1$
⋯
$N(\mu_0, \sigma^2)$
$N(\mu_1, \sigma_1^2 = \lambda\sigma^2)$
Scenario 2 (S2): $h < \kappa$
The mean changes before the variance
1
2
⋯
$h - 1$
h
⋯
$\kappa - 1$
κ
$\kappa + 1$
⋯
$N(\mu_0, \sigma^2)$
$N(\mu_1, \sigma^2)$
$N(\mu_1, \sigma_1^2 = \lambda\sigma^2)$
Scenario 3 (S3): $h > \kappa$
The mean changes after the variance
1
2
⋯
$\kappa - 1$
κ
⋯
$h - 1$
h
$h + 1$
⋯
$N(\mu_0, \sigma^2)$
$N(\mu_0, \sigma_1^2 = \lambda\sigma^2)$
$N(\mu_1, \sigma_1^2 = \lambda\sigma^2)$

Figure 1: The different scenarios.

From Figure 1 we see the following:

Scenario 1: The mean and the variance change simultaneously from μ_0 to μ_1 and from σ^2 to σ_1^2, respectively. Note that, it is assumed that the shift in the process parameters occurs somewhere between samples $\kappa - 1$ and κ.

Scenario 2: The change in the mean from μ_0 to μ_1 occurs before the change in the variance from σ^2 to σ_1^2.

Scenario 3: The change in the variance from σ^2 to σ_1^2 occurs before the change in the mean from μ_0 to μ_1.

Because it is assumed that the process variance σ^2 is unknown, the first sample is used to obtain an initial estimate of σ^2. Thus, in the remainder of this article σ^2 is assumed to denote a point estimate of the unknown variance. This initial estimate is continuously updated using the new incoming samples as they are collected as long as the estimated value of σ^2 does not change, i.e. is not detected using the control chart. The control chart and the plotting statistic is based on the in-control distribution of the process. The two sample test statistic for testing the hypothesis at time r that the two independent samples (the measurements of the r^{th} sample alone and the measurements of the first $r-1$ samples combined) are from normal distributions with the same unknown variance, is based on the statistic

$$U_r^* = \frac{S_r^2}{S_{r-1}^{2\text{pooled}}} \qquad \text{for} \quad r = 2, 3, \dots\,,$$

(2.1)

$$\text{where} \quad S_{r-1}^{2\text{pooled}} = \frac{\sum_{i=1}^{r-1} n_i S_i^2}{\sum_{i=1}^{r-1} n_i} \quad \text{and} \quad S_i^2 = \frac{1}{n_i}\sum_{k=1}^{n_i}(X_{ik}-\mu_i)^2 \quad \text{for } i=1,2,\dots,r\,.$$

[Take note: μ_i denotes the known population mean of sample i.]

The focus will be on the part where the process is out-of-control, i.e. encountered a shift, since the exact distribution of the plotting statistic is then unknown. To simplify the notation used in expression (2.1), following a change in the process variance between samples $\kappa-1$ and κ, define the random variable

$$U_0^* = U_\kappa^* = \frac{S_\kappa^2}{S_{\kappa-1}^{2\text{pooled}}}\,. \tag{2.2}$$

The subscript of the random variable U_0^* indicates the number of samples after the parameter has changed, with zero indicating that it is the first sample after the process encountered a permanent upward or downward step shift in the variance.

Note that, the three scenarios can theoretically occur with equal probability as there would be no reason to expect (without additional information such as expert knowledge about the process being monitored) that the mean would sustain a change prior to the variance (and vice versa). In fact, it might be more realistic to argue that in practice the mean and variance would change simultaneously in the event of a "special cause" as such an event might change the entire underlying process generating distribution and hence both the location and variability might be affected. Having said the aforementioned, the likelihood of the three scenarios will most likely depend on the interaction between the underlying process distribution and the special causes that may occur. The focus of this article is on scenario 2 since the results for the other scenarios follow by means of simplifications (by setting the noncentrality parameter equal to zero) and will be shown as remarks.

Suppose that the process variance has changed between samples (time periods) $\kappa - 1$ and $\kappa > 1$ from σ^2 to $\sigma_1^2 = \lambda\sigma^2$ where λ is unknown, $\lambda \neq 1$ and $\lambda > 0$, but the process mean also encountered an unknown sustained shift between samples (time periods) $h-1$ and h where $1 < h < \kappa$. Note that, in practice h, κ and λ would be unknown (but deterministic) values. Consider the sample variance, i.e. S_i^2, before and after the shifts in the process mean and variance took place:

Before the shift in the mean:

$$\begin{aligned} \text{Samples:} &\quad i = 1, 2, ..., h-1\,. \\ \text{Distribution:} &\quad X_{ik} \sim N\big(\mu_0, \sigma^2\big)\,. \end{aligned}$$

$$\begin{aligned} S_i^2 &= \frac{1}{n_i}\sum_{k=1}^{n_i}(X_{ik}-\mu_0)^2 \ , \\ \frac{n_i\,S_i^2}{\sigma^2} &\sim \chi^2_{n_i} \ . \end{aligned}$$

After the shift in the mean:

$$\begin{aligned} \text{Samples:} &\ \ i = h, ..., \kappa-1\,. \\ \text{Distribution:} &\ \ X_{ik} \sim N\big(\mu_1 = \mu_0 + \xi_0\,\sigma,\, \sigma^2\big)\,. \end{aligned}$$

[Take note: The observer is unaware of the shift in the process mean and therefore still wrongly assumes $X_{ik} \sim N(\mu_0, \sigma^2)$.
This is the key to the noncentral case because the plotting statistic and transformations (see Section 6) depends on the in-control distribution.]

$$\begin{aligned} S_i^2 &= \frac{1}{n_i}\sum_{k=1}^{n_i}(X_{ik}-\mu_0)^2 \ , \\ n_i\,S_i^2 &= \sum_{k=1}^{n_i}(X_{ik}-\mu_1+\mu_1-\mu_0)^2 \ , \\ \frac{n_i\,S_i^2}{\sigma^2} &= \sum_{k=1}^{n_i}\left(\frac{X_{ik}-\mu_1}{\sigma}+\frac{\mu_1-\mu_0}{\sigma}\right)^2 \\ &= \sum_{k=1}^{n_i}(Z_{ik}+\xi_0)^2 \qquad \text{where} \quad Z_{ik} \sim N(0,1) \\ &\sim \chi'^2_{n_i}\left(\sum_{k=1}^{n_i}\xi_0^2\right) = \chi'^2_{n_i}(\delta_i) \qquad \text{where} \quad \delta_i = \sum_{k=1}^{n_i}\xi_0^2 = n_i\xi_0^2 > 0 \\ &\qquad\qquad\qquad\qquad\qquad\qquad\quad \text{with} \quad \xi_0 = \frac{\mu_1-\mu_0}{\sigma} \ . \end{aligned}$$

After the shift in the mean and variance:

Samples: $i = \kappa, \kappa+1, \dots$.
Distribution: $X_{ik} \sim N\big(\mu_1 = \mu_0 + \xi_1\sigma_1,\, \sigma_1^2 = \lambda\sigma^2\big)$.

[Take note: The observer is unaware of the shifts in the process parameters and therefore still wrongly assumes $X_{ik} \sim N(\mu_0, \sigma^2)$.]

$$\begin{aligned}
S_i^2 &= \frac{1}{n_i}\sum_{k=1}^{n_i}(X_{ik}-\mu_0)^2 \ , \\
n_i S_i^2 &= \sum_{k=1}^{n_i}(X_{ik}-\mu_1+\mu_1-\mu_0)^2 \ , \\
\frac{n_i S_i^2}{\sigma_1^2} &= \sum_{k=1}^{n_i}\left(\frac{X_{ik}-\mu_1}{\sigma_1}+\frac{\mu_1-\mu_0}{\sigma_1}\right)^2 \\
&= \sum_{k=1}^{n_i}(Z_{ik}+\xi_1)^2 \qquad \text{where} \quad Z_{ik} \sim N(0,1) \\
&\sim \chi'^2_{n_i}\left(\sum_{k=1}^{n_i}\xi_1^2\right) = \chi'^2_{n_i}(\delta_i) \qquad \text{where} \quad \delta_i = \sum_{k=1}^{n_i}\xi_1^2 = n_i\xi_1^2 > 0 \\
&\qquad\qquad\qquad\qquad\qquad\qquad\quad \text{with} \quad \xi_1 = \frac{\mu_1-\mu_0}{\sigma_1} \ .
\end{aligned}$$

Remark 2.1.

(i) $\chi^2_{n_i}$ denotes a central χ^2 random variable with degrees of freedom n_i (see Johnson *et al.* (1995), Chapter 18).

(ii) $\chi'^2_{n_i}(\delta_i)$ denotes a noncentral χ^2 random variable with degrees of freedom n_i and noncentrality parameter δ_i (see Johnson *et al.* (1995), Chapter 29).

(iii) The degrees of freedom is assumed to be n_i, since the mean is not estimated because it is assumed that the mean is a fixed / deterministic value before and after the shift. In case the mean is unknown and has to be estimated too, the degrees of freedom changes from n_i to $n_i - 1$ and the μ_0 would be replaced by $\hat{\mu}_0$, i.e. an estimate of μ_0.

(iv) The shift in the mean, before the variance changed, is modelled as follows: $\xi_0 = \frac{\mu_1-\mu_0}{\sigma}$, i.e. $\mu_1 = \mu_0 + \xi_0\sigma$.

(v) The shift in the mean, after the variance changed, is modelled as follows: $\xi_1 = \frac{\mu_1-\mu_0}{\sigma_1}$, i.e. $\mu_1 = \mu_0 + \xi_1\sigma_1$.

(vi) The pivotal quantity $\frac{n_i S_i^2}{\sigma_1^2} \sim \chi'^2_{n_i}(\delta_i)$ after the shift in the variance reduces to a central chi-squared random variable if the process mean did not change, i.e. when $\mu_1 = \mu_0$ (see Adamski *et al.* (2012)).

Following a change in the variance between samples $\kappa-1$ and κ, define the following random variable:

$$
\begin{aligned}
U_0^* &= \frac{S_\kappa^2}{S_{\kappa-1}^{2\text{pooled}}} = \sum_{i=1}^{\kappa-1} n_i \times \frac{S_\kappa^2}{\sum_{i=1}^{h-1} n_i S_i^2 + \sum_{i=h}^{\kappa-1} n_i S_i^2} \\
&= \frac{\sum_{i=1}^{\kappa-1} n_i}{n_\kappa} \times \frac{\frac{n_\kappa S_\kappa^2}{\sigma_1^2} \times \frac{\sigma_1^2}{\sigma^2}}{\sum_{i=1}^{h-1} \frac{n_i S_i^2}{\sigma^2} + \sum_{i=h}^{\kappa-1} \frac{n_i S_i^2}{\sigma^2}} = \frac{\sum_{i=1}^{\kappa-1} n_i}{n_\kappa} \times \frac{\lambda\, \chi'^2_{n_\kappa}(\delta_\kappa)}{\sum_{i=1}^{\kappa-1} \chi'^2_{n_i}(\delta_i)} ,
\end{aligned}
$$

where $\lambda = \frac{\sigma_1^2}{\sigma^2}$ indicates the unknown size of the shift in the variance

$$
\text{and } \delta_i = \begin{cases} 0 & \text{for } i = 1,...,h-1 , \\ n_i \xi_0^2 > 0 \quad \text{with } \xi_0 = \frac{\mu_1-\mu_0}{\sigma} & \text{for } i = h,...,\kappa-1 , \\ n_\kappa \xi_1^2 > 0 \quad \text{with } \xi_1 = \frac{\mu_1-\mu_0}{\sigma_1} & \text{for } i = \kappa . \end{cases}
$$

$\big[$Take note: $\sum_{i=1}^{h-1} \chi^2_{n_i} \overset{d}{=} \sum_{i=1}^{h-1} \chi'^2_{n_i}(0).\big]$

In general, at sample $\kappa+j$, where $\kappa > 1$ and $j = 1,2,...,p$, we define the following sequence of random variables (all based on the two sample test statistic for testing the equality of variances):

$$
\begin{aligned}
U_j^* &= \frac{S_{\kappa+j}^2}{S_{\kappa+j-1}^{2\text{pooled}}} \\
&= \sum_{i=1}^{\kappa+j-1} n_i \times \frac{S_{\kappa+j}^2}{\sum_{i=1}^{h-1} n_i S_i^2 + \sum_{i=h}^{\kappa-1} n_i S_i^2 + \sum_{i=\kappa}^{\kappa+j-1} n_i S_i^2} \\
&= \frac{\sum_{i=1}^{\kappa+j-1} n_i}{n_{\kappa+j}} \times \frac{\frac{n_{\kappa+j}\, S_{\kappa+j}^2}{\sigma_1^2} \times \frac{\sigma_1^2}{\sigma^2}}{\sum_{i=1}^{h-1} \frac{n_i S_i^2}{\sigma^2} + \sum_{i=h}^{\kappa-1} \frac{n_i S_i^2}{\sigma^2} + \sum_{i=\kappa}^{\kappa+j-1} \frac{n_i S_i^2}{\sigma_1^2} \times \frac{\sigma_1^2}{\sigma^2}} \\
&= \frac{\sum_{i=1}^{\kappa+j-1} n_i}{n_{\kappa+j}} \times \frac{\lambda\, \chi'^2_{n_{\kappa+j}}(\delta_{\kappa+j})}{\sum_{i=1}^{\kappa-1} \chi'^2_{n_i}(\delta_i) + \lambda \sum_{i=\kappa}^{\kappa+j-1} \chi'^2_{n_i}(\delta_i)} \qquad \text{with } \lambda = \frac{\sigma_1^2}{\sigma^2} ,
\end{aligned}
$$

$$
\text{where } \delta_i = \begin{cases} 0 & \text{for } i = 1,...,h-1 , \\ n_i \xi_0^2 > 0 \quad \text{with } \xi_0 = \frac{\mu_1-\mu_0}{\sigma} & \text{for } i = h,...,\kappa-1 , \\ n_i \xi_1^2 > 0 \quad \text{with } \xi_1 = \frac{\mu_1-\mu_0}{\sigma_1} & \text{for } i = \kappa,...,\kappa+j . \end{cases}
$$

To simplify matters going forward and for notational purposes we omit the factors $\sum_{i=1}^{\kappa-1} n_i/n_\kappa$ and $\sum_{i=1}^{\kappa+j-1} n_i/n_{\kappa+j}$, respectively, in U_0^* and U_j^*, since they do not contain any random variables, and also drop the * superscript, and therefore the random variables of interest are:

$$
\begin{aligned}
U_0 &= \frac{\lambda W_0}{X} , \\
U_j &= \frac{\lambda W_j}{X + \lambda \sum_{k=0}^{j-1} W_k} , \qquad j = 1,2,...,p \quad \text{and} \quad \lambda > 0 ,
\end{aligned}
\tag{2.3}
$$

where

$\lambda \;=\; \frac{\sigma_1^2}{\sigma^2}$ indicates the unknown size of the shift in the variance,

$X \;=\; \sum_{i=1}^{\kappa-1} \chi'^2_{n_i}(\delta_i) \sim \chi'^2_a(\delta_a)$, i.e. X is a noncentral chi-squared random variable with degrees of freedom, $a{=}\sum_{i=1}^{\kappa-1} n_i$ and noncentrality parameter $\delta_a = \sum_{i=h}^{\kappa-1}\delta_i$, $h<\kappa$ where $\delta_i = n_i\xi_0^2$ with $\xi_0 = \frac{\mu_1-\mu_0}{\sigma}$,

$W_i \;\sim\; \chi'^2_{v_i}(\delta_i)$, i.e. W_i is a noncentral chi-squared random variable with degrees of freedom $v_i = n_{\kappa+i}$ and noncentrality parameter $\delta_i = n_{\kappa+i}\xi_1^2$ with $\xi_1 = \frac{\mu_1-\mu_0}{\sigma_1}$, $i = 0,1,...,p$.

Take note that X represents the sum of $\kappa-1$ independent noncentral χ^2 random variables, i.e. $\chi'^2_{n_1},...,\chi'^2_{n_{\kappa-1}}$ since we assume the samples are independent.

Remark 2.2. Scenarios 1 and 3 can be obtained as follows:

(i) When the process mean and variance change simultaneously (scenario 1), i.e. $h=\kappa$, then $\delta_a = 0$. The superscript (S1) in the expressions that follow indicate scenario 1 as discussed and shown in Figure 1. From (2.3) it then follows that

$$U_0^{(S1)} = \frac{\lambda W_0}{X}\,,$$
$$U_j^{(S1)} = \frac{\lambda W_j}{X+\lambda\sum_{k=0}^{j-1}W_k}\,, \qquad j=1,2,...,p \quad \text{and} \quad \lambda>0\,,$$

where

$X = \sum_{i=1}^{\kappa-1}\chi^2_{n_i} \sim \chi^2_a$ with $a = \sum_{i=1}^{\kappa-1} n_i$,

$W_i {\sim} \chi'^2_{v_i}(\delta_i)$ with $v_i{=}n_{\kappa+i}$, $\delta_i{=}n_{\kappa+i}\xi_1^2$ and $\xi_1{=}\frac{\mu_1-\mu_0}{\sigma_1}$, $i{=}0,1,...,p$.

(ii) For scenario 3, the process variance has changed between samples (time periods) $\kappa-1$ and $\kappa>1$, but the process mean encountered a sustained shift between samples (time periods) $h-1$ and h where $h>\kappa$, i.e. the mean changed after the variance. The random variables in (2.3) will change as follows:

$$U_0^{(S3)} = \frac{\lambda W_0}{X}\,,$$
$$U_j^{(S3)} = \frac{\lambda W_j}{X+\lambda\sum_{k=0}^{j-1}W_k}\,, \qquad j=1,2,...,p \quad \text{and} \quad \lambda>0\,,$$

where

$X = \sum_{i=1}^{\kappa-1}\chi^2_{n_i} \sim \chi^2_a$ with $a = \sum_{i=1}^{\kappa-1} n_i$,

$$W_i \sim \chi'^2_{v_i}(\delta_i) \;\text{ with }\; v_i = n_{\kappa+i},\; \delta_i = \begin{cases} 0 & \text{for } i=0,1,...,h{-}1\,, \\ n_{\kappa+i}\xi_1^2 \text{ and } \xi_1 = \frac{\mu_1-\mu_0}{\sigma_1} & \\ & \text{for } i = h, h{+}1,...,p\,. \end{cases}$$

(iii) If the process mean remains unchanged and only the process variance encountered a sustained shift, the components X and W_i in (2.3) will reduce to central chi-squared random variables. The joint distribution of the random variables (2.3) will then be the generalized multivariate beta distribution derived by Adamski *et al.* (2012), with the only difference being the degrees of freedom of the chi-squared random variables. This shows that the solution to the run-length distribution of a Q-chart used to monitor the parameter θ in the Exp(θ) distribution (when θ is unknown) is similar to the solution to the run-length distribution when monitoring the variance with a Q-chart in case of a $N(\mu_0, \sigma^2)$ distribution where μ_0 is known and σ^2 is unknown.

3. THE EXACT DENSITY FUNCTION

In this section the joint distribution of the random variables U_0, U_1, U_2 (see (2.3)) is derived, i.e. the first three random variables following a change in the variance. In section 4 the multivariate extension is considered with a detailed proof. The reason for this unorthodox presentation of results is to first demonstrate the different marginals for the trivariate case.

Theorem 3.1. *Let X, W_i with $i = 0,1,2$ be independent noncentral chi-squared random variables with degrees of freedom a and v_i and noncentrality parameters δ_a and δ_i with $i = 0,1,2$, respectively. Let $U_0 = \frac{\lambda W_0}{X}$, $U_1 = \frac{\lambda W_1}{X+\lambda W_0}$ and $U_2 = \frac{\lambda W_2}{X+\lambda W_0+\lambda W_1}$ (see (2.3)) and $\lambda > 0$. The joint density of (U_0, U_1, U_2) is given by*

$$f(u_0, u_1, u_2)$$

$$\begin{aligned}
&= \frac{e^{-\left(\frac{\delta_a+\delta_0+\delta_1+\delta_2}{2}\right)} \lambda^{\frac{a}{2}}\, \Gamma\left(\frac{a+v_0+v_1+v_2}{2}\right)}{\Gamma\left(\frac{a}{2}\right) \Gamma\left(\frac{v_0}{2}\right) \Gamma\left(\frac{v_1}{2}\right) \Gamma\left(\frac{v_2}{2}\right)}\, u_0^{\frac{v_0}{2}-1} u_1^{\frac{v_1}{2}-1} u_2^{\frac{v_2}{2}-1} (1+u_0)^{\frac{v_1}{2}+\frac{v_2}{2}} \\
&\quad \times (1+u_1)^{\frac{v_2}{2}} \Big[\lambda + u_0 + u_1(1+u_0) + u_2\,(1+u_0)\,(1+u_1)\Big]^{-\left(\frac{a+v_0+v_1+v_2}{2}\right)} \\
&\quad \times \Psi_2^{(4)}\left[\frac{a+v_0+v_1+v_2}{2}; \frac{a}{2}, \frac{v_0}{2}, \frac{v_1}{2}, \frac{v_2}{2}; \frac{\lambda\delta_a}{2z}, \frac{\delta_0 u_0}{2z}, \frac{\delta_1 u_1\,(1+u_0)}{2z}, \frac{\delta_2 u_2\,(1+u_0)\,(1+u_1)}{2z}\right], \\
&\qquad\qquad\qquad\qquad\qquad\qquad\qquad\qquad u_j > 0\,, \quad j = 0,1,2\;,
\end{aligned} \tag{3.1}$$

where $z = \lambda + u_0 + u_1(1+u_0) + u_2\,(1+u_0)\,(1+u_1)$ and $\Psi_2^{(4)}$ the confluent hypergeometric function in four variables (see Sánchez et al. (2006) or Srivastava & Kashyap (1982)).

Proof: The expression for the joint density of (U_0, U_1, U_2) is obtained by setting $p = 2$ in (4.1) and applying result A.2 of Sanchez *et al.* (2006). □

Remark 3.1.

(i) For the special case when $\lambda = 1$ (i.e. the process variance did not encounter a shift although the mean did), this trivariate density (3.1) simplifies to

$$
\begin{aligned}
&f(u_0, u_1, u_2) \\
&= \frac{e^{-\left(\frac{\delta_a+\delta_0+\delta_1+\delta_2}{2}\right)}\,\Gamma\!\left(\frac{a+v_0+v_1+v_2}{2}\right)}{\Gamma\!\left(\frac{a}{2}\right)\Gamma\!\left(\frac{v_0}{2}\right)\Gamma\!\left(\frac{v_1}{2}\right)\Gamma\!\left(\frac{v_2}{2}\right)}\; u_0^{\frac{v_0}{2}-1}\, u_1^{\frac{v_1}{2}-1}\, u_2^{\frac{v_2}{2}-1}(1+u_0)^{\frac{v_1}{2}+\frac{v_2}{2}}\,(1+u_1)^{\frac{v_2}{2}} \\
&\quad\times \Big[(1+u_0)\,(1+u_1)\,(1+u_2)\Big]^{-\left(\frac{a+v_0+v_1+v_2}{2}\right)} \\
&\quad\times \Psi_2^{(4)}\left[\tfrac{a+v_0+v_1+v_2}{2};\, \tfrac{a}{2}, \tfrac{v_0}{2}, \tfrac{v_1}{2}, \tfrac{v_2}{2};\, \tfrac{\delta_a}{2y}, \tfrac{\delta_0 u_0}{2y}, \tfrac{\delta_1 u_1 (1+u_0)}{2y}, \tfrac{\delta_2 u_2\,(1+u_0)\,(1+u_1)}{2y}\right],
\end{aligned}
$$

where $y = (1+u_0)\,(1+u_1)\,(1+u_2)$.

(ii) When the shift in the mean and the variance occurs simultaneously (scenario 1), we have that $\delta_a = 0$, and it follows that the trivariate density (3.1) is given by

$$
\begin{aligned}
&f(u_0, u_1, u_2) \\
&= \frac{e^{-\left(\frac{\delta_0+\delta_1+\delta_2}{2}\right)}\lambda^{\frac{a}{2}}\,\Gamma\!\left(\frac{a+v_0+v_1+v_2}{2}\right)}{\Gamma\!\left(\frac{a}{2}\right)\Gamma\!\left(\frac{v_0}{2}\right)\Gamma\!\left(\frac{v_1}{2}\right)\Gamma\!\left(\frac{v_2}{2}\right)}\; u_0^{\frac{v_0}{2}-1}\, u_1^{\frac{v_1}{2}-1}\, u_2^{\frac{v_2}{2}-1}(1+u_0)^{\frac{v_1}{2}+\frac{v_2}{2}}\,(1+u_1)^{\frac{v_2}{2}} \\
&\quad\times \Big[\lambda + u_0 + u_1(1+u_0) + u_2\,(1+u_0)\,(1+u_1)\Big]^{-\left(\frac{a+v_0+v_1+v_2}{2}\right)} \\
&\quad\times \Psi_2^{(3)}\left[\tfrac{a+v_0+v_1+v_2}{2};\, \tfrac{v_0}{2}, \tfrac{v_1}{2}, \tfrac{v_2}{2};\, \tfrac{\delta_0 u_0}{2z}, \tfrac{\delta_1 u_1\,(1+u_0)}{2z}, \tfrac{\delta_2 u_2\,(1+u_0)\,(1+u_1)}{2z}\right],
\end{aligned}
$$

where $z = \lambda + u_0 + u_1(1+u_0) + u_2\,(1+u_0)\,(1+u_1)$ with $\Psi_2^{(3)}$ the confluent hypergeometric function in three variables.

(iii) When monitoring the variance and the mean did not change, i.e. $\delta_a = \delta_0 = \delta_1 = \delta_2 = 0$, the trivariate density (3.1) simplifies to the generalized multivariate beta distribution, derived by Adamski *et al.* (2012):

$$
\begin{aligned}
&f(u_0, u_1, u_2) \\
&= \frac{\lambda^{\frac{a}{2}}\,\Gamma\!\left(\frac{a+v_0+v_1+v_2}{2}\right)}{\Gamma\!\left(\frac{a}{2}\right)\Gamma\!\left(\frac{v_0}{2}\right)\Gamma\!\left(\frac{v_1}{2}\right)\Gamma\!\left(\frac{v_2}{2}\right)}\; u_0^{\frac{v_0}{2}-1}\, u_1^{\frac{v_1}{2}-1}\, u_2^{\frac{v_2}{2}-1}(1+u_0)^{\frac{v_1}{2}+\frac{v_2}{2}}\,(1+u_1)^{\frac{v_2}{2}} \\
&\quad\times \Big[\lambda + u_0 + u_1(1+u_0) + u_2\,(1+u_0)\,(1+u_1)\Big]^{-\left(\frac{a+v_0+v_1+v_2}{2}\right)}.
\end{aligned}
$$

3.1. Bivariate cases

Theorem 3.2. *Let X, W_i with $i=0,1,2$ be independent noncentral chi-squared random variables with degrees of freedom a and v_i and noncentrality parameters δ_a and δ_i with $i=0,1,2$, respectively. Let $U_0=\frac{\lambda W_0}{X}$, $U_1=\frac{\lambda W_1}{X+\lambda W_0}$ and $U_2=\frac{\lambda W_2}{X+\lambda W_0+\lambda W_1}$ and $\lambda>0$.*

(**a**) *The joint density of (U_0,U_1) is given by*

$$\begin{aligned}(3.2)\qquad & f(u_0,u_1)\\ = {} & \frac{e^{-\left(\frac{\delta_a+\delta_0+\delta_1}{2}\right)}\lambda^{\frac{a}{2}}\,\Gamma\left(\frac{a+v_0+v_1}{2}\right)}{\Gamma\left(\frac{a}{2}\right)\Gamma\left(\frac{v_0}{2}\right)\Gamma\left(\frac{v_1}{2}\right)}\; u_0^{\frac{v_0}{2}-1}\, u_1^{\frac{v_1}{2}-1}(1+u_0)^{\frac{v_1}{2}}\,\Big[\lambda+u_0+u_1(1+u_0)\Big]^{-\left(\frac{a+v_0+v_1}{2}\right)}\\ & \times\Psi_2^{(3)}\left[\frac{a+v_0+v_1}{2};\frac{a}{2},\frac{v_0}{2},\frac{v_1}{2};\frac{\lambda\,\delta_a}{2\Big[\lambda+u_0+u_1(1+u_0)\Big]},\frac{\delta_0\,u_0}{2\Big[\lambda+u_0+u_1(1+u_0)\Big]},\frac{\delta_1 u_1\,(1+u_0)}{2\Big[\lambda+u_0+u_1(1+u_0)\Big]}\right],\\ & \qquad u_j>0\,,\quad j=0,1\;.\end{aligned}$$

(**b**) *The joint density of (U_0,U_2) is given by*

$$\begin{aligned}(3.3)\qquad & f(u_0,u_2)\\ = {} & \frac{e^{-\left(\frac{\delta_a+\delta_0+\delta_1+\delta_2}{2}\right)}\lambda^{\frac{a}{2}}\,\Gamma\left(\frac{a+v_0+v_1+v_2}{2}\right)\Gamma\left(\frac{a+v_0}{2}\right)}{\Gamma\left(\frac{a}{2}\right)\Gamma\left(\frac{v_0}{2}\right)\Gamma\left(\frac{v_2}{2}\right)\Gamma\left(\frac{a+v_0+v_1}{2}\right)}\; u_0^{\frac{v_0}{2}-1}(1+u_0)^{-\left(\frac{a+v_0}{2}\right)}\,u_2^{\frac{v_2}{2}-1}\\ & \times(1+u_2)^{-\left(\frac{a+v_0+v_1+v_2}{2}\right)}\sum_{k_1=0}^{\infty}\sum_{k_2=0}^{\infty}\sum_{k_3=0}^{\infty}\sum_{k_4=0}^{\infty}\sum_{k_5=0}^{\infty}\frac{\left(\frac{a+v_0+v_1+v_2}{2}\right)_{k_1+k_2+k_3+k_4+k_5}}{\left(\frac{a}{2}\right)_{k_1}\left(\frac{v_0}{2}\right)_{k_2}\left(\frac{v_2}{2}\right)_{k_4}}\\ & \times\frac{\left(\frac{a+v_0}{2}\right)_{k_1+k_2+k_5}}{\left(\frac{a+v_0+v_1}{2}\right)_{k_1+k_2+k_3+k_5}\,k_1!\,k_2!\,k_3!\,k_4!\,k_5!}\left(\frac{\lambda\,\delta_a}{2\,(1+u_0)\,(1+u_2)}\right)^{k_1}\\ & \times\left(\frac{\delta_0\,u_0}{2\,(1+u_0)\,(1+u_2)}\right)^{k_2}\left(\frac{\delta_1}{2\,(1+u_2)}\right)^{k_3}\left(\frac{\delta_2\,u_2}{2\,(1+u_2)}\right)^{k_4}\left(\frac{1-\lambda}{(1+u_0)\,(1+u_2)}\right)^{k_5},\\ & \qquad u_j>0\,,\quad j=0,2\;.\end{aligned}$$

(**c**) *The joint density of (U_1,U_2) is given by*

$$\begin{aligned}(3.4)\qquad & f(u_1,u_2)\\ = {} & \frac{e^{-\left(\frac{\delta_a+\delta_0+\delta_1+\delta_2}{2}\right)}\lambda^{\frac{a}{2}}\,\Gamma\left(\frac{a+v_0+v_1+v_2}{2}\right)}{\Gamma\left(\frac{v_1}{2}\right)\Gamma\left(\frac{v_2}{2}\right)\Gamma\left(\frac{a+v_0}{2}\right)}\; u_1^{\frac{v_1}{2}-1}(1+u_1)^{-\left(\frac{a+v_0+v_1}{2}\right)}\,u_2^{\frac{v_2}{2}-1}\\ & \times(1+u_2)^{-\left(\frac{a+v_0+v_1+v_2}{2}\right)}\sum_{k_1=0}^{\infty}\sum_{k_2=0}^{\infty}\sum_{k_3=0}^{\infty}\sum_{k_4=0}^{\infty}\sum_{k_5=0}^{\infty}\frac{\left(\frac{a+v_0+v_1+v_2}{2}\right)_{k_1+k_2+k_3+k_4+k_5}}{\left(\frac{a}{2}\right)_{k_1}\left(\frac{v_1}{2}\right)_{k_3}\left(\frac{v_2}{2}\right)_{k_4}}\;\times\end{aligned}$$

$$\times \frac{\left(\frac{a}{2}\right)_{k_1+k_5}}{\left(\frac{a+v_0}{2}\right)_{k_1+k_2+k_5} k_1!\,k_2!\,k_3!\,k_4!\,k_5!} \left(\frac{\lambda\,\delta_a}{2\,(1+u_1)\,(1+u_2)}\right)^{k_1}$$

$$\times\left(\frac{\delta_0}{2\,(1+u_1)\,(1+u_2)}\right)^{k_2} \left(\frac{\delta_1\, u_1}{2\,(1+u_1)\,(1+u_2)}\right)^{k_3} \left(\frac{\delta_2\, u_2}{2\,(1+u_2)}\right)^{k_4} \left(\frac{1-\lambda}{(1+u_1)\,(1+u_2)}\right)^{k_5},$$

$$u_j > 0\,, \quad j=1,2\ .$$

Proof: (**a**) Expanding $\Psi_2^{(4)}(\cdot)$ in equation (3.1) in series form and integrating this trivariate density with respect to u_2, yields

$$f(u_0,u_1)$$

$$= \frac{e^{-\left(\frac{\delta_a+\delta_0+\delta_1+\delta_2}{2}\right)}\lambda^{\frac{a}{2}}\,\Gamma\!\left(\frac{a+v_0+v_1+v_2}{2}\right)}{\Gamma(\frac{a}{2})\Gamma(\frac{v_0}{2})\Gamma(\frac{v_1}{2})\Gamma(\frac{v_2}{2})}\; u_0^{\frac{v_0}{2}-1}\, u_1^{\frac{v_1}{2}-1}\,(1+u_0)^{\frac{v_1+v_2}{2}}\,(1+u_1)^{\frac{v_2}{2}}$$

$$\times \sum_{k_1=0}^{\infty}\sum_{k_2=0}^{\infty}\sum_{k_3=0}^{\infty}\sum_{k_4=0}^{\infty} \frac{\left(\frac{a+v_0+v_1+v_2}{2}\right)_{k_1+k_2+k_3+k_4}}{\left(\frac{a}{2}\right)_{k_1}\left(\frac{v_0}{2}\right)_{k_2}\left(\frac{v_1}{2}\right)_{k_3}\left(\frac{v_2}{2}\right)_{k_4} k_1!k_2!k_3!k_4!}\left(\frac{\lambda\delta_a}{2}\right)^{k_1}$$

$$\times\left(\frac{\delta_0 u_0}{2}\right)^{k_2}\left(\frac{\delta_1 u_1(1+u_0)}{2}\right)^{k_3}\left(\frac{\delta_2(1+u_0)(1+u_1)}{2}\right)^{k_4}$$

$$\times\int_0^\infty u_2^{\frac{v_2}{2}+k_4-1}\Big[\lambda+u_0+u_1\,(1+u_0)+u_2(1+u_0)(1+u_1)\Big]^{-\left(\frac{a+v_0+v_1+v_2}{2}+k_1+k_2+k_3+k_4\right)} du_2\ .$$

Take note:

$$\int_0^\infty u_2^{\frac{v_2}{2}+k_4-1}\Big[\lambda+u_0+u_1(1+u_0)+u_2(1+u_0)(1+u_1)\Big]^{-\left(\frac{a+v_0+v_1+v_2}{2}+k_1+k_2+k_3+k_4\right)} du_2$$

$$= \Big[\lambda+u_0+u_1(1+u_0)\Big]^{-\left(\frac{a+v_0+v_1+v_2}{2}+k_1+k_2+k_3+k_4\right)}$$

$$\times\int_0^\infty u_2^{\frac{v_2}{2}+k_4-1}\left[1+\frac{u_2(1+u_0)(1+u_1)}{\lambda+u_0+u_1\,(1+u_0)}\right]^{-\left(\frac{a+v_0+v_1+v_2}{2}+k_1+k_2+k_3+k_4\right)} du_2\ .$$

Using Gradshteyn and Ryzhik (2007) Eq. 3.194.3 p. 315, the joint density of U_0 and U_1 in expression (3.2) follows after simplification.

Remark 3.2.

(**i**) Alternatively, the proof of this theorem can be derived by substituting $p=1$ in (4.1).

(**ii**) If $\delta_a=\delta_0=\delta_1=0$, the density simplifies to the bivariate distribution derived by Adamski *et al.* (2012):

$$
\begin{aligned}
&f(u_0,u_1)\\
={}& \frac{\lambda^{\frac{a}{2}}\Gamma\left(\frac{a+v_0+v_1}{2}\right)}{\Gamma(\frac{a}{2})\Gamma(\frac{v_0}{2})\Gamma(\frac{v_1}{2})}u_0^{\frac{v_0}{2}-1}\left(1+u_0\right)^{-\left(\frac{a+v_0}{2}\right)}u_1^{\frac{v_1}{2}-1}\left(1+u_1\right)^{-\left(\frac{a+v_0+v_1}{2}\right)}\\
&\times\left[\frac{\lambda+u_0+u_1(1+u_0)}{(1+u_0)(1+u_1)}\right]^{-\left(\frac{a+v_0+v_1}{2}\right)}.
\end{aligned}
$$

This can be rewritten using the binomial series ${}_1F_0(\alpha;z)=(1-z)^{-\alpha}$, for $|z|<1$ (Mathai (1993) p. 25) with $1-z=\frac{\lambda+u_0+u_1(1+u_0)}{(1+u_0)(1+u_1)}$. Therefore

$$
\begin{aligned}
&f(u_0,u_1)\\
={}& \frac{\Gamma(\frac{a+v_0+v_1}{2})\lambda^{\frac{a}{2}}}{\Gamma(\frac{a}{2})\Gamma(\frac{v_0}{2})\Gamma(\frac{v_1}{2})}u_0^{\frac{v_0}{2}-1}\left(1+u_0\right)^{-\left(\frac{a+v_0}{2}\right)}u_1^{\frac{v_1}{2}-1}\left(1+u_1\right)^{-\left(\frac{a+v_0+v_1}{2}\right)}\\
&\times\ {}_1F_0\left(\frac{a+v_0+v_1}{2};\frac{1-\lambda}{(1+u_0)(1+u_1)}\right).
\end{aligned}
$$

(**b**) Expanding $\Psi_2^{(4)}(\cdot)$ in equation (3.1) in series form and integrating the trivariate density (3.1) with respect to u_1, it follows that

$$
\begin{aligned}
&f(u_0,u_2)\\
={}& \frac{e^{-\left(\frac{\delta_a+\delta_0+\delta_1+\delta_2}{2}\right)}\lambda^{\frac{a}{2}}\,\Gamma\left(\frac{a+v_0+v_1+v_2}{2}\right)}{\Gamma(\frac{a}{2})\Gamma(\frac{v_0}{2})\Gamma(\frac{v_1}{2})\Gamma(\frac{v_2}{2})}\;u_0^{\frac{v_0}{2}-1}\left(1+u_0\right)^{\frac{v_1+v_2}{2}}u_2^{\frac{v_2}{2}-1}\\
&\times\sum_{k_1=0}^{\infty}\sum_{k_2=0}^{\infty}\sum_{k_3=0}^{\infty}\sum_{k_4=0}^{\infty}\frac{\left(\frac{a+v_0+v_1+v_2}{2}\right)_{k_1+k_2+k_3+k_4}}{\left(\frac{a}{2}\right)_{k_1}\left(\frac{v_0}{2}\right)_{k_2}\left(\frac{v_1}{2}\right)_{k_3}\left(\frac{v_2}{2}\right)_{k_4}k_1!k_2!k_3!k_4!}\left(\frac{\lambda\delta_a}{2}\right)^{k_1}\left(\frac{\delta_0u_0}{2}\right)^{k_2}\\
&\times\left(\frac{\delta_1(1+u_0)}{2}\right)^{k_3}\left(\frac{\delta_2u_2(1+u_0)}{2}\right)^{k_4}\int_0^{\infty}u_1^{\frac{v_1}{2}+k_3-1}\left(1+u_1\right)^{\frac{v_2}{2}+k_4}\\
&\times\Big[\lambda+u_0+u_1\left(1+u_0\right)+u_2(1+u_0)(1+u_1)\Big]^{-\left(\frac{a+v_0+v_1+v_2}{2}+k_1+k_2+k_3+k_4\right)}du_1\,.
\end{aligned}
$$

Using Gradshteyn and Ryzhik (2007) Eq. 3.197.5 p. 317 and Eq. 9.131.1 p. 998, it follows that

$$
\begin{aligned}
f(u_0,u_2)={}&\frac{e^{-\left(\frac{\delta_a+\delta_0+\delta_1+\delta_2}{2}\right)}\lambda^{\frac{a}{2}}\,\Gamma\left(\frac{a+v_0+v_1+v_2}{2}\right)}{\Gamma(\frac{a}{2})\Gamma(\frac{v_0}{2})\Gamma(\frac{v_1}{2})\Gamma(\frac{v_2}{2})}\;u_0^{\frac{v_0}{2}-1}\left(1+u_0\right)^{\frac{v_1+v_2}{2}}u_2^{\frac{v_2}{2}-1}\\
&\times\sum_{k_1=0}^{\infty}\sum_{k_2=0}^{\infty}\sum_{k_3=0}^{\infty}\sum_{k_4=0}^{\infty}\frac{\left(\frac{a+v_0+v_1+v_2}{2}\right)_{k_1+k_2+k_3+k_4}}{\left(\frac{a}{2}\right)_{k_1}\left(\frac{v_0}{2}\right)_{k_2}\left(\frac{v_1}{2}\right)_{k_3}\left(\frac{v_2}{2}\right)_{k_4}k_1!k_2!k_3!k_4!}\\
&\times\left(\frac{\lambda\delta_a}{2(1+u_0)(1+u_2)}\right)^{k_1}\left(\frac{\delta_0u_0}{2(1+u_0)(1+u_2)}\right)^{k_2}\left(\frac{\delta_1(1+u_0)}{2(1+u_0)(1+u_2)}\right)^{k_3}
\end{aligned}
$$

$$\times \left(\tfrac{\delta_2 u_2(1+u_0)}{2(1+u_0)(1+u_2)}\right)^{k_4} \frac{\Gamma\left(\frac{v_1}{2}+k_3\right)\Gamma\left(\frac{a+v_0}{2}+k_1+k_2\right)}{\Gamma\left(\frac{a+v_0+v_1}{2}+k_1+k_2+k_3\right)} \left[(1+u_0)(1+u_2)\right]^{-\left(\frac{a+v_0+v_1+v_2}{2}\right)}$$

$$\times\, {}_2F_1\!\left(\tfrac{a+v_0+v_1+v_2}{2}+k_1+k_2+k_3+k_4, \tfrac{a+v_0}{2}+k_1+k_2; \tfrac{a+v_0+v_1}{2}+k_1+k_2+k_3; \tfrac{1-\lambda}{(1+u_0)(1+u_2)}\right).$$

Expanding the Gauss hypergeometric function, ${}_2F_1(\cdot)$ (see Gradshteyn and Ryzhik (2007)), in series form, the desired result (3.3) follows after simplification.

(**c**) Proof follows similarly as in (b). □

3.2. Univariate cases

Theorem 3.3. *Let X, W_i with $i = 0, 1, 2$ be independent noncentral chi-squared random variables with degrees of freedom a and v_i and noncentrality parameters δ_a and δ_i with $i = 0, 1, 2$, respectively. Let $U_0 = \frac{\lambda W_0}{X}$, $U_1 = \frac{\lambda W_1}{X+\lambda W_0}$ and $U_2 = \frac{\lambda W_2}{X+\lambda W_0+\lambda W_1}$ and $\lambda > 0$. The marginal density of*

(**a**) *U_0 is given by*

$$f(u_0) = \frac{e^{-\left(\frac{\delta_a+\delta_0}{2}\right)}\lambda^{\frac{a}{2}}\Gamma\left(\frac{a+v_0}{2}\right)}{\Gamma(\frac{a}{2})\Gamma(\frac{v_0}{2})} u_0^{\frac{v_0}{2}-1} (u_0+\lambda)^{-\left(\frac{a+v_0}{2}\right)} \times \Psi_2\left(\frac{a+v_0}{2}; \frac{a}{2}, \frac{v_0}{2}; \frac{\lambda\delta_a}{2(u_0+\lambda)}, \frac{\delta_0 u_0}{2(u_0+\lambda)}\right), \qquad u_0 > 0\,, \tag{3.5}$$

with Ψ_2 the Humbert confluent hypergeometric function of two variables (see Sanchez et al. (2006)),

(**b**) *U_1 is given by*

$$f(u_1) = \frac{e^{-\left(\frac{\delta_a+\delta_0+\delta_1}{2}\right)}\lambda^{\frac{a}{2}}\Gamma\left(\frac{a+v_0+v_1}{2}\right)}{\Gamma(\frac{v_1}{2})\Gamma\left(\frac{a+v_0}{2}\right)} u_1^{\frac{v_1}{2}-1} (1+u_1)^{-\left(\frac{a+v_0+v_1}{2}\right)} \times \sum_{k_1=0}^{\infty}\sum_{k_2=0}^{\infty}\sum_{k_3=0}^{\infty}\sum_{k_4=0}^{\infty} \frac{\left(\frac{a+v_0+v_1}{2}\right)_{k_1+k_2+k_3+k_4}\left(\frac{a}{2}\right)_{k_1+k_4}}{\left(\frac{a}{2}\right)_{k_1}\left(\frac{v_1}{2}\right)_{k_3}\left(\frac{a+v_0}{2}\right)_{k_1+k_2+k_4} k_1!k_2!k_3!k_4!} \times \left(\frac{\lambda\delta_a}{2(1+u_1)}\right)^{k_1}\left(\frac{\delta_0}{2(1+u_1)}\right)^{k_2}\left(\frac{\delta_1 u_1}{2(1+u_1)}\right)^{k_3}\left(\frac{1-\lambda}{(1+u_1)}\right)^{k_4}, \qquad u_1 > 0\,, \tag{3.6}$$

(**c**) *U_2 is given by*

$$
\begin{aligned}
f(u_2) \;=\; & \frac{e^{-\left(\frac{\delta_a+\delta_0+\delta_1+\delta_2}{2}\right)}\lambda^{\frac{a}{2}}\,\Gamma\left(\frac{a+v_0+v_1+v_2}{2}\right)}{\Gamma(\frac{v_2}{2})\Gamma\left(\frac{a+v_0+v_1}{2}\right)}\; u_2^{\frac{v_2}{2}-1}(1+u_2)^{-\left(\frac{a+v_0+v_1+v_2}{2}\right)} \\
& \times \sum_{k_1=0}^{\infty}\sum_{k_2=0}^{\infty}\sum_{k_3=0}^{\infty}\sum_{k_4=0}^{\infty}\sum_{k_5=0}^{\infty} \frac{\left(\frac{a+v_0+v_1+v_2}{2}\right)_{k_1+k_2+k_3+k_4+k_5}\left(\frac{a}{2}\right)_{k_1+k_5}}{\left(\frac{a}{2}\right)_{k_1}\left(\frac{v_2}{2}\right)_{k_4}\left(\frac{a+v_0+v_1}{2}\right)_{k_1+k_2+k_3+k_5}\,k_1!k_2!k_3!k_4!k_5!} \qquad (3.7)\\
& \times \left(\frac{\lambda\delta_a}{2(1+u_2)}\right)^{k_1}\left(\frac{\delta_0}{2(1+u_2)}\right)^{k_2}\left(\frac{\delta_1}{2(1+u_2)}\right)^{k_3}\left(\frac{\delta_2 u_2}{2(1+u_2)}\right)^{k_4}\left(\frac{1-\lambda}{(1+u_2)}\right)^{k_5}, \\
& \hfill u_2>0\,.
\end{aligned}
$$

Proof: (**a**) Using Gradshteyn and Ryzhik (2007) Eq. 3.194.3 p. 315, the result (3.5) follows after simplification.

Remark 3.3. If $\delta_a = \delta_0 = 0$, the density simplifies to the univariate distribution derived by Adamski *et al.* (2012), namely

$$
f(u_0) \;=\; \frac{\lambda^{\frac{a}{2}}\,\Gamma\left(\frac{a+v_0}{2}\right)}{\Gamma\left(\frac{a}{2}\right)\Gamma\left(\frac{v_0}{2}\right)}\; u_0^{\frac{v_0}{2}-1}(u_0+\lambda)^{-\left(\frac{a+v_0}{2}\right)}\,.
$$

(**b**) Using the definition of the beta type II integral function (see Prudnikov *et al.* (1986) Eq. 2.2.4(24) p. 298) yields the desired result.

(**c**) Proof follows similarly as in (b). □

4. MULTIVARIATE EXTENSION

In this section the noncentral generalized multivariate beta type II distribution is proposed.

Theorem 4.1. *Let X, W_i with $i = 0, 1, 2, ..., p$ be independent noncentral chi-squared random variables with degrees of freedom a and v_i and noncentrality parameters δ_a and δ_i with $i = 0, 1, 2, ..., p$, respectively. Let $U_0 = \frac{\lambda W_0}{X}$, and $U_j = \frac{\lambda W_j}{X+\lambda\sum_{k=0}^{j-1}W_k}$ where $j = 1, 2, ..., p$, and $\lambda > 0$. The joint density of $(U_0, U_1, ..., U_p)$*

is given by

$$
\begin{aligned}
& f\left(u_0, u_1, ..., u_p\right) \\
&= \frac{e^{-\left(\frac{\delta_a+\delta_0+\delta_1+\ldots+\delta_p}{2}\right)}\Gamma\left(\frac{a}{2}+\sum\limits_{j=0}^{p}\frac{v_j}{2}\right)\lambda^{\frac{a}{2}}}{\Gamma\left(\frac{a}{2}\right)\Gamma\left(\frac{v_0}{2}\right)\cdots\Gamma\left(\frac{v_p}{2}\right)} \left(\prod_{j=0}^{p} u_j^{\frac{v_j}{2}-1}\right)\left(\prod_{k=0}^{p-1}\left(1+u_k\right)^{\sum\limits_{j=k+1}^{p}\frac{v_j}{2}}\right) \\
& \times\left(\lambda+u_0+\sum_{j=1}^{p}u_j\prod_{k=0}^{j-1}\left(1+u_k\right)\right)^{-\left(\frac{a}{2}+\sum\limits_{j=0}^{p}\frac{v_j}{2}\right)} \\
& \times\Psi_2^{(p+2)}\left[\frac{a}{2}+\sum_{j=0}^{p}\frac{v_j}{2};\frac{a}{2},\frac{v_0}{2},...,\frac{v_p}{2};\frac{\lambda\delta_a}{2z},\frac{\delta_0u_0}{2z},\frac{\delta_1u_1(1+u_0)}{2z},...,\frac{\delta_pu_p\prod\limits_{k=0}^{j-1}(1+u_k)}{2z}\right], \\
& \qquad\qquad u_j>0,\quad j=1,2,...,p\ ,
\end{aligned}
\tag{4.1}
$$

where $z=\lambda+u_0+\sum\limits_{j=1}^{p}u_j\prod\limits_{k=0}^{j-1}\left(1+u_k\right)$ *and* $\Psi_2^{(p+2)}$ *the confluent hypergeometric function in* $p+2$ *variables.*

Proof: The joint density of $X, W_0, W_1, ..., W_p$ is

$$
\begin{aligned}
& f\left(x, w_0, w_1, ..., w_p\right) \\
&= \frac{e^{-\left(\frac{\delta_a+\delta_0+\delta_1+\ldots+\delta_p}{2}\right)}}{2^{\frac{a+v_0+\ldots+v_p}{2}}\Gamma\left(\frac{a}{2}\right)\Gamma\left(\frac{v_0}{2}\right)\cdots\Gamma\left(\frac{v_p}{2}\right)}\ {}_0F_1\left(\tfrac{a}{2};\tfrac{\delta_a x}{4}\right)\ {}_0F_1\left(\frac{v_0}{2};\frac{\delta_0w_0}{4}\right)\ {}_0F_1\left(\frac{v_1}{2};\frac{\delta_1w_1}{4}\right) \\
& \times\ {}_0F_1\left(\frac{v_2}{2};\frac{\delta_2w_2}{4}\right)\cdots\ {}_0F_1\left(\frac{v_p}{2};\frac{\delta_pw_p}{4}\right) \\
& \times\ x^{\frac{a}{2}-1}w_0^{\frac{v_0}{2}-1}w_1^{\frac{v_1}{2}-1}w_2^{\frac{v_2}{2}-1}\cdots w_p^{\frac{v_p}{2}-1}e^{-\frac{1}{2}\left(x+w_0+w_1+w_2+\ldots+w_p\right)}
\end{aligned}
$$

where ${}_0F_1\left(a;z\right)=\sum\limits_{j=0}^{\infty}\frac{\Gamma(a)}{\Gamma(a+j)}\frac{z^j}{j!}=\sum\limits_{j=0}^{\infty}\frac{z^j}{(a)_jj!}$ where $\left(\alpha\right)_j$ is the Pochhammer coefficient defined as $\left(\alpha\right)_j=\alpha\left(\alpha+1\right)\cdots\left(\alpha+j-1\right)=\frac{\Gamma(\alpha+j)}{\Gamma(\alpha)}$ (see Johnson *et al.* (1995), Chapter 1).

Let $U=X$, $U_0=\frac{\lambda W_0}{X}$ and $U_j=\frac{\lambda W_j}{X+\lambda\sum_{k=0}^{j-1}W_k}$ where $j=1,2,...,p$.

This gives the inverse transformation: $X=U$, $W_0=\frac{1}{\lambda}U_0U$ and $W_j=\frac{1}{\lambda}U_j\left(U+\lambda\sum_{k=0}^{j-1}W_k\right)=\frac{1}{\lambda}U_jU\prod_{k=0}^{j-1}\left(1+U_k\right)$ where $j=1,2,...,p$, with Jacobian

$$J\left(x,w_0,..,w_p\rightarrow u,u_0,..,u_p\right)=\frac{u}{\lambda}\prod_{j=1}^{p}\frac{u\prod\limits_{k=0}^{j-1}(1+u_k)}{\lambda}=\left(\frac{u}{\lambda}\right)^{p+1}\prod_{k=0}^{p-1}\left(1+u_k\right)^{p-k}.$$

Thus, the joint density of $U, U_0, U_1, ..., U_p$ is

$$\begin{aligned} f\left(u, u_0, .., u_p\right) &= \frac{e^{-\left(\frac{\delta_a+\delta_0+\delta_1+...+\delta_p}{2}\right)} \lambda^{\left(-\sum\limits_{j=0}^{p} \frac{v_j}{2}\right)}}{2^{\frac{a+v_0+...+v_p}{2}} \Gamma(\frac{a}{2})\Gamma(\frac{v_0}{2})...\Gamma(\frac{v_p}{2})} \, {}_0F_1\left(\tfrac{a}{2}; \tfrac{\delta_a u}{4}\right) \, {}_0F_1\left(\tfrac{v_0}{2}; \tfrac{\delta_0 u_0 u}{4\lambda}\right) \\ &\times \left(\prod_{j=1}^{p} {}_0F_1\left(\frac{v_j}{2}; \frac{\delta_j u_j u \prod\limits_{k=0}^{j-1}(1+u_k)}{4\lambda}\right)\right) u^{\frac{a}{2}+\sum\limits_{j=0}^{p}\frac{v_j}{2}-1} u_0^{\frac{v_0}{2}-1} \left(\prod_{j=1}^{p} u_j^{\frac{v_j}{2}-1}\right) \\ &\times \left(\prod_{k=0}^{p-1} (1+u_k)^{\sum\limits_{j=k+1}^{p} \frac{v_j}{2}}\right) e^{-\frac{u}{2}\left(1+\frac{u_0}{\lambda}+\sum\limits_{j=1}^{p}\frac{u_j}{\lambda}\prod\limits_{k=0}^{j-1}(1+u_k)\right)} . \end{aligned}$$

Note that $\prod_{j=1}^{p} \left[\prod_{k=0}^{j-1} (1+u_k)\right]^{\frac{v_j}{2}-1} = \prod_{k=0}^{p-1} (1+u_k)^{\sum_{j=k+1}^{p} \frac{v_j}{2}-(p-k)}$. Expanding the ${}_0F_1(\cdot)$ expressions in series form, integrating with respect to u and using the definition of the gamma integral function (see Prudnikov *et al.* (1986) Eq. 2.3.3(1), p. 322) yields the result (4.1). □

Remark 4.1. If $\delta_a = \delta_0 = \delta_1 = ... = \delta_p = 0$, the distribution with density given in (4.1) simplifies to the multivariate distribution derived by Adamski *et al.* (2012)

$$\begin{aligned} f\left(u_0, u_1, ..., u_p\right) &= \frac{\Gamma\left(\frac{a}{2}+\sum\limits_{j=0}^{p}\frac{v_j}{2}\right)\lambda^{\frac{a}{2}}}{\Gamma(\frac{a}{2})\Gamma(\frac{v_0}{2})...\Gamma(\frac{v_p}{2})} \left(\prod_{j=0}^{p} u_j^{\frac{v_j}{2}-1}\right) \left(\prod_{k=0}^{p-1} (1+u_k)^{\sum\limits_{j=k+1}^{p}\frac{v_j}{2}}\right) \\ &\times \left(\lambda + u_0 + \sum_{j=1}^{p} u_j \prod_{k=0}^{j-1} (1+u_k)\right)^{-\left(\frac{a}{2}+\sum\limits_{j=0}^{p}\frac{v_j}{2}\right)} . \end{aligned}$$

5. SHAPE ANALYSIS

In this section the shape of the univariate and bivariate marginal densities will be illustrated and the influence of the noncentrality parameters will be investigated.

Panels (i) and (ii) of Figure 2 illustrate the effect of the noncentrality parameters δ_a and δ_0 on the univariate marginal density of U_0 (see equation (3.5)).

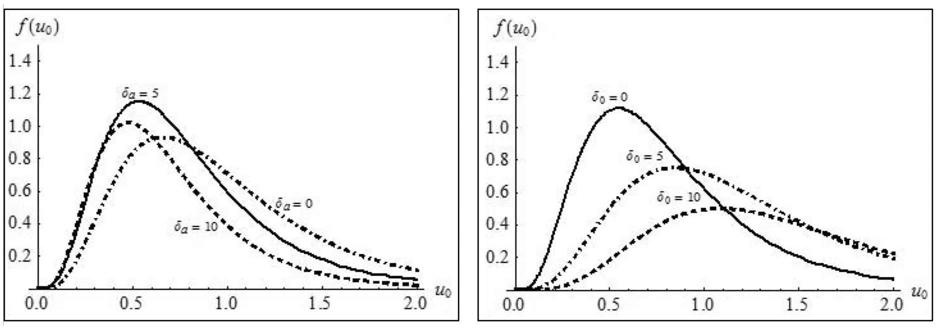

(**i**) Role of δ_a for $\delta_0 = 2$.

(**ii**) Role of δ_0 for $\delta_a = 0$.

Figure 2: The marginal density function for different values of the parameters δ_a and δ_0 for $\lambda = 1.5$, $\kappa = 3$, $a = 20$ and $\nu_0 = 10$.

In terms of the process control application the parameters can be interpreted as follows:

a: pooled number of observations before the shift in the unknown variance took place,

v_0: sample size at time period κ, the first sample following the shift in the variance; the shift in the variance took place between samples $\kappa - 1$ and κ,

δ_a: noncentrality parameter that quantifies the change in the mean before the change in the variance took place,

[Take note: if the mean and variance changes simultaneously, then $\delta_a = 0$.]

δ_0: noncentrality parameter that quantifies the change in the mean after the change in the variance took place,

λ: size of the unknown shift in the variance.

Panel (i) shows the effect of δ_a; we observe that as δ_a increases the density initially moves towards the vertical axis and then towards the horizontal axis. In panel (ii) the density moves towards the horizontal axis for bigger values of δ_0. The influence of the parameters a, v_0 and λ on the marginal density is discussed in detail in Adamski *et al.* (2012).

Panels (i) to (iv) of Figure 3 illustrate the effect of the noncentrality parameters δ_a, δ_0 and δ_1 on the bivariate density of U_0, U_1 (see equation (3.2)) for $\lambda = 1.5$, $\kappa = 3$, $a = 20$, $v_0 = v_1 = 10$. For $\lambda < 1$ the pattern is similar. The effect of λ is addressed in Adamski *et al.* (2012).

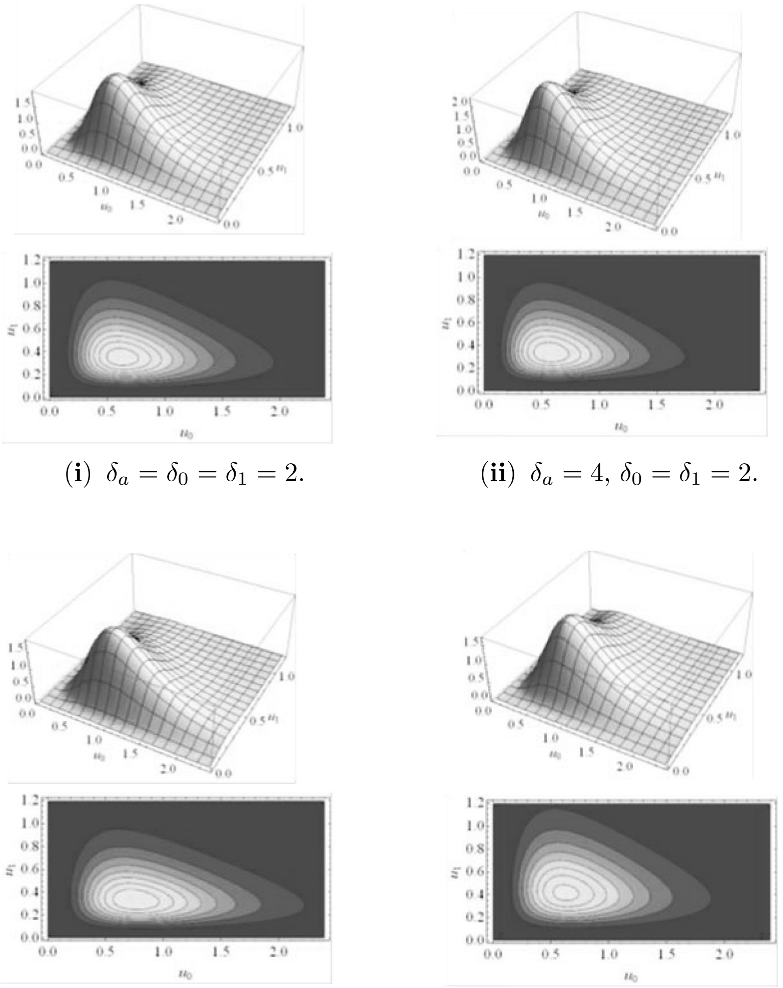

(i) $\delta_a = \delta_0 = \delta_1 = 2$.

(ii) $\delta_a = 4$, $\delta_0 = \delta_1 = 2$.

(iii) $\delta_a = 2$, $\delta_0 = 4$, $\delta_1 = 2$.

(iv) $\delta_a = \delta_0 = 2$, $\delta_1 = 4$.

Figure 3: The bivariate density of U_0, U_1.

6. PROBABILITY CALCULATIONS

A practical example (based on simulated data) of calculating the probability that a control chart will signal after the process variance and mean encountered a sustained shift, is considered.

At time period κ the plotting statistic for the Q-chart is constructed by calculating the statistic $U_0^* = \frac{S_\kappa^2}{S_{\kappa-1}^{2pooled}}$, transforming this statistic to obtain a standard normal random variable, denoted $Q\left(U_0^*\right)$ and plotting $Q\left(U_0^*\right)$ on a Shewhart-type chart where the control limits are $UCL/LCL = \pm 3$ and the centerline is $CL = 0$ (see Human and Chakraborti (2010)). When transforming the statistic to a normal random variable, Q-charts make use of the classical probability integral transformation theorem (see Quesenberry (1991)).

The marginal density of U_0 can be used to determine the probability of detecting the shift in the process variance immediately, i.e. when collecting the first sample after the shift took place. Once a shift in the process parameter occurred, the run-length is the number of samples collected from time κ (i.e. first sample after the change) until an out-of-control signal is observed (i.e. a plotting statistic plots on or outside the control limits). The discrete random variable defining the run-length is called the run-length random variable and typically denoted by N. The distribution of N is called the run-length distribution. The probability of detecting a shift immediately, in other words, the probability of a run-length of one, is the likelihood that a signal is obtained at time κ. The probability that the run-length is one, is one minus the probability that the random variable, U_0^*, plots between the control limits,

$$\text{(6.1)} \qquad \Pr(N=1) \;=\; 1-\int_{LCL}^{UCL} f(u_0^*)\,du_0^* \;=\; 1-\int_{LCL_\kappa}^{UCL_\kappa} f(u_0)\,du_0 \;.$$

Take note that the difference between the random variables U_0^* and U_0 (refer to the definitions on page 7 and 8 of the introduction) will be incorporated in the control limits of the control chart.

When the process is in-control, i.e. $\lambda = 1$ and the process mean did not encounter a shift, $U_0^* = \dfrac{W_0/n_\kappa}{X/\sum_{i=1}^{\kappa-1} n_i} \sim F\left(n_\kappa, \sum_{i=1}^{\kappa-1} n_i\right)$, then the Q plotting statistic is given by $Q\left(U_0^*\right) = \Phi^{-1}\left[F\left(U_0^*\right)\right]$ and the control limits UCL_κ and LCL_κ are determined as follows:

$$\begin{array}{rrcl}
 & -3 < & \Phi^{-1}\left[F\left(U_0^*\right)\right] & < 3 \\
\Longleftrightarrow & \Phi(-3) < & F\left(U_0^*\right) & < \Phi(3) \\
\Longleftrightarrow & F^{-1}\left[\Phi(-3)\right] < & U_0^* & < F^{-1}\left[\Phi(3)\right] \\
\Longleftrightarrow & \dfrac{F^{-1}\left[\Phi(-3)\right]}{\frac{\sum_{i=1}^{\kappa-1} n_i}{n_\kappa}} < & U_0 & < \dfrac{F^{-1}\left[\Phi(3)\right]}{\frac{\sum_{i=1}^{\kappa-1} n_i}{n_\kappa}}
\end{array}$$

where

$F(\cdot)$ denotes the cumulative distribution function of the F distribution,

$F^{-1}(\cdot)$ denotes the inverse of the cumulative distribution function of the F distribution,

$\Phi(\cdot)$ denotes the standard normal cumulative distribution function,

$\Phi^{-1}(\cdot)$ denotes the inverse of the standard normal cumulative distribution function.

Therefore $UCL_\kappa = \frac{F^{-1}[\Phi(3)]}{\frac{\sum_{i=1}^{\kappa-1} n_i}{n_\kappa}}$ and $LCL_\kappa = \frac{F^{-1}[\Phi(-3)]}{\frac{\sum_{i=1}^{\kappa-1} n_i}{n_\kappa}}$. Note that LCL_κ and UCL_κ depend on κ whereas LCL and UCL equals -3 and 3, respectively (regardless the value of κ).

The probability that the run-length is two can be calculated by defining the following two events:

Let $A = \{LCL_\kappa < U_0 < UCL_\kappa\}$ and $B = \{LCL_{\kappa+1} < U_1 < UCL_{\kappa+1}\}$. Then,

$$\begin{aligned} \text{(6.2)} \qquad \Pr(N\!=\!2) &= \Pr(A \cap B^C) \;=\; \Pr(A) - \Pr(A \cap B) \\ &= \int_{LCL_\kappa}^{UCL_\kappa} f(u_0)\, du_0 \;-\; \int_{LCL_{\kappa+1}}^{UCL_{\kappa+1}} \int_{LCL_\kappa}^{UCL_\kappa} f(u_0, u_1)\, du_0\, du_1 \;. \end{aligned}$$

The run-length probabilities for higher values of N can be calculated in a similar fashion.

Consider the following data set to illustrate the control chart and the use of the proposed density functions to determine the run-length probabilities. Twenty samples of size 5 were generated. The first 10 samples were generated from a $N(10,1)$ distribution. Between samples 10 and 11 the process mean and variance encountered a sustained shift, therefore the last 10 samples were generated from a $N(11.5, 1.5)$ distribution. Take note that when calculating the sample variance, the practitioner is unaware of the change in the mean. The simulated data set is given in Table 1 and the control chart in Figure 4. Note that there is no plotting

Table 1: Simulated data set.

Sample (i)	X_{i1}	X_{i2}	X_{i3}	X_{i4}	X_{i5}	Sample variance	U_i^*	Plotting statistic
1	9.672	10.328	9.061	9.606	10.471	0.295	NA	NA
2	12.064	10.689	10.332	8.618	9.949	1.352	4.581	−1.553
3	10.085	10.603	9.986	9.634	10.866	0.251	0.305	1.276
4	8.653	9.371	8.830	10.893	11.324	1.226	1.940	−1.049
5	10.187	9.001	9.234	10.266	8.701	0.676	0.865	0.054
6	9.560	10.738	10.617	8.831	12.225	1.487	1.957	−1.173
7	8.387	11.668	9.590	10.064	9.204	1.238	1.405	−0.672
8	11.194	9.137	7.822	10.723	11.034	1.701	1.825	−1.110
9	10.181	10.413	11.128	10.890	8.524	0.889	0.865	0.033
10	10.761	9.953	11.530	9.330	10.034	0.674	0.666	0.388
11	11.175	11.963	13.257	12.327	13.857	7.227	7.382	−4.012
12	12.850	12.132	11.727	10.362	11.309	3.499	2.262	−1.548
13	9.964	12.275	10.585	11.670	11.529	2.129	1.245	−0.525
14	11.955	11.450	12.625	11.627	11.306	3.434	1.971	−1.312
15	11.981	12.890	11.306	11.725	9.372	3.470	1.863	−1.216
16	10.184	8.689	11.045	11.428	11.687	1.546	0.785	0.160
17	10.651	10.974	10.282	11.372	9.324	0.758	0.390	1.055
18	10.375	12.098	10.711	11.556	9.884	1.496	0.799	0.134
19	10.480	11.489	12.726	12.910	10.191	3.677	1.984	−1.350
20	12.701	11.517	10.126	11.659	11.727	3.069	1.575	−0.936

statistic that corresponds to sample number / time 1 as this sample is used to obtain an initial estimate of the process variance. The process is effectively monitored from sample 2 onwards. This process is declared out-of-control at sample number 11 since this is the first sample where a plotting statistic plots on or outside the control limits.

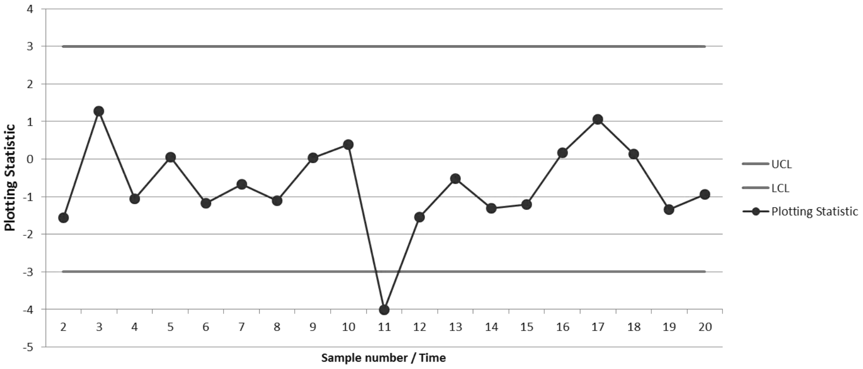

Figure 4: Control chart.

The software package Mathematica was used to calculate the probabilities by using the summation form of the Humbert function in equation (3.5). Based on the information of the simulated data set, we have (i) $v_i = n_i = n = 5$ (equal sample sizes at each point in time), (ii) $\kappa = 11$, (iii) $\delta_a = 0$ (i.e. the mean and variance changed simultaneously between sample number 10 and 11), (iv) $\delta_0 = 5$ and (v) $\lambda = 1.5$. The probability of detecting the shift in the process variance immediately at time period 11 is calculated using (6.1):

$$\begin{aligned}\Pr(N=1) &= 1 - \int_{LCL_{\kappa=11}}^{UCL_{\kappa=11}} f(u_0)\,du_0 = 1 - \int_{0.004632685}^{0.470157314} f(u_0)\,du_0 \\ &= 0.177224\end{aligned}$$

where

$$\begin{aligned}UCL_{\kappa=11} &= \frac{F_{5,50}^{-1}\left[\Phi\,(3)\right]}{10} = \frac{F_{5,50}^{-1}\left[0.998650102\right]}{10} = \frac{4.701573136}{10} \\ &= 0.470157314\ ,\end{aligned}$$

$$\begin{aligned}LCL_{\kappa=11} &= \frac{F_{5,50}^{-1}\left[\Phi\,(-3)\right]}{10} = \frac{F_{5,50}^{-1}\left[0.001349898\right]}{10} = \frac{0.04632684922}{10} \\ &= 0.004632685\ .\end{aligned}$$

The probability of detecting the shift in the process variance at time period 12 is calculated using (6.2):

$$\begin{aligned}\Pr(N\!=\!2) &= \int_{0.004632685}^{0.470157314} f(u_0)\,du_0 - \int_{0.004221604}^{0.420758373}\int_{0.004632685}^{0.470157314} f(u_0,u_1)\,du_0\,du_1\\ &= 0.090598\ .\end{aligned}$$

These run-length probabilities can then be used to estimate the average run-length (ARL) using the formula $E(N) = ARL = \sum\limits_{k=1}^{\infty} k \Pr(N\!=\!k) \approx \sum\limits_{k=1}^{M} k \Pr(N\!=\!k)$. The accuracy of the ARL estimate will depend on the cut-off M. The probabilities can be evaluated using the multivariate density function in (4.1) or using Monte Carlo simulation. The evaluation of high dimensional multiple integrals become increasingly more complex (i.e. time consuming and resource intensive) as the dimension increases and is beyond the scope of this article.

Table 2 summarises the effect of the different parameters on the probability to detect the shift in the variance immediately.

Table 2: Probabilities for different parameter values.

Role of	δ_a	δ_0	n_i	κ	λ	$\Pr(N\!=\!1)$	Comment
$\lambda = \dfrac{\sigma_1^2}{\sigma^2}$	0	5	5	11	0.5 1 1.5	0.015147 0.048686 0.177224	The larger the step shift, the higher the probability.
κ	0	5	5	3 5 11	1.5	0.057861 0.110475 0.177224	The more historical samples available before the shift took place, the higher the probability.
n	0	5	1 5 10	11	1.5	0.166158 0.177224 0.171251	The larger the sample size, the probability initially increases and then decreases.
δ_0	0	0 2 5	5	11	1.5	0.015941 0.060114 0.177224	The larger δ_0 (i.e. the relative change in the mean), the higher the probability.

7. CONCLUDING REMARKS

Adamski *et al.* (2012) recently introduced a new generalized multivariate beta distribution with density in closed form, where a distribution is needed for the run-length of a Q-chart that monitors the process mean when measurements are from an exponential distribution with unknown parameter. In this paper the distributions are proposed for the case when measurements from each sample are independent and identically distributed normal random variables and we are monitoring the unknown spread when the known mean encountered a sustained shift. We have generalized the proposed model to the multivariate case and we hope that the results presented in this paper will be useful in the Statistical Process Control field.

ACKNOWLEDGMENTS

This work is based upon research supported by the National Research Foundation, South Africa (Grant: FA2007043000003 and the Thuthuka programme: TTK20100707000011868). We also acknowledge the valuable suggestions from Professor Filipe Marques and the anonymous referees whom helped in approving this paper.

REFERENCES

[1] Adamski, K.; Human, S.W. and Bekker, A. (2012). A generalized multivariate beta distribution: control charting when the measurements are from an exponential distribution, *Statistical Papers*, **53**, 1045–1064.

[2] Gradshteyn, I.S. and Ryzhik, I.M. (2007). *Table of Integrals, Series, and Products*, Academic Press, Amsterdam.

[3] Gupta, A.K.; Orozco-Castaneda, J.M. and Nagar, D.K. (2009). Noncentral bivariate beta distribution, *Statistical Papers*, **52**, 139–152.

[4] Human, S.W. and Chakraborti, S. (2010). Q charts for the exponential distribution, *JSM 2010 Proceedings, Section On Quality And Productivity*, Vancouver, British Columbia, Canada.

[5] Johnson, N.L.; Kotz, S. and Balakrishnan, N. (1995). *Continuous Univariate Distributions*, Vol. 2 (second edition), John Wiley & Sons, New York.

[6] Mathai, A.M. (1993). *A Handbook Of Generalized Special Functions For Statistical And Physical Sciences*, Clarendon Press, Oxford.

[7] Montgomery, D.C. (2009). *Statistical Quality Control: A Modern Introduction*, 6th ed., John Wiley, New York.

[8] Quesenberry, C.P. (1991). SPC Q Charts for start-up processes and short or long runs, *Journal Of Quality Technology*, **23**(3), 213–224.

[9] Patnaik, J.H. (1949). The non-central χ^2 and F-distributions and their applications, *Biometrika*, **36**, 202–232.

[10] Pe, T. and Drygas, H. (2006). An alternative representation of noncentral beta and F distributions, *Statistical Papers*, **47**, 311–318.

[11] Prudnikov, A.P.; Brychkov, Y.A. and Marichev, O.I. (1986). *Integrals and Series, Volume I: Elementary Functions*, Gordon and Breach, New York.

[12] Sanchez, L.E. and Nagar, D.K. (2003). Non-central matrix-variate Dirichlet distribution, *Taiwanese Journal Of Mathematics*, **7**(3), 477–491.

[13] Sanchez, L.E.; Nagar, D.K. and Gupta, A.K. (2006). Properties of noncentral Dirichlet distributions, *Computers and Mathematics with Applications*, **52**, 1671–1682.

[14] Srivastava, H.M. and Kashyap, B.R.K. (1982). *Special Functions in Queuing Theory And Related Stochastic Processes*, Academic Press, New York.

[15] Tang, P.C. (1938). The power function of the analysis of variance tests with tables and illustrations of their use, *Statistical Research Memoirs*, **2**, 126–150.

[16] Troskie, C.G. (1967). Noncentral multivariate Dirichlet distributions, *South African Statistical Journal*, **1**, 21–32.

REVSTAT – Statistical Journal
Volume 11, Number 1, March 2013, 45–65

USE OF SURVIVAL MODELS IN A REFINERY

Authors: Sílvia Madeira
– Phd in Mathematics, ECT of University of Évora, Portugal
silvia.madeira@galpenergia.com

Paulo Infante
– CIMA/DMAT, ECT of University of Évora, Portugal
pinfante@uevora.pt

Filipe Didelet
– EST, IPS Setúbal, Portugal
filipe.didelet@estsetubal.ips.pt

Abstract:

- Statistical methods are nowadays increasingly useful in industrial engineering. From plant design reliability to equipment analysis, there is much to cover with statistical models in order to improve the efficiency of systems. At Sines refinery we found it useful to apply a Cox model to a particular critical equipment trying to find process variables that cause its vibration as well as to apply well known distributions to baseline hazard rate.

Key-Words:

- *reliability; maintenance; time between failures; Kaplan–Meier; Cox proportional hazards.*

AMS Subject Classification:

- 62N01, 62P30, 90B25.

1. INTRODUCTION

As industries became more competitive, their methods to improve results are intimately related to efficiency. Although efficiency can be achieved with technology, it only can be reliable based on the fact that the system is prepared for failures, managing them the best way. Failures can be classified as follows: avoided, predictable or inevitable. In each case, knowing equipment behaviour helps companies to manage spare parts, man-hours and maintenance issues that will improve reliability and save money [12]. Reliability studies are then a priority and this work has been written to support decisions based on reliability models and according to standards [8].

Sines refinery has been concerned with the shut-downs made by the Turbo-Expander equipment in the FCC unit (Fluid Catalytic Cracking). As it was having problems due to a vibration failure mode causing FCC unit shut-down since year 2000, it was decided to investigate the origin of the vibration. Expander manufacturers and other entities that have this kind of equipment have investigated this problem as it is a big economical issue for the companies as we can see in [4] and [6]. They highly recommend investigating efficiency in order to detect scaling deposition in expander rotor blades. It is believed that the composition of some particles resulting from process reaction are the key for scaling, not just erosion. On 2011 turnaround, the procedure of changing the expander's rotor and shroud was not complete. Only the rotor was changed. This has caused a slight gap between the shroud and the rotor blades due to shroud erosion. This gap is believed to cause less resistance and then, less particles deposition. However, results of Cox Proportional Hazards [2] [3] demonstrate components in these particles to be linked with high values of expander vibration and with times to failure. In Section 3 we have a brief description of the equipment and contextualization of the subject. In Section 4 we will refer to the goal of this work and variables definition. Then we will present some parametric and non-parametric approaches using Kaplan–Meier estimator and Cox Proportional Hazards in Section 5, and a parametric adjustment to the null model with parametric models. Finally, Section 6 is dedicated to some general considerations of this work.

2. MODELS

Several approaches were tried and reviews for different models were studied, although not all of them could fit on the data and conditions of our study. Cox Proportional Hazards had a strong focus because of its flexibility, but some approaches using Competing Risks Theory as we can see in Fine and Gray [5] or Lunn and McNeil [11] were not possible due the complexity of the system.

As we have both time-dependent and independent events it was very difficult to articulate a model and find covariates that could meet the assumptions needed. Additive interaction used by Li and Chambless [10] was proposed but due to the nature of the data and the way that some covariates are monitored make it impossible to use. We will then use the best possible models to fit our data that meet the required conditions for the assumptions needed.

3. FRAMING AND DEFINITIONS

3.1. Configuration of the FCC Power Recover Unit at Sines refinery

A PRU (Power Recover Unit) is composed of an expander, a main air blower, a turbine, a gear box and a motor/generator which recovers the flue gas from the process to generate energy and steam. At Sines refinery we can find a particular configuration of the PRU as we can see in Figure 1. This configuration

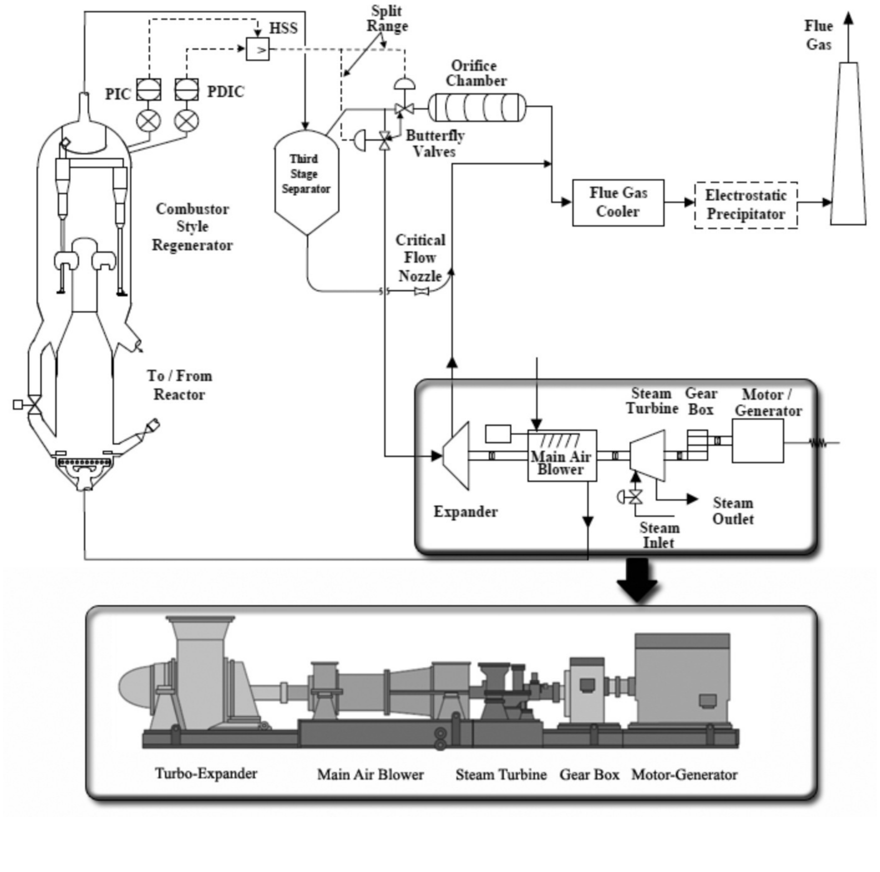

Figure 1: FCC and PRU train.

brings an additional problem to the system. The fact that the expander is coupled with the other equipment leads to unwanted shut-downs of all FCC units whenever the expander has a shut-down. As a shut-down implies high costs, the main goal is to avoid it. Pareto analysis was done on all PRU failure modes so the main failure mode can be easily identified. It was clear that the vibration failure mode was the principal reason for the problems in the expander. Actually, this equipment is supposed to have a reliability of 99%, and its only intrinsic failure is vibration.

3.2. Expander — What is it and how does it work?

The Turbo-Expander (Figure 2) is composed of the nose cone, the rotor blades, the stator ring, the shaft and the casings. Process flue gas reaches the expander rotor blades at a pressure of about 2.1 barg and a temperature of 700° Celsius degrees. The flow at this pressure and temperature is here transformed into mechanical energy, making the rotor blades rotate as well as the shaft at approximately 5700 rpm, held by the steam turbine. This mechanical energy is thus transformed in electrical energy through the generator that is coupled with the expander in the same shaft. In Figure 3 we can see process flue gas come inside the expander casing (grey arrows) that reaches the rotor blades being cooled (white arrow), and then, exhausting through the exhaust casing (black arrows). During this process some particles can set down on the rotor blades.

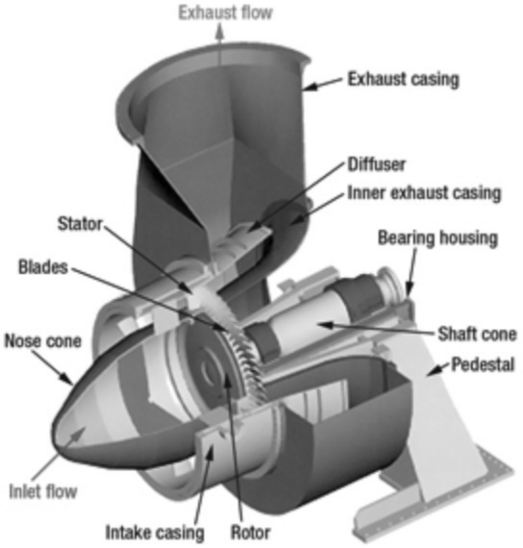

Figure 2: Turbo-Expander.

As deposition may not be uniformly distributed by the blades, it will cause imbalance at high rotation, and thus, cause vibration. The trip value is set to $v\,\mu$m (microns) — where v is a predefined target — and when this value is reached, either the trip (shut-down due to go beyond the threshold values) can occur or operational staff can choose to try to make a controlled shut-down once it is unavoidable.

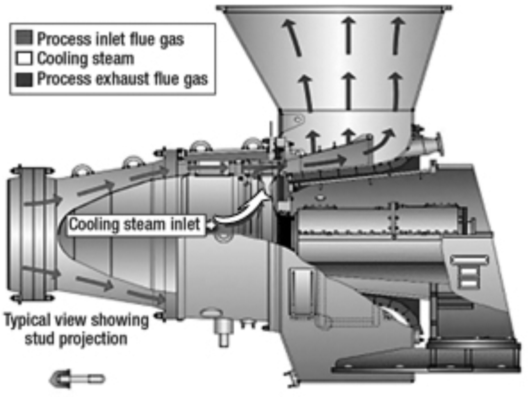
▨ Process inlet flue gas
□ Cooling steam
■ Process exhaust flue gas
Cooling steam inlet
Typical view showing stud projection

Figure 3: Turbo-Expander flue gas flow.

4. TIMES TO EXPANDER VIBRATION FAILURE MODE

In order to investigate the root cause of the problem, all shut-down events were recorded and variables that were suspected to be related with the expander vibration were recorded through the on-line monitoring system of all instrumented variables, since year 2000. There were also concerns with the fact that vibration due to imbalance in the rotor blades caused by deposition can be due to mechanical reasons, chemical reasons, or a combination of both. As flue gas is the product of combustion of coke, compounds that are produced in this reaction can be carried out with flue gas and reach the expander. Tiny particles as well as some chemical combinations that can produce a kind of glue effect can cause deposition. This is a theory supported by the industrial community [4] and the present work has demonstrated some compounds and their characteristics to be important reasons. However, in the past, some internal mechanical damage either in the regenerator and 3$^{\text{rd}}$ stage separator have been shown to be a good reason for particles to easily reach the turbo expander and cause vibration. To explain the reasons that lead to scaling is not the subject of this work, but the fact that it may exist. However, it is important to refer that we have several hypotheses for scaling and none must be rejected.

Reasons for scaling:

a) Erosion combined with more tiny particles can cause deposition;

b) Some chemical compounds combined with each other can act as glue and cause deposition;

c) Vapour is not at the correct temperature/pressure and will cause scaling combined with flue gas particles;

Reasons for high concentrations of tiny particles to reach the expander:

a) Internal damage in the regenerator, or internal damage in the 3rd stage separator.

Internal damage is not easily detected which makes this a major challenge. Scaling can be due a combination of factors that we actually don't know if they are happening or not at the same time. Another problem is that the point of collection of particles for analysis is not immediately before the expander so, in practice, we can only infer what's reaching expander from particles that are being regenerated.

From all possible variables that can influence the system, we have:

Table 1: Variables description.

variable	description	variable	description
vnd	Vanadium (ppm)	*c*	Carbon (%)
ni	Nickel (ppm)	*re*	RE_2O_3 – Rare-earth oxides (%)
fe	Iron (%)	*abd*	Apparent Bulk Density (g/cc)
cu	Copper (ppm)	*alo*	Al_2O_3 Alumina Oxide (%)
pb	Lead (%)	*aps*	Average Particle Size (microns)
na	Sodium (%)	*pv*	Particules' Pore Volume (cc/g)
po	P_2O_5 – Phosphorus Pentoxide (%)	*mat*	Micro activity Test
mgo	MgO – Magnesium Oxide (ppm)	*sa*	Particles' Surface Area (m^2/g)
cf	Coke Factor	*vpb*	Vapour pressure (barg)
gf	Gas factor	*vib*	Vibration Values (microns)
pin	Inlet Pressure (barg)	*car*	Main Air Blower Flow (%)
pout	Exhaust Pressure (barg)	*cr*	Reactor Feedstock (t/h)
tpin	Inlet Temperature (°C)	*bp*	Bypass Valve (%)
tpout	Exhaust Temperature (°C)	*pt*	Particles Size (%)

5. SURVIVAL MODELS

Several approaches were tried to correlate some particles' compounds and attributes as well as with process variables such as temperature, pressure, among others, with times to vibration failures using survival models.

1. First approach — Use the times to expander failure and correlate them with particles' compounds and attributes and with process physical variables. For this, we have recorded all shut-down events since year 2000, censoring those that were not by vibration. Whenever there is a shut-down, a "as good as new condition" is reached for turbo-expander due to the thermal shock produced by equipment cooling.
2. Second approach — Use times to high vibration and correlate them with particles' compounds and attributes and with process physical variables, as high vibration values can end in a shut-down or not. High vibration values are harmful for the equipment, and they may not cause a shut-down but they must be avoided, and are here treated as an event. For this, we have recorded all shut-down events and high vibration values (higher than $v/3\,\mu$m) since year 2000, censoring shut-downs that were not by vibration. Whenever there is a shut-down or a high vibration value and the value drops again after some short time, a good as new condition is considered.

5.1. Kaplan–Meier estimators

First, we have made a non-parametric approach using the Kaplan–Meier estimator [9] (using software R) to obtain the survival curves for times to expander vibration failure mode. As we have right censored data and the intervals between events are typically non uniform, Kaplan–Meier is a good approach.

Let $R(t)$ be the probability that a member from a given population will have a lifetime exceeding t. For a sample of size N from the list of observations, let the observed times until the shut-down of the N sample observations be $t_1 \leq t_2 \leq t_3 \leq \cdots \leq t_n$. Corresponding to each t_i is n_i, the number "at risk" just prior to time t_i, and d_i, the number of shut-downs at time t_i. The Kaplan–Meier estimator is the non-parametric maximum likelihood estimate of $R(t)$. It is a product of the form:

$$\hat{R}(t) = \prod_{t_i<t} \frac{n_i - d_i}{n_i}\;. \tag{5.1}$$

5.1.1. First Approach — Only shut-downs are considered

In these Kaplan–Meier curves for times to expander vibration failure mode, we know that reliability keeps high for values under $v/2\,\mu$m. Therefore, one of the goals here is to predict when vibration values become dangerous and a potential spark for the fast increase in its values. Although reliability never drops below 50% (Figure 4), it is important to find the reasons for the shut-downs as they are an important economical factor.

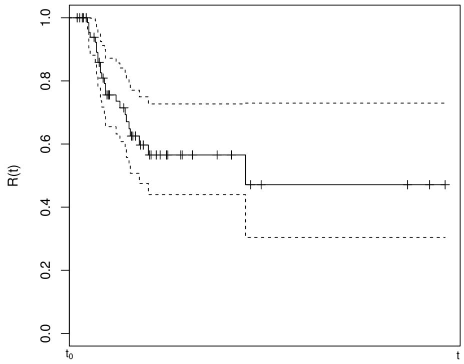

Figure 4: Kaplan–Meier for the null model — Approach 1.

5.1.2. Second Approach — High vibration values are considered

The curve in Figure 5 shows us that high vibration values are recurrent although shut-downs are not. The reliability values quickly decrease and when t_1 is reached, we have less than 50% of reliability for high vibration values.

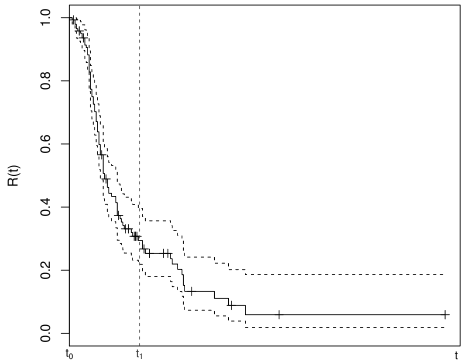

Figure 5: Kaplan–Meier for the null model — Approach 2.

The question here, is that high vibration values can lead to one of two situations: — particles deposited in rotor blades can drop due to imbalance caused by high vibration, or — imbalance can increase as a result of high vibration and get out of control leading to trip vibration values and cause a shut-down. Here is just a matter of "mechanical free will". That's why it is important to check causes for high vibration values.

5.2. Cox Proportional Hazards Model

Survival models were studied, first with a non-parametric approach with Kaplan–Meier, and then, a semi-parametric approach was tried using Cox proportional hazards. Cox model allows analysis of life times in which the outcome variable is the time until the latest event, being censoring or failure, and is characterised by the coefficients (β's) which measure the effects of covariates on the hazard rate:

$$h(t) = h_0(t)\exp\big\{\beta_1 x_1 + \cdots + \beta_p x_p\big\}\,, \tag{5.2}$$

with:

- h_0: baseline hazard rate function;
- $\beta_1, ..., \beta_p$: model parameters;
- $x_1, ..., x_p$: explanatory covariates.

Let Y_i denote the observed time (either censoring time or event time) for observation i, and let C_i be the indicator that the time corresponds to an event (i.e. if $C_i = 1$ the event occurred and if $C_i = 0$ the time is a censoring time, which is, a general shut-down). We used the partial likelihood method for the parameters using Breslow's [1] estimate:

$$L(\beta) = \prod_{i:C_i=1} \frac{\theta_i}{\sum_{j:Y_j\le Y_i}\theta_j}\,, \tag{5.3}$$

with

$$\theta_j = \exp\big\{\hat{\beta}_j\big\} \tag{5.4}$$

As it is a multivariate regression, correlation between covariates must be carefully studied. Once vibration can be consequence of the other covariates, it was not included for now in our models. Models were developed in order to avoid joining correlated covariates, which had a Pearson's correlation value above 0.75 or because experts show us that chemically speaking, when some covariate increases, another one will also increase (or vice-versa). All variables here presented are continuous, and whenever a covariate is as significant as when categorized as when continuous, it will be used in its categorized form, in order to simplify model interpretation. Models adjustments were made according Hosmer and Lemeshow [7] modelling stages.

5.2.1. First Approach — Only shut-downs are considered

Univariate analysis was made to the covariates and those with significance below 25% were considered in the multivariate model. Both forward and backward methods were tested using R software, and the best fit was achieved for each. Because this is a dynamic system, each time there is a shut-down, the event is uploaded to the database and the model is tested again. Some variables were added to the initial tested model because they were shown to be relevant, and have, individually, good explanatory values. However, sometimes when together, they have poor explanatory values. Variable *vib* corresponds to the vibration and shall not be accompanying other variables in the same model due to collinearity. From the possible 28 covariates, only 22, according the criterion of correlation, can be used. Only 10 from these variables are significant at 10%. Choosing only those variables with p-values below 25% of significance and after using backward and forward techniques, only 8 of them were used, and Model 1 was reached as shown in Table 2. Previously, in an initial approach we have used two different models, one for chemical and another one for physical variables, but with the introduction of new variables, this has shown not to be the best solution.

Table 2: Cox model 1.

variable	β	$se(\beta)$	p-value
nix	-3.12	0.88	0.0004
fe	-11.18	5.68	0.0492
sa	0.11	0.03	0.0003
na	-24.01	6.63	0.0003
vpb	0.86	0.36	0.0179
mgo	43.53	20.26	0.0316
cfx	-328.5	97.29	0.0007
tpin	-0.24	0.06	0.0000
cfx:tpin	0.46	0.14	0.0007

62.8% of the variation can be explained by this model, with a concordance value of 0.899 and a likelihood ratio test with a p-value effectively zero. Variable *sa* is the surface area of the particles and seems to be an important variable to take into consideration. This variable explains about 18.4% of data variation in its univariate analysis. An increase in the surface area of the particles means that they are more able to break and produce fine particles, and the increase of one unit of *sa* increases the risk by about 5.5%. Coke factor (*cf*) and vanadium *vnd* are important variables as well as they explain 15% and 11.5% of data variation respectively in the univariate analysis. In Model 1 *sa* has an associated risk of 11.6%. Except for *sa*, *mgo* and *vpb* covariates, all the other covariates that are not in an interaction (*ni*, *fe*, *na*), are indicating that if they are trending downward, the risk will largely increase. We know also that for the increase in one unit of *vpb* the associated risk increases almost 2.5 times keeping the other covariates constant. Magnesium can be a contaminant metal when combined with other components, and makes sense that the increase of one unit will exponentially increase the covariate effect. Variable *cfx* is the categorized variable (0 and 1) for coke factor and the cut-off point used for it was its mean because of its better interpretation, and if it is trending downward it may indicate a higher risk. Inlet temperature *tpin* can be a good monitoring variable for the same reason as *cf*. Coke factor is related with temperature in the regenerator and thus, also with the quantity of contaminant metals, so this interaction makes all sense. Statistically speaking, we can say that for the *cfx* value of 0, the risk will decrease regardless of the value of the inlet temperature (*tpin*), but if the *cfx* value is 1, the risk will increase, with a higher risk (287 times) for inlet temperature values under the 1$^{\text{st}}$ quartile. Also this means that for inlet temperatures above its mean, and when *cfx* goes from 0 to 1, the risk starts to increase as we can see in Figure 6.

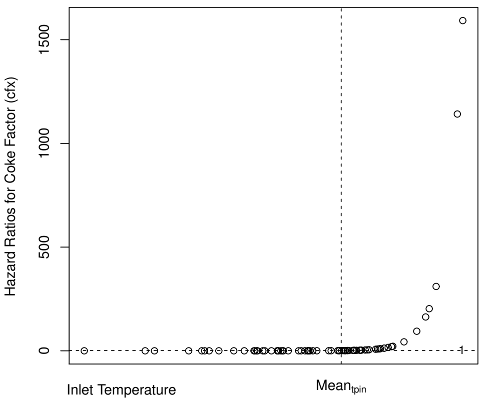

Figure 6: Interaction *cfx:tpin*, *tpin* fixed.

In Figure 7a we have the survival estimates for the quartiles and in Figure 7b we have the Kaplan–Meier estimate of model 1. Model 1 is quite satisfactory, with good results in its residuals analysis, and linear correlation tests were made and they suggest that none of the covariates violate the proportional hazards assumptions (see Appendix A). Realistic possible scenarios can be used and the survival estimates are given for two examples in Figure 8a and Figure 8b. As we can see, when the magnesium variable increases its concentration, reliability decreases.

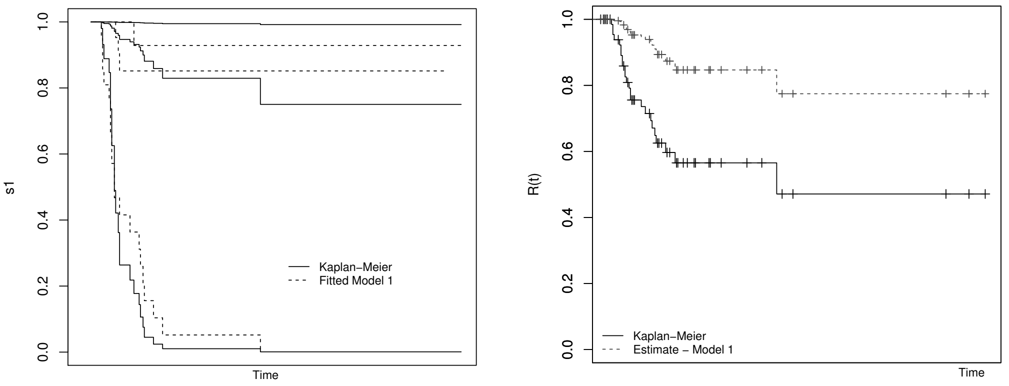

(a) Survival estimates for the quartiles (Model 1).

(b) Model 1 estimate via KM.

Figure 7: Estimate analysis for model 1.

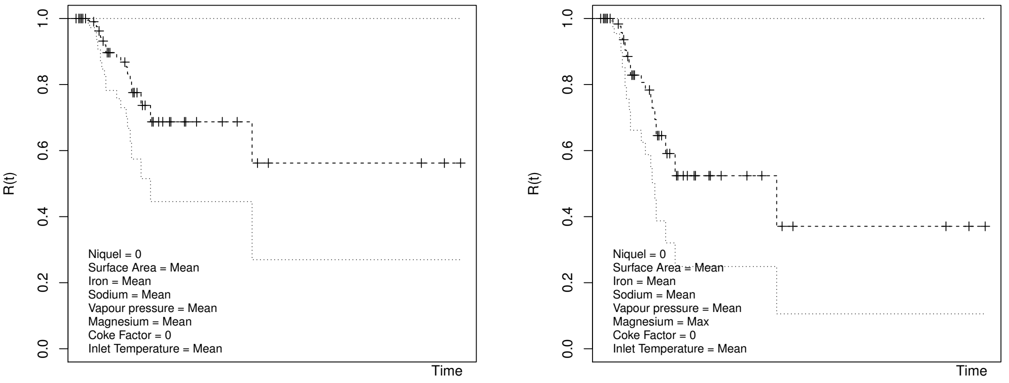

(a) Scenario 1.

(b) Scenario 2.

Figure 8: Reliability for different scenarios.

5.2.2. Second Approach — High vibration values are considered

Model 2 uses the second approach and supports the idea that our event is “high vibration”. Times to high vibration values and shut-downs are here analysed instead of only times to shut-down failures. Thus, using the same process variables, we achieve the Cox model 2 in Table 3. In this model, more than finding the reasons for shut-downs, is to find the reasons for scaling. High vibrations can be a spark for a shut-down and the line that bounds the two situations (shut-down or not) is just a question of the way the scaling is being heterogeneously distributed on the rotor blades, and how much imbalance it will cause. Comparing these results with the previous model (model 1), we found some variables in common.

Table 3: Cox model 2.

variable	β	$se(\beta)$	p-value
fe	−6.49	2.01	0.0013
tpin	−0.05	0.01	0.0002
tpout	−0.01	0.01	0.0278
re	−0.95	0.28	0.0008
mgo	−66.48	21.33	0.0018
na	−202.8	58.24	0.0005
cf	−3.22	1.77	0.0691
gf	−2.81	0.69	0.0000
mgo:na	240.2	68.87	0.0005
cf:gf	1.65	0.49	0.0008

Nevertheless, some covariates that are not in common seem to have individually, a high significance in both models, such as *sa* and *vpb*. However, when together in the models they lose their significance. Approximately 35% of data variation are explained by this model, with a concordance value of 0.74 and a likelihood ratio test with a p-value effectively zero. We can see that the common covariates with model 1 (*fe*, *tpin*, *mgo*, *na* and *cf*), are monitoring variables as well as exhaust temperature (*tpout*). Magnesium oxide (*mgo*) is a very problematic component when combined with sodium (*na*, which is a poison for the process and combined with some metals can act as "glue"). For *mgo* and *na* interaction (Figure 9) we

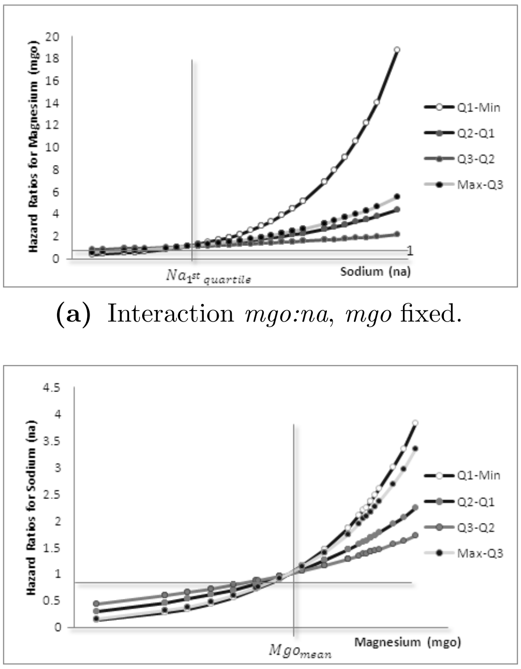

(a) Interaction *mgo:na*, *mgo* fixed.

(b) Interaction *mgo:na*, *na* fixed.

Figure 9: Interaction *mgo:na* for model 2.

have that for magnesium values fixed above the 3$^{\text{rd}}$ quartile, the risk can increase from 22% to 4 times as much depending on sodium increase, but we have a clear interaction when we set *na* at its maximum value and we see that the risk increases 18 times for values below *mgo*'s 1$^{\text{st}}$ quartile, although it always increases for all *mgo* quartiles' variations. Coke factor (*cf*) indicates the amount of produced coke in the process and it can be a monitoring variable as it isn't a protective factor. Gas factor *gf* is concerned with the amount of produced gases and it can be read as a monitoring variable as well. In Figure 10 we can see that for coke factor and gas factor interaction, if we set *cf* value for its maximum, we will have a large risk increase when we increase *gf*. At the same time, when we set the values for *gf* and make *cf* increase, the hazard rates will increase for high values of *gf*.

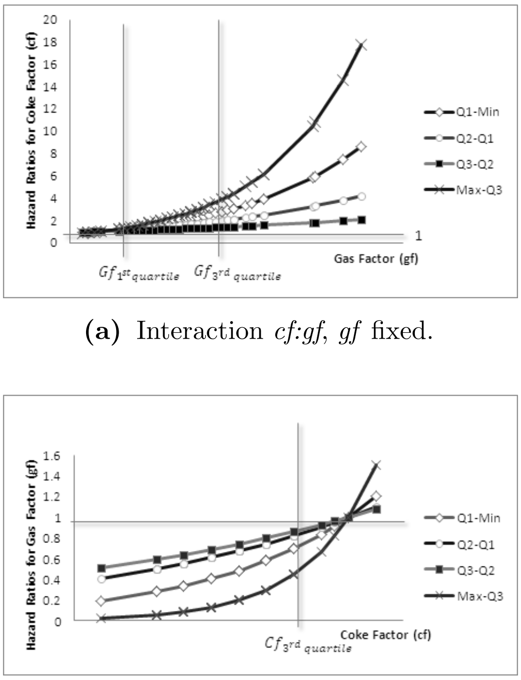

(a) Interaction *cf:gf*, *gf* fixed.

(b) Interaction *cf:gf*, *cf* fixed.

Figure 10: Interaction *cf:gf* for model 2.

We can see in Figure 11a, that we have a better survival estimate than in model 1, with a good fit to the quartiles. Linear correlation suggest that none of the covariates violate the proportional hazards assumption as for model 1, and the residual analysis didn't show problematic points that may be interfering in the model (see Appendix B). As with model 1, two different scenarios were considered for model 2. We can see in Figure 12a the reliability curve for model 2 considering the mean for all variables. As we increase *cf* (Figure 12b) keeping all other variables constant, we see that the reliability curve have a higher slope and decreases faster.

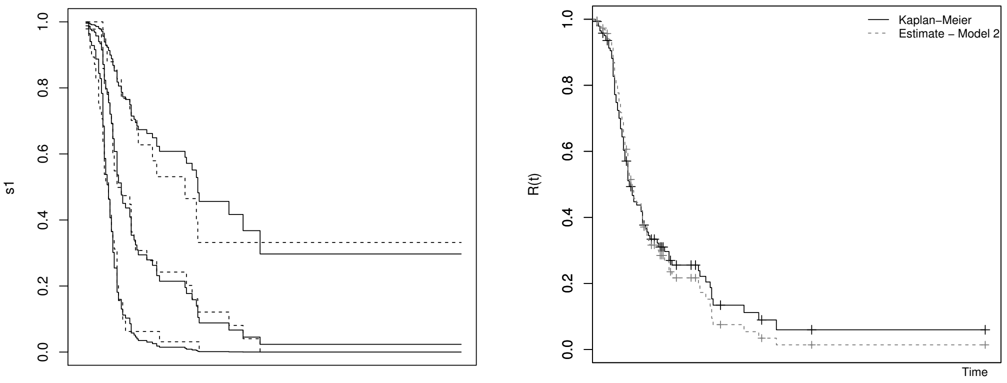

(a) Survival estimates for the quartiles (Model 2).

(b) Model 2 estimate via KM.

Figure 11: Estimate analysis for model 2.

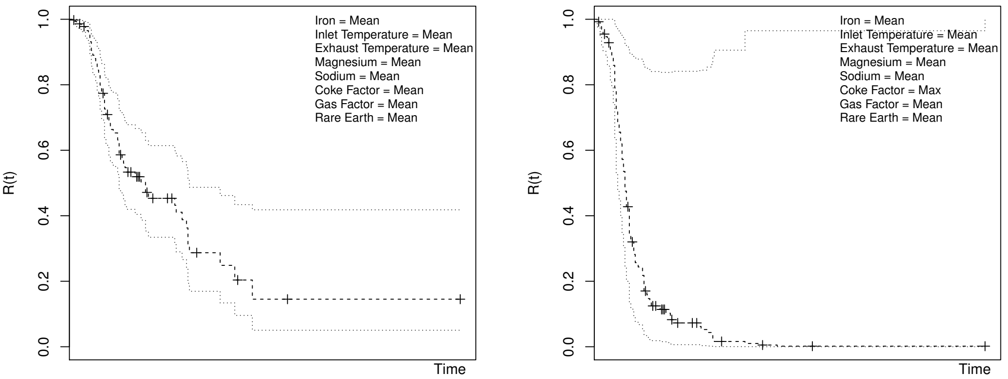

(a) Scenario 1.

(b) Scenario 2.

Figure 12: Reliability for different scenarios.

5.3. Parametric Models

In order to have a first parametric model, we have proceeded to parametric approaches for the baseline hazard rate determination. As we can see, none of the tested distributions are presenting a good fit, however, the log-normal has the lowest AIC (Figure 13). In order to find a better parametric fit, only times before t_1 were considered. We can see a better approach is achieved with the log-normal distribution in Figure 14, which has the lowest AIC. According to the AIC value we also have the log-normal distribution as a good fit for the baseline hazard as shown in Figure 15.

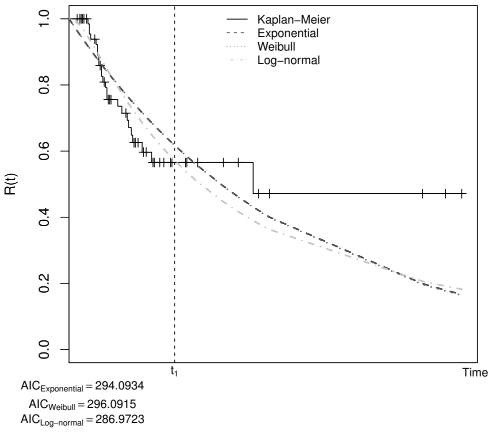

Figure 13: Parametric models for the null model (model 1).

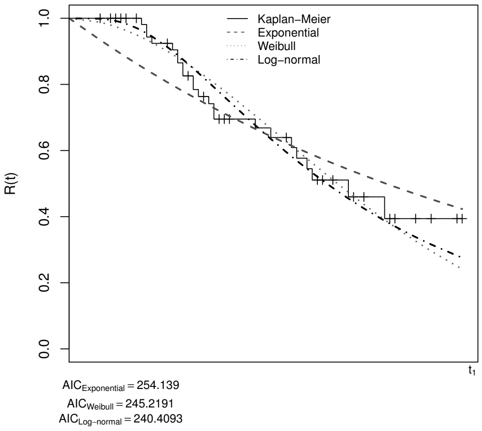

Figure 14: Parametric models for the null model (model 1) until time t_1.

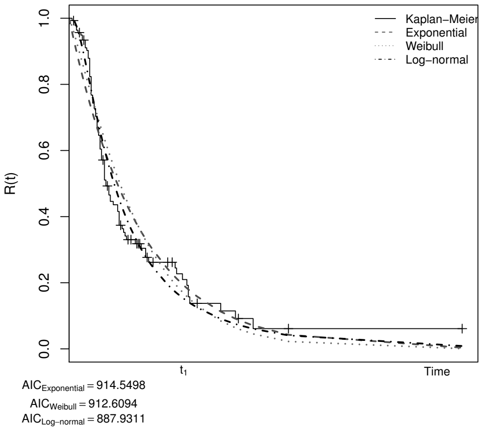

Figure 15: Parametric models for the model 2.

6. CONCLUDING REMARKS

For the proposed problem in Section 4, the consistency of some covariates in tested models make them a subject of investigation. Some covariates such as surface area should be definitely monitored, as well as the inlet and exhaust temperatures trend. It seems that sodium, magnesium and iron are influential variables for the increase of the risk of high vibration values, and should be monitored, although all these variables are very difficult to control as they depend on the reactor feedstock and reactor temperatures. Investigation on this subject will be ongoing as it can help to find the reasons for the so non-welcome shutdowns. Future work will be done to mechanical equipment in order to optimize, if possible, predictive maintenance scenarios.

APPENDIX A

Here we have the residual analysis for model 1. We can see that proportionality assumption is verified when we analyse Figure 16. Deviance residuals and martingale residuals where analysed as well as score residuals and for all cases possible outliers or influential observations where removed to check the availability of the model. In all cases the coefficients never changed their values above 25%.

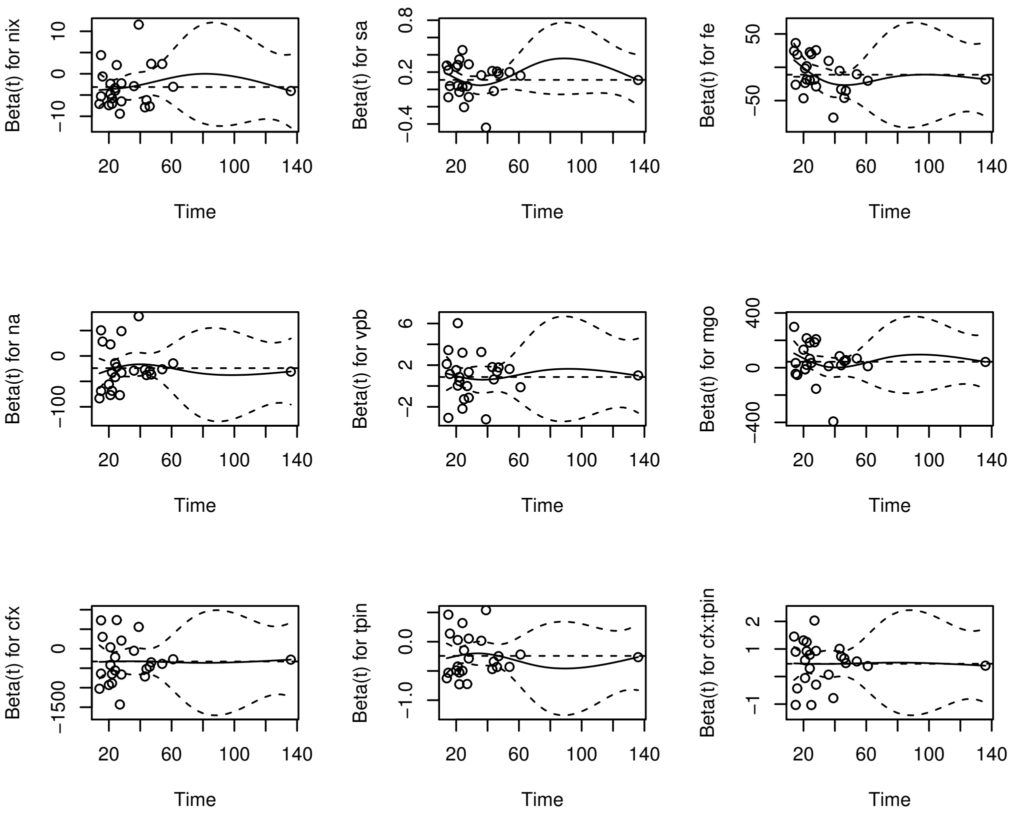

Figure 16: Schoenfeld residuals for model 1.

APPENDIX B

As for model 1 the proportionality assumption was checked via Schoenfeld residuals.We can see that proportionality assumption is verified when we analyse Figure 17. Just like model 1, model 2 has been checked for influential observations with no significant change in its coefficients.

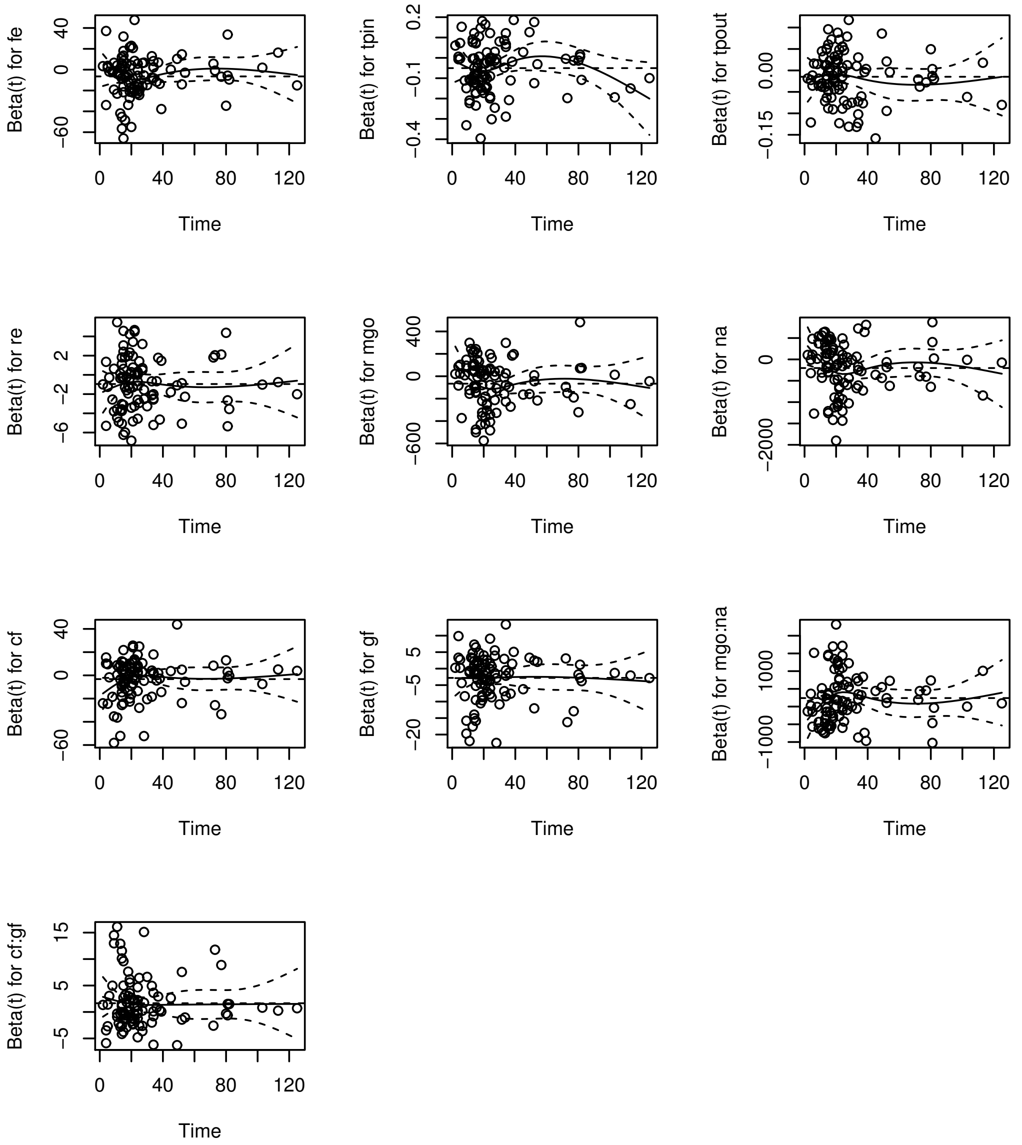

Figure 17: Schoenfeld residuals for model 2.

ACKNOWLEDGMENTS

This study was supported on behalf of FCT (Portuguese Foundation for Science and Technology) and Galp Energia, the insertion company for the PhD. The second author is member of CIMA-UE, research center supported financially by the FCT.

REFERENCES

[1] Breslow, N.E. (1972). Regression models and life tables (with discussion) by D.R. Cox, *Journal of the Royal Statistical Society, Series B*, **34**, 187–220.

[2] Cox, D.R. (1972). Regression models and life tables (with discussion), *Journal of the Royal Statistical Society, Series B*, **34**, 187–220.

[3] Cox, D.R. and Oakes, D. (1984). *Analysis of Survival Data*, Chapman and Hall, London.

[4] Diangu, H. (2011). Analysis on causes of scaling in flue gas turbine of FCCU and countermeasures, *China Petroleum Processing and Petrochemical Technology*, **13**(1), 66–74.

[5] Fine, J.P. and Gray, R.J. (1999). A proportional hazards model for the subdistribution of a competing risk, *Journal of the American Statistical Association*, **94**, 496–509.

[6] Gladys, N. and Laura, V. (1999). Analysis of rotor-blade failure due to high-temperature corrosion/erosion, *Surface and Coatings Technology*, **120–121**, 145–150.

[7] Hosmer, D.W. and Lemeshow, S. (2000). *Applied Logistic Regression*, Wiley, New York.

[8] ISO 14224:2006 (2006). *Petroleum and Natural Gas Industries — Collection and Exchange of Reliability and Maintenance Data for Equipment*, International Standard Organization, Second Edition.

[9] Kaplan, E.L. and Meier, P. (1958). Nonparametric estimation from incomplete observations, *J. Amer. Statist. Assn.*, **53**, 457–481.

[10] Li, R. and Chambless, L. (2007). Test for additive interaction in proportional hazards models, *Annals of Epidemiology*, **17**(3), 237–236.

[11] Lunn, M. and McNeil, D. (1995). Applying Cox regression to competing risks, *Biometrics*, **51**(2), 524–532.

[12] Rausand, M. and Hoyland, A. (2004). *System Reliability Theory — Models, Statistical Methods and Applications*, Second Edition, Wiley.

REVSTAT – Statistical Journal
Volume 11, Number 1, March 2013, 67–82

ROBUST METHODS IN ACCEPTANCE SAMPLING

Authors: Elisabete Carolino
– Escola Superior de Tecnologias da Saúde de Lisboa (IPL), Portugal
lizcarolino@gmail.com

Isabel Barão
– Faculdade de Ciências (UL), Portugal
mibarao@fc.ul.pt

Abstract:

- In the quality control of a production process (of goods or services), from a statistical point of view, the focus is either on the process itself with application of Statistical Process Control or on its frontiers, with application of Acceptance Sampling (AS) and Experimental Design. AS is used to inspect either the process output (final product) or the process input (raw material). The purpose of the design of a sampling plan is to determine a course of action that, if applied to a series of lots of a given quality, and based on sampling information, leads to a specified risk of accepting/rejecting them. Thus AS yields quality assurance. The classic AS by variables is based on the hypothesis that the observed quality characteristics follow the Gaussian distribution (treated in classical standards). This is sometimes an abusive assumption that leads to wrong decisions. AS for non-Gaussian variables, mainly for variables with asymmetric and/or heavy tailed distributions, is a relevant topic. When we have a known non-Gaussian distribution we can build specific AS plans associated with that distribution. Alternatively, we can use the Gaussian classical plans with robust estimators of location and scale — for example, the total median and the sample median as location estimates, and the full range, the sample range and the interquartile range, as scale estimates. In this work we will address the problem of determining AS plans by variables for Extreme Value distributions (Weibull and Fréchet) with known shape parameter. Classical plans, specific plans and plans using the robust estimates for location are determined and compared.

Key-Words:

- *quality control; acceptance sampling; acceptance sampling by variables; robust methods.*

1. INTRODUCTION

Acceptance Sampling (AS) is used to inspect either the output process — final product — or the input — initial product. On a lot-by-lot basis, a random sample is taken from the lot and based on the information given by the sample a decision is taken: to accept or to reject the lot. The purpose of AS is to determine a course of action, not to estimate lot quality. It prescribes a procedure that, if applied to a series of lots, will give a specified risk of accepting lots of given quality. An AS plan indicates the rules for accepting or rejecting a lot that is being inspected. Acceptance sampling is a compromise between no inspection and 100% inspection. It is likely to be used under the following conditions:

- When 100% inspection is tiring the percentage of nonconforming items passed may be higher than under a scientifically designed sampling plan.
- When the cost of inspection is high and the loss arising from the passing of a nonconforming unit is not great. It is possible in some cases that no inspection at all will be the cheapest plan.
- When inspection is destructive. In this case sampling must be employed.

There are two approaches to AS in the literature. The first approach is AS by attributes, in which the product is specified as conforming or nonconforming (defective) based on a certain criteria and the number of nonconforming units is counted. The other approach is AS by variables, if the item inspection leads to a continuous measurement. In comparison to sampling plans by attributes, sampling plans by variables have the advantage of usually resulting in considerable savings in sample size for comparable assurance. The main disadvantage of the classical case of the acceptance sampling by variables is that it is based on the hypothesis that the observed quality characteristic follows a Gaussian distribution. References to this section are ([4]), ([12]), ([9]), ([13]).

In Acceptance Sampling there are two kinds of decisions based on the sample, to accept or to reject the lot, and two kinds of errors associated:

- Type I error: consists of incorrectly rejecting a lot that is really acceptable. The probability of making a type I error is α, also called *producer's risk*.
- Type II error: consists of incorrectly accepting a lot that is really unacceptable. The probability of making a type II error is β, also called *consumer's risk*.

The producer wishes the acceptance of "good" lots with high probability $(1-\alpha)$ and the consumer wishes the acceptance of "bad" lots with small probability (β).

In the determination of an AS plan the aim is to calculate the sample size, n, to be taken from the lot and the acceptability constant, k, that satisfy the conditions referred to as the *producer's risk* and the *consumer's risk*. There are two quality values that we need to define ([14]):

- *AQL — Acceptable Quality Level* — the worst quality level that is still considered acceptable. The *AQL* is a percent defective that is the base line requirement for the quality of the producer's product.
- *LTPD — Lot Tolerance Percent Defective* — the poorest quality in an individual lot that should be accepted, the level of quality where it is desirable to reject most lots. The *LTPD* is a designated high defect level that would be unacceptable to the consumer.

To prevent "good" lots from being rejected and "bad" lots from being accepted, we calculate the values of n and k by solving the system

$$\begin{cases} P_{\mathrm{ac}}(\omega = AQL) \;=\; 1-\alpha\,, \\ P_{\mathrm{ac}}(\omega = LTPD) \;=\; \beta\,, \end{cases} \tag{1.1}$$

where $P_{\mathrm{ac}}(\omega) = \mathrm{P}(\text{accept the lot} \,|\, \omega)$ designates the acceptance probability (function of n and k) and ω the non conforming proportion. If we let ω vary in $[0,1]$, we can establish the operating characteristic curve, *OC-curve*, $P_{\mathrm{ac}}(\omega)$. This curve shows the lot acceptance probability in accordance with its quality, given by the nonconforming proportion. This is the most used way of determining an AS plan: to specify 2 desired points on the *OC-curve* and solve for the (n,k) that uniquely determines the *OC-curve* going through these points $(AQL, 1-\alpha)$ and $(LTPD, \beta)$ ([8]). Alternatively the above system can be solved for k and *LTPD*, as will be used later for comparison purposes.

In AS, sampling plans can be built up with a single specification limit (the upper or lower) or with two specification limits (the upper and the lower). This latter situation is theoretically more complex since the two previous procedures have to be added into one. For more details see ([3]).

Let X denote the random variable that represents the quality characteristic inspected. For simplicity, in the next sections we will assume that there is a single specification limit, the upper limit U, so the nonconforming proportion is given by $\omega = P(X \geq U)$. In section 2 we will review the classical case where X is assumed to follow a Gaussian distribution. In section 3 we will derive AS plans when X follows an Extreme Value distribution (Weibull and Fréchet). As a particular case of Weibull distribution we obtain the results for the exponential distribution studied in ([2]) and ([11]). In the section 4 robust estimators for location are presented. In section 5, classical plans, specific plans and plans using the robust estimates for location are compared by means of the *OC-curve*. The main conclusions are driven in section 6.

2. ACCEPTANCE SAMPLING FOR GAUSSIAN VARIABLES

The acceptance sampling by variables in the Gaussian case was solved in theory and for application in American Standard, MIL-STD 414 (updated several times in details). The most recent international version is ([1]).

Consider that the quality characteristic of interest, X, follows a Gaussian distribution, with mean μ and standard deviation σ, $X \frown N(\mu,\sigma)$ and that a sample of size n is taken from the lot for AS purposes. The nonconforming proportion is given by $\omega = P(X \geq U) = 1 - \Phi\big(\frac{U-\mu}{\sigma}\big)$. The lot is accepted if the estimated nonconforming proportion based on the sample is "small" or an associated quality index Q is "big". The definition of Q depends on the standard deviation of X being known or unknown, as follows.

2.1. σ known

If σ is known the quality index Q is defined as $Q = \frac{U-\overline{X}}{\sigma}$ and the criterion of acceptance is $Q = \frac{U-\overline{X}}{\sigma} \geq k$. The values of n and k are the solution of the system

$$\begin{cases} P\big(Q \geq k \,|\, \omega = AQL\big) \;=\; 1-\alpha\,, \\ P\big(Q \geq k \,|\, \omega = LTPD\big) \;=\; \beta\,, \end{cases}$$

and are given by

$$\begin{cases} k \;=\; \dfrac{z_{1-\alpha}\, z_{LTPD} - z_\beta\, z_{AQL}}{z_\beta - z_{1-\alpha}}\,, \\ n \;=\; \left(\dfrac{z_{1-\alpha} - z_\beta}{z_{LTPD} - z_{AQL}}\right)^2, \end{cases}$$

where z_p denotes the p-probability quantile of the standard Gaussian distribution. For details see ([4]) and ([12]).

2.2. σ unknown

If σ is unknown the criterion of acceptance is $Q = \frac{U-\overline{X}}{S} \geq k$, with $S^2 = \sum_{i=1}^{n} \frac{(X_i-\overline{X})^2}{n-1}$ the unbiased estimator of σ^2. The values of n and k result from the resolution of the system

$$\begin{cases} P_{\rm ac}\big(Q \geq k \,|\, \omega = AQL\big) \;=\; 1-\alpha\,, \\ P_{\rm ac}\big(Q \geq k \,|\, \omega = LTPD\big) = \beta\,, \end{cases}$$

or from the equivalent

$$\begin{cases} F_{t,\nu=n-1,\delta=\sqrt{n}\,z_{AQL}}\big(-k\sqrt{n}\big) \;=\; 1-\alpha\,, \\ F_{t,\nu=n-1,\delta=\sqrt{n}\,z_{LTPD}}\big(-k\sqrt{n}\big) \;=\; \beta\,, \end{cases}$$

where $F_{t,\nu,\delta}(\cdot)$ represents the distribution function of the non-central t variable with ν degrees of freedom and non-centrality parameter δ ([4]) and ([12]).

3. ACCEPTANCE SAMPLING FOR NON-GAUSSIAN VARIABLES

At this point, we will take a closer look at two specific distributions that are widely used in Statistical Quality Control, namely the Weibull and Fréchet distributions.

The procedure to be used for non-Gaussian variables is analogous to that used for the Gaussian case. We start by defining the quality index for each case and compare its observed value with the constant k of acceptance, considering the situations of known and unknown parameters. To define the AS plan for each case, we must solve system (1.1).

Let us consider the Weibull distribution, Weibull(θ,δ), with probability density function (*pdf*) $f_X(x)=\frac{\theta}{\delta}\left(\frac{x}{\delta}\right)^{\theta-1}e^{-\left(\frac{x}{\delta}\right)^{\theta}}$, $x>0$, $\delta>0$, $\theta>0$, and the Fréchet distribution, Fréchet(θ,δ), with *pdf* $f_X(x)=\frac{\theta}{\delta}\left(\frac{x}{\delta}\right)^{-\theta-1}e^{-\left(\frac{x}{\delta}\right)^{-\theta}}$, $x>0$, $\delta>0$, $\theta>0$, and let $\hat{\theta}$ and $\hat{\delta}$ represent the maximum likelihood estimators of their respective dispersion and shape parameters based on a random sample of size n. Considering that $Y=\frac{2n\hat{\delta}^{\theta}}{\delta^{\theta}}\frown\chi^2_{2n}$, in the Weibull case, and that $Y=\frac{2n\hat{\delta}^{-\theta}}{\delta^{-\theta}}\frown\chi^2_{2n}$, in the Fréchet case, the results of Table 1 are obtained (for details see ([3])).

Table 1: Non-Conforming proportion, Criterion of acceptance and Acceptance Sampling plans for the Weibull and Fréchet cases.

Distribution		Weibull (θ,δ)	Fréchet (θ,δ)
Non-Conforming Proportion $\omega=P\big(X>U\big)$		$e^{-\left(\frac{U}{\delta}\right)^{\theta}}$	$1-e^{-\left(\frac{U}{\delta}\right)^{-\theta}}$
Criterion of acceptance	θ known	$Q_U=\left(\frac{U}{\widehat{\delta}}\right)^{\theta}\geq k$	$Q_U=\left(\frac{U}{\widehat{\delta}}\right)^{-\theta}\leq k$
	θ unknown	$Q_U=\left(\frac{U}{\widehat{\delta}}\right)^{\widehat{\theta}}\geq k$	$Q_U=\left(\frac{U}{\widehat{\delta}}\right)^{-\widehat{\theta}}\leq k$
AS plans: values of k and n	θ known	$\begin{cases} n=-\dfrac{k\,\chi^2_{2n;\beta}}{2\,ln(LTPD)} \\ k=-\dfrac{2n\,ln(AQL)}{\chi^2_{2n;1-\alpha}} \end{cases}$ *	$\begin{cases} n=-\dfrac{k\,\chi^2_{2n;1-\beta}}{2\,ln(1-LTPD)} \\ k=-\dfrac{2n\,ln(1-AQL)}{\chi^2_{2n;\alpha}} \end{cases}$
	θ unknown	**	**

* Note that, this system is equal to the exponential case, ([2]).

** Since the exact distribution of Q_U is unknown analytically, to determine the values of n and k that satisfy the system (1.1) we have to proceed with simulation methods.

4. ROBUST ESTIMATORS FOR LOCATION

As we referred previously, when we have a non-Gaussian distribution we can build specific AS plans associated with that distributions.

As also mentioned, the classical plans (Gaussian case) assume normality of the data and they use $\overline{X}$ as an estimator of μ. However, when data is Non-Gaussian, $\overline{X}$ may not be the best estimator, mainly when the distribution is asymmetric and/or has heavy tails.

Thus, alternatively, as robust estimators for μ, we suggest the sample median $(\widetilde{X})$ and total median $(\widetilde{X}_T)$, respectively, given by

$$\widetilde{X} = \begin{cases} X_{(m)} & \text{if } n = 2m-1\,, \\ \dfrac{X_m + X_{m+1}}{2} & \text{if } n = 2m\,, \end{cases}$$

$m \geq 1$ and $\widetilde{X}_T = \sum_{i=1}^{n} a_i X_{(i)}$, such that $a_i = a_{n-i+1}, \forall\, i = 1, ..., n,\ 0 < a_1 < a_2 < ... < a_{\left[\frac{n}{2}\right]},\ \sum_{i=1}^{n} a_i = 1$.

Considering these estimators for the mean value, the quality index of classical plans is, respectively $Q_N^{'} = \frac{U-\widetilde{X}}{\sigma}$ and $Q_N^{''} = \frac{U-\widetilde{X}_T}{\sigma}$, and the criterion of acceptance, for each case is $Q_N^{'} = \frac{U-\widetilde{X}}{\sigma} \geq k_n^{'}$ and $Q_N^{''} = \frac{U-\widetilde{X}_T}{\sigma} \geq k_n^{''}$. When we work with $Q_N^{'}$, we use the distribution of $\widetilde{X}$. When we work with $Q_N^{''}$, we need to use simulation methods, since its distribution is unknown.

For calculating the weight of the tails, we used the index, τ,([10]),

$$\tau(F) = \frac{1}{2}\left(\frac{F^{-1}(0.99) - F^{-1}(0.5)}{F^{-1}(0.75) - F^{-1}(0.5)} + \frac{F^{-1}(0.5) - F^{-1}(0.01)}{F^{-1}(0.5) - F^{-1}(0.25)}\right) \Big/ \left(\frac{z_{0.99} - z_{0.5}}{z_{0.75} - z_{0.5}}\right),$$

where $F^{-1}(p)$ represents the p-quantile of the distribution F and z_p represents de the p-quantile of the standard Gaussian distribution.

To assess the degree of skewness, Fisher's skewness coefficient, c_1, was used, given by $c_1(F) = \frac{\mu_3}{\sigma^3}$, where F represents the distribution of the data, μ_3 represents the third-order central moment of the distribution F and σ represents the standard deviation of the distribution F.

According to ([7]), for asymmetric distributions, the best estimator for the mean value is

- $\overline{X}$, if $c_1 < 0.9$ independently of the value of n or if $n > 16$ independently of the value of c_1;

- $\widetilde{X}_T$, if $0.9 \le c_1 \le 3.69$ and $n \le 16$;
- $\widetilde{X}$, if $c_1 > 3.69$ and $n = 3$ or 4;
- $\widetilde{X}_T$, if $c_1 > 3.69$ and $5 \le n \le 16$.

For the tail weight index (τ), the best estimator for the mean value is

- $\overline{X}$, if $\tau < 1.01$ independently of the value of n;
- $\widetilde{X}_T$, if $1.01 \le \tau \le 1.8$ and $n \ge 5$;
- $\widetilde{X}$, if $\tau > 1.8$ and $n = 3$ or 4;
- $\widetilde{X}_T$, if $\tau > 1.8$ and $n \ge 5$.

5. SOME RESULTS

Our main questions are: what miscalculations occur if X is Weibull and we use a standard AS plan for Gaussian X instead? What alternatives can we use? Can we use robust estimators for the location in the Gaussian case?

As we said before, the determination of the specific sampling plan is based on the solution of the System (1.1). Usually α, β, AQL and *LTPD* are fixed and the system is solved for n and k. For comparison of the plans it is more convenient to fix n (taken from the standard) and solve the system to calculate k and *LTPD*. The comparison of the results will, essentially, be based on *LTPD* or/and the *OC-curve*.

To exemplify what we propose, we consider distributions with different degrees of asymmetry and tail weight index. So we are going to compare the Gaussian case with the Weibull ($\theta = 7$ and $\theta = 1$) and Fréchet ($\theta = 5$) cases. We will consider $\alpha = 5\%$, $\beta = 10\%$, $AQL = 1\%$ and several values of n, taken from the standard.

5.1. Comparisons of Gaussian and specific plans

If the quality characteristic is a non-Gaussian variable and if we use the values of the standard (apply the classical plans), the producers risk (5%) is miscalculated and misleading. We have, therefore, to carry out the adjustment of the α's for the *OC-curves* which pass in the point $(AQL, 1-\alpha)$, and so we can compare the sampling plans. For more details see ([3]). Table 2 shows the results for the exponential case.

Table 2: Results of α's adjustment, exponential case.

Sample size, n	Adjusted α
10	0.036
15	0.038
20	0.039
30	0.041
35	0.041
50	0.043
75	0.044
100	0.045
150	0.046
200	0.046

Table 3 shows the comparison results of the Gaussian case (given by the standard) versus the exponential case, based on *LTPD* and k.

Table 3: Comparison of *LTPD* and k, between Gaussian case (σ known) and exponential case.

Sample size, n	$AQL = 1\%$					
	Standard (α is not 5%) Gaussian data Gaussian fit		Exponential data Gaussian fit		Exponential data Exponential fit	
	$LTPD_N(\%)$	k_N	$LTPD_{EN}(\%)$	k_{EN}	$LTPD_E(\%)$	k_E
10	8.06	1.81	16.13	1.76	16.13	2.93
15	5.81	1.90	11.45	1.87	11.45	3.16
20	4.73	1.96	9.08	1.93	9.08	3.30
30	3.66	2.03	6.68	2.01	6.68	3.49
35	3.35	2.05	5.99	2.03	5.99	3.56
50	2.79	2.09	4.73	2.08	4.73	3.70
75	2.34	2.14	3.73	2.13	3.73	3.85
100	2.10	2.16	3.20	2.16	3.20	3.94
150	1.84	2.19	2.65	2.19	2.65	4.05
200	1.70	2.21	2.36	2.21	2.36	4.12

Examining the results presented in Tables 2 and 3, it can be seen that if the quality characteristic is an exponential variable and if we use the values of the standard (classic case), the producer's risk (as well as the consumer's) is miscalculated. For example, given $AQL = 1\%$, $n = 10$ and if we want a producer's risk of 5%, standards give the values of k and *LTPD*, respectively, 1.81 and 8.06%.

But in fact, with this k the real risk of the producer is 6.36% (the risk of 5% is illusory and misleading) and the real consumer's non-conforming fraction is 16.13% (instead of 8.06%). Therefore, to ensure a risk of 5% the standard shall be calculated with a risk of 3.6%, yielding the acceptance constant, k, in the last but one column of Table 3.

Tables 4 and 5 show the results of the Weibull case with $\theta = 7$. These results show, once again, that abusively using AS plans for Gaussian variables,

Table 4: Simulation results: estimated α for Gaussian case when α of Weibull ($\theta = 7$, $\delta = 10$) case is 0.05 and 95% Confidence Interval for α.

Sample size, n	Adjusted α	95% Confidence Interval for α	
		Lower limit	Upper limit
10	0.055	0.042	0.069
15	0.053	0.041	0.068
20	0.053	0.040	0.067
30	0.053	0.041	0.067
35	0.052	0.039	0.066
50	0.052	0.040	0.066
75	0.052	0.040	0.065
100	0.051	0.039	0.065
150	0.051	0.039	0.066
200	0.051	0.038	0.066

Table 5: Comparison of *LTPD* and k, between the Gaussian case and the Weibull ($\theta = 7$, $\delta = 10$) case.

Sample size, n	$AQL = 1\%$					
	Standard (α is not 5%) Gaussian data Gaussian fit		Weibull data Gaussian fit		Weibull data Weibull fit	
	$LTPD_N(\%)$	k_N	$LTPD_{WN}(\%)$	k_{WN}	$LTPD_W(\%)$	k_W
10	8.06	1.81	21.00	1.76	16.13	2.93
15	5.81	1.90	14.00	1.87	11.45	3.16
20	4.73	1.96	12.00	1.93	9.08	3.30
30	3.66	2.03	9.00	2.01	6.68	3.49
35	3.35	2.05	7.50	2.03	5.99	3.56
50	2.79	2.09	6.00	2.08	4.73	3.70
75	2.34	2.14	5.00	2.13	3.73	3.85
100	2.10	2.16	4.00	2.16	3.20	3.94
150	1.84	2.19	3.00	2.19	2.65	4.05
200	1.70	2.21	2.36	2.21	2.36	4.12

when we have an exponential or Weibull variable, implies serious risks for the consumer and/or the producer. Comparing the last column of Tables 3 and 5, we can see that the results for the exponential and Weibull cases are equal, i.e., the plans are θ invariant.

The same kind of precautions has to be taken in the Fréchet distribution for the calculation of the risks α and β, and the constants k and $LTPD$.

5.2. Comparisons of specific and robust AS plans

The plots in Figures 1 and 2 show, for $n = 5$, the operating characteristic curves, *OC-curves*, $P_{\text{ac}}(\omega)$ for:

- the Gaussian case with sample mean (—○—);
- the Gaussian case with sample median (Figure 1) and total median (Figure 2) (—□—) with Weibull data;
- Weibull case with $\theta = 7$, $\delta = 10$ (—●—). This distribution has $c_1 = -0.463$ and $\tau = 0.990$.

Observing the graphs of Figures 1 and 2, it appears that the mean sample produces better results than the sample median or the total median. The *OC-curve* of the Gaussian case with sample mean is closer to the specific case and is below of the *OC-curves* of the Gaussian case with sample median and total median. For other values of n, the results are similar. $\overline{X}$ is the best estimator for this type of distribution.

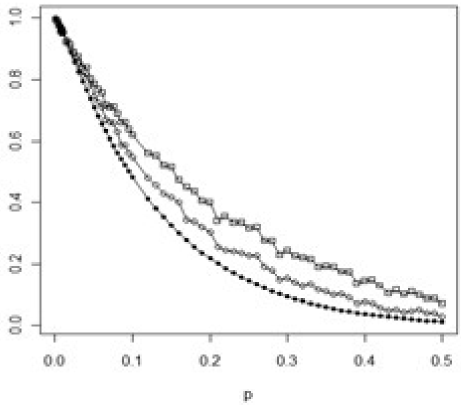

Figure 1: Comparison of OC-curves, $P_{\text{ac}}(p)$, $p \in [0;1]$ — range of non-conforming proportion — between Weibull (simulated values) and Gaussian case, $n = 5$:
(—□—) Gaussian case with σ known and sample median;
(—○—) Gaussian case with σ known and sample mean;
(—●—) Weibull case with θ known.

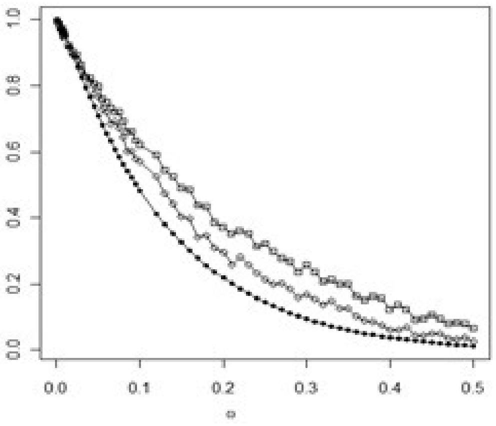

Figure 2: Comparison of OC-curves, $P_{\rm ac}(p)$, $p \in [0;1]$ — range of non-conforming proportion — between Weibull (simulated values) and Gaussian case, $n=5$:
(—□—) Gaussian case with σ known and total median;
(—○—) Gaussian case with σ known and sample mean;
(—●—) Weibull case with θ known.

The plots in Figures 3 and 4 show, for $n = 5$, the *OC-curves*, $P_{\rm ac}(\omega)$ for:

- the Gaussian case with sample mean (—○—);
- the Gaussian case with sample median (Figure 3) and total median (Figure 4) (—□—) with Weibull data;
- Weibull case with $\theta = 1$, $\delta = 10$ (exponential case) (—●—). This distribution has $c_1 = 6.619$ and $\tau = 2.260$.

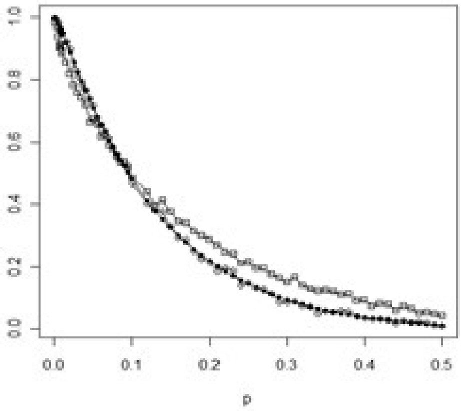

Figure 3: Comparison of OC-curves, $P_{\rm ac}(p)$, $p \in [0;1]$ — range of non-conforming proportion — between Weibull ($\theta=1$) (simulated values) and Gaussian case, $n=5$:
(—□—) Gaussian case with σ known and sample median;
(—○—) Gaussian case with σ known and sample mean;
(—●—) Weibull case with θ known.

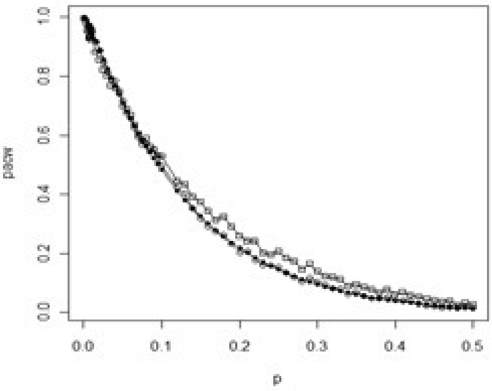

Figure 4: Comparison of OC-curves, $P_{\rm ac}(p)$, $p \in [0;1]$ — range of non-conforming proportion — between Weibull ($\theta = 1$) (simulated values) and Gaussian case, $n = 5$:
(–□–) Gaussian case with σ known and total median;
(–○–) Gaussian case with σ known and sample mean;
(–●–) Weibull case with θ known.

In this special case (exponential) $\overline{X}$ is the best estimator for this type of distribution, it produces the best results. This is a special case, since it contradicts the results obtained by ([7]). We can see that, after adjusting for the α's, the *OC-curves* of the specific case and the classic case with mean sample are coincident, and there is, therefore no alternative to improve the results. For other values of n, the results are similar.

The plots in Figures 5 and 6 show, for $n = 5$, the *OC-curves*, $P_{\rm ac}(\omega)$ for:

- the Gaussian case with sample mean (–○–);
- the Gaussian case with sample median (Figure 5) and total median (Figure 6) (–□–) with Fréchet data;
- Fréchet case with $\theta = 5$, $\delta = 10$ (–●–). This distribution has $c_1 = 3.535$ and $\tau = 1.357$.

In this case $\widetilde{X}_T$ is the best estimator for this type of distribution, i.e., we get the best results relatively to $\widetilde{X}$ and $\overline{X}$. For other values of n, the results are similar.

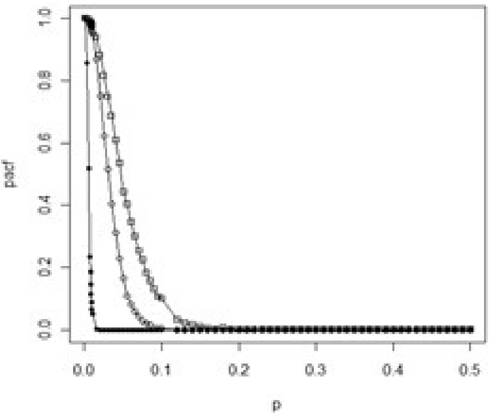

Figure 5: Comparison of OC-curves, $P_{\mathrm{ac}}(p)$, $p \in [0;1]$ — range of non-conforming proportion — between Fréchet ($\theta = 1$) (simulated values) and Gaussian case, $n = 5$:
(–□–) Gaussian case with σ known and sample median;
(–○–) Gaussian case with σ known and sample mean;
(–●–) Fréchet case with θ known.

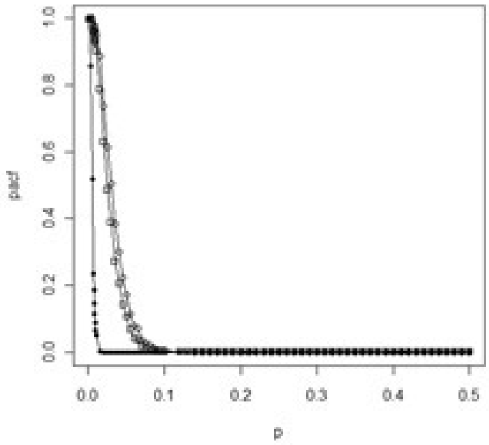

Figure 6: Comparison of OC-curves, $P_{\mathrm{ac}}(p)$, $p \in [0;1]$ — range of non-conforming proportion — between Fréchet ($\theta = 1$) (simulated values) and Gaussian case, $n = 5$:
(–□–) Gaussian case with σ known and total median;
(–○–) Gaussian case with σ known and sample mean;
(–●–) Fréchet case with θ known.

6. CONCLUSIONS

It is important to note that standard sampling plans by variables are not to be used indiscriminately, when the normality assumption may be questioned. Application of an incorrect sampling plan can cause damage to the producer and to the consumer.

If data comes from the Weibull model with $\theta = 1$, i.e., the exponential case, and if we apply the standard k determined for the Gaussian case, the producer's risk (level) of the AS plan will no longer be 5%, but will be lower, what is convenient for the producer. The values of the *LTPD*, important for the consumer, are also miscalculated when using the wrong model. However, after adjusting the α's, the AS plans are equal.

If data comes from the Weibull model with $\theta \neq 1$ and we use the appropriate AS plan (considering this distribution), as expected, we get better results than if we use the standard AS plan (assuming Gaussian case), as the *OC-curve* for the Weibull plan is below the one for the standard plan (Figure 1).

The results of using the statistics $Q_N^{'}$ and $Q_N^{''}$ are (except in the exponential case) in agreement with those obtained by ([7]), ([5]) and ([6]), i.e., the efficiency of the robust estimators for location depends on the asymmetry and the tail weight of the data distribution. When the distribution of the quality characteristic is Weibull, $\theta = 7$, so has a low skewness coefficient and a low tail weight index (Figures 1 and 2), $\overline{X}$ produces better results than the $\widetilde{X}$ and the $\widetilde{X}_T$, as expected. When the distribution of the quality characteristic is Fréchet, $\theta = 5$, so has a high skewness coefficient and a high tail weight index (Figures 5 and 6), $\widetilde{X}_T$ produces better results than the $\overline{X}$ and the $\widetilde{X}$.

So, when faced with the problem of determining AS plans for quality characteristics with non-Gaussian variables but we are able to adequately model the data and estimate its parameters, which usually is not easy, we can use specific AS plans. Alternatively, mainly for variables with asymmetric and/or heavy tailed distributions, robust AS plans are to be considered as a good alternative to the classical plans.

ACKNOWLEDGMENTS

We want to thank Professor Fernanda Figueiredo for the valuable suggestions. We also acknowledge the valuable suggestions from the referees.

REFERENCES

[1] ANSI/ASQC Z1.9-2011 (2011). *Sampling Procedures and Tables for Inspection by Variables for Percent Nonconforming*, ASQ, Milwaukee, WI (USA).

[2] Carolino, E.; Casquilho, M. and Barão, M. (2007). Amostragem de aceitação para uma variável assimétrica: a Exponencial, *Actas do XIV Congresso Anual da Sociedade Portuguesa de Estatística*, 281–292.

[3] Carolino, Elisabete (2012). *Amostragem de Aceitação para Variáveis não Gaussianas*, PhD Dissertation (in portuguese), FCUL, Portugal.

[4] Duncan, A.J. (1986). *Quality Control and Industrial Statistics*, 5th edition, IRWIN, USA.

[5] Figueiredo, F. and Gomes, M.I. (2004). The total median in statistical quality control, *Applied stochastic models in business and industry*, **20**, 339–353.

[6] Figueiredo, F. and Gomes, M.I. (2009). Monitoring industrial processes with robust control charts, *Revstat*, **7**, 151–170.

[7] Figueiredo, F.O. (2003). *Controlo Estatístico da Qualidade e Métodos Robustos*, PhD Dissertation (in portuguese), FCUL, Portugal.

[8] Gomes, M.I.; Figueiredo, F. and Barão, M.I. (2010). *Controlo Estatístico da Qualidade*, Segunda Edição revista e aumentada, Edições SPE.

[9] Guenther, William C. (1977). *Sampling Inspection in Statistical Quality Control*, First published, Whitstable Litho Ltd, GB.

[10] Hoaglin, David C.; Mosteller, Frederick and Tuckey, John W. (2000). *Understanding Robust and Explanatory Data Analysis*, John Wiley and Sons, Inc., New York.

[11] Levinson, W. (1997). Watch out for non-normal distributions of impurities, *Chemical Engineering Progress*, 70–76.

[12] Montgomery, D.C. (2004). *Introduction to Statistical Quality Control*, 5th edition, John Wiley and Sons, Inc., New York, USA.

[13] Schilling, E.G. and Neubauer, D.V. (2009). *Acceptance sampling in Quality Control*, 2nd ed., Chapman and Hall / CRC, New York, USA.

[14] Wetherill, G.B. and Brown, D.W. (1991). *Statistical Process Control*, Chapman and Hall, London, UK.

REVSTAT – Statistical Journal
Volume 11, Number 1, March 2013, 83–104

THE SKEW-NORMAL DISTRIBUTION IN SPC

Authors: Fernanda Figueiredo
– CEAUL and Faculdade de Economia da Universidade do Porto, Portugal
otilia@fep.up.pt

M. Ivette Gomes
– Universidade de Lisboa, FCUL, DEIO and CEAUL, Portugal
ivette.gomes@fc.ul.pt

Abstract:

- Modeling real data sets, even when we have some potential (as)symmetric models for the underlying data distribution, is always a very difficult task due to some uncontrollable perturbation factors. The analysis of different data sets from diverse areas of application, and in particular from *statistical process control* (SPC), leads us to notice that they usually exhibit moderate to strong asymmetry as well as light to heavy tails, which leads us to conclude that in most of the cases, fitting a normal distribution to the data is not the best option, despite of the simplicity and popularity of the Gaussian distribution. In this paper we consider a class of skew-normal models that include the normal distribution as a particular member. Some properties of the distributions belonging to this class are enhanced in order to motivate their use in applications. To monitor industrial processes some control charts for skew-normal and bivariate normal processes are developed, and their performance analyzed. An application with a real data set from a cork stopper's process production is presented.

Key-Words:

- *bootstrap control charts; false alarm rate; heavy-tails; Monte Carlo simulations; probability limits; run-length; shewhart control charts; skewness; skew-normal distribution; statistical process control.*

AMS Subject Classification:

- 62G05, 62G35, 62P30, 65C05.

1. INTRODUCTION

The most commonly used standard procedures of *statistical quality control* (SQC), control charts and acceptance sampling plans, are often implemented under the assumption of normal data, which rarely holds in practice. The analysis of several data sets from diverse areas of application, such as, *statistical process control* (SPC), reliability, telecommunications, environment, climatology and finance, among others, leads us to notice that this type of data usually exhibit moderate to strong asymmetry as well as light to heavy tails. Thus, despite of the simplicity and popularity of the Gaussian distribution, we conclude that in most of the cases, fitting a normal distribution to the data is not the best option. On the other side, modeling real data sets, even when we have some potential (as)symmetric models for the underlying data distribution, is always a very difficult task due to some uncontrollable perturbation factors.

This paper focus on the parametric family of skew-normal distributions introduced by O'Hagan and Leonard (1976), and investigated with more detail by Azzalini (1985, 1986, 2005), among others.

Definition 1.1. A random variable (rv) Y is said to have a location-scale skew-normal distribution, with location at λ, scale at δ and shape parameter α, and we denote $Y \sim SN(\lambda, \delta^2, \alpha)$, if its probability density function (pdf) is given by

$$(1.1) \qquad f(y;\lambda,\delta,\alpha) \,=\, \frac{2}{\delta}\,\phi\biggl(\frac{y-\lambda}{\delta}\biggr)\,\Phi\biggl(\alpha\,\frac{y-\lambda}{\delta}\biggr), \qquad y\in\mathbb{R} \;\; (\alpha,\lambda\in\mathbb{R},\;\delta\in\mathbb{R}^+)\;,$$

where ϕ and Φ denote, as usual, the pdf and the cumulative distribution function (cdf) of the standard normal distribution, respectively. If $\lambda = 0$ and $\delta = 1$, we obtain the standard skew-normal distribution, denoted by $SN(\alpha)$.

This class of distributions includes models with different levels of skewness and kurtosis, apart from the normal distribution itself ($\alpha = 0$). In this sense, it can be considered an extension of the normal family. Allowing departures from the normal model, by the introduction of the extra parameter α that controls the skewness, its use in applications will provide more robustness in inferential methods, and perhaps better models to fit the data, for instance, when the empirical distribution has a shape similar to the normal, but exhibits a slight asymmetry. Note that even in potential normal situations there is some possibility of having disturbances in the data, and the skew-normal family of distributions can describe the process data in a more reliable and robust way. In applications it is also important to have the possibility of regulating the thickness of the tails, apart of the skewness.

The cdf of the skew-normal rv Y defined in (1.1) is given by

$$(1.2) \qquad F(y;\lambda,\delta,\alpha) \,=\, \Phi\!\left(\frac{y-\lambda}{\delta}\right) - 2\,T\!\left(\frac{y-\lambda}{\delta},\alpha\right), \quad y\in\mathbb{R}\ \ (\alpha,\lambda\in\mathbb{R},\ \delta\in\mathbb{R}^+)\ ,$$

where $T(h,b)$ is the Owen's T function (integral of the standard normal bivariate density, bounded by $x=h$, $y=0$ and $y=b\,x$), tabulated in Owen (1956), and that can be defined by $T(h,b) = \dfrac{1}{2\pi}\displaystyle\int_0^b \Big\{ \mathrm{e}^{-\frac{1}{2}h^2(1+x^2)}/(1+x^2) \Big\}\, dx,\ (b,h)\in\mathbb{R}\times\mathbb{R}.$

Although the pdf in (1.1) has a very simple expression the same does not happen with the cdf in (1.2), but this is not a problem that leads us to avoid the use of the skew-normal distribution. We have access to the R package 'sn' (version 0.4-17) developed by Azzalini (2011), for instance, that provides functions related to the skew-normal distribution, including the density function, the distribution function, the quantile function, random number generators and maximum likelihood estimates. The moment generating function of the rv Y is given by $M_Y(t) = 2\,\exp\!\big(\lambda t + \delta^2 t^2/2\big)\,\Phi(\theta\delta t)$, $\forall\, t\in\mathbb{R}$, where $\theta = \alpha/\sqrt{1+\alpha^2} \in (-1,1)$, and there exist finite moments of all orders.

Other classes of skew normal distributions, for the univariate and the multivariate case, together with the related classes of skew-t distributions, have been recently revisited and studied in the literature. For details see Fernandez and Steel (1998), Abtahi *et al.* (2011) and Jamalizadeb *et al.* (2011), among others. In this paper some control charts based on the skew-normal distribution are proposed. They still are parametric control charts, and should be compared with the so-called nonparametric or distribution-free control charts that require even less restrictive assumptions, a topic out of the scope of this paper. We merely mention that the nonparametric charts have the same in-control run-length distribution for every continuous distribution, and thus, are by definition robust. In the literature several Shewhart, CUSUM and EWMA type nonparametric control charts have been proposed. Most of them are devised to monitor the location and are based on well-known nonparametric test statistics. For a recent overview on the latest developments on nonparametric control charts, see Chakraborti *et al.* (2011) and references therein.

This paper is organized as follows. Section 2 provides some information about the family of skew-normal distributions, in what concerns properties, random sample generation and inference. Section 3 presents bootstrap control charts for skew-normal processes and some simulation results about their performance. Control charts based on specific statistics with a skew normal distribution are considered to monitor bivariate normal processes, and their properties evaluated. In Section 4, an application in the field of SQC is provided. The paper ends with some conclusions and recommendations in Section 5.

2. THE UNIVARIATE SKEW-NORMAL FAMILY OF DISTRIBUTIONS

Without loss of generality, we are going to enhance some properties of this family of distributions by considering a standard skew-normal rv X, with pdf

$$f(x;\alpha) \,=\, 2\,\phi(x)\,\Phi(\alpha x)\;, \qquad x\in\mathbb{R}\;\;(\alpha\in\mathbb{R})\;. \tag{2.1}$$

Note that, if $Y \sim SN(\lambda,\delta^2,\alpha)$ then $X = \dfrac{Y-\lambda}{\delta} \sim SN(\alpha)$.

2.1. An overview of some properties

In Figure 1 we illustrate the shape of the pdf of X for several values of α. We easily observe the shape parameter α controls the direction and the magnitude of the skewness exhibited by the pdf. As $\alpha \to \pm\infty$ the asymmetry of the pdf increases, and if the sign of α changes, the pdf is reflected on the opposite side of the vertical axis. For $\alpha > 0$ the pdf exhibits positive asymmetry, and for $\alpha < 0$ the asymmetry is negative.

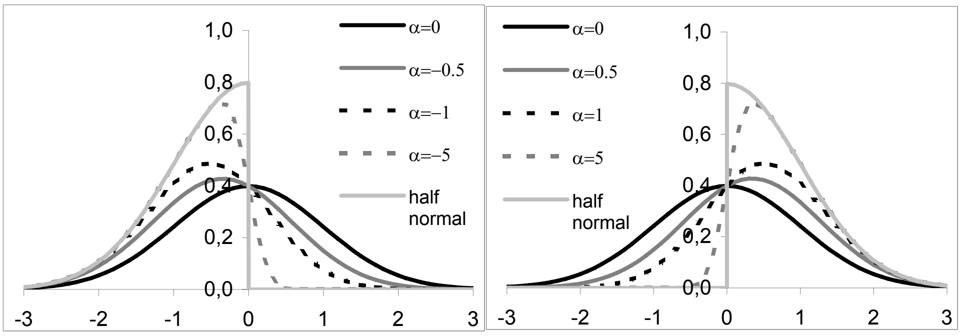

Figure 1: Density functions of standard skew-normal distributions with shape parameter α and the negative and positive half-normal pdf's.

From the Definition 2.1, we easily prove the following results:

Proposition 2.1. *As $\alpha \to \pm\infty$ the pdf of the rv X converges to a half-normal distribution. If $\alpha \to +\infty$, the pdf converges to $f(x) = 2\,\phi(x)$, $x \geq 0$, and if $\alpha \to -\infty$, the pdf converges to $f(x) = 2\,\phi(x)$, $x \leq 0$.*

Proposition 2.2. *If $X \sim SN(\alpha)$ then the rv $W = |X|$ has a half-normal distribution with pdf given by $f(w) = 2\,\phi(w)$, $w \geq 0$, and the rv $T = X^2$, the square of a half-normal distribution, has a pdf given by $f(t) = \frac{1}{\sqrt{2\pi}}\, t^{-1/2}\, e^{-t^2/2}$, $t \geq 0$, i.e., has a chi-square distribution with 1 degree of freedom.*

Denoting the usual sign function by sign(·) and taking $\theta = \alpha/\sqrt{1+\alpha^2}$, the rv X with a standard skew-normal distribution $SN(\alpha)$ has mean value given by

$$\mathbb{E}(X) = \sqrt{\frac{2}{\pi}}\,\theta \underset{\alpha\to\pm\infty}{\longrightarrow} \operatorname{sign}(\alpha) \times 0.79788 \ ,$$

and variance equal to

$$\mathbb{V}(X) = 1 - \frac{2}{\pi}\,\theta^2 \underset{\alpha\to\pm\infty}{\longrightarrow} 0.36338 \ .$$

The Fisher coefficient of skewness is given by

$$\beta_1 = \frac{(4-\pi)\,\sqrt{2\,\theta^6/\pi^3}}{\sqrt{-8\theta^6/\pi^3 + 12\,\theta^4/\pi^2 - 6\,\theta^2/\pi + 1}} \underset{\alpha\to\pm\infty}{\longrightarrow} \operatorname{sign}(\alpha) \times 0.99527 \ .$$

From these expressions we easily observe that the mean value and the degree of skewness of the $SN(\alpha)$ distribution increases with $|\alpha|$ while the variance decreases, but they all converge to a finite value.

Taking into consideration the large asymmetry of the $SN(\alpha)$ distribution when $\alpha \to \pm\infty$, and the fact that the kurtosis coefficient expresses a balanced weight of the two-tails, we shall here evaluate separately the right-tail weight and the left-tail weight of the $SN(\alpha)$ distribution through the coefficients $\tau_{\rm R}$ and $\tau_{\rm L}$ defined by

$$\tau_{\rm R} := \left(\frac{F^{-1}(0.99) - F^{-1}(0.5)}{F^{-1}(0.75) - F^{-1}(0.5)}\right) \left(\frac{\Phi^{-1}(0.99) - \Phi^{-1}(0.5)}{\Phi^{-1}(0.75) - \Phi^{-1}(0.5)}\right)^{-1}$$

and

$$\tau_{\rm L} := \left(\frac{F^{-1}(0.5) - F^{-1}(0.01)}{F^{-1}(0.5) - F^{-1}(0.25)}\right) \left(\frac{\Phi^{-1}(0.5) - \Phi^{-1}(0.01)}{\Phi^{-1}(0.5) - \Phi^{-1}(0.25)}\right)^{-1} ,$$

where F^{-1} and Φ^{-1} denote the inverse functions of the cdf of the $SN(\alpha)$ and of the cdf of the standard normal distributions, respectively. These coefficients are based on the tail-weight coefficient τ defined in Hoaglin *et al.* (1983) for symmetric distributions. For the normal distribution, $\tau_{\rm L} = \tau_{\rm R} = 1$. If the distribution F has a right (left) tail heavier than the normal tails, $\tau_{\rm R} > 1$ ($\tau_{\rm L} > 1$), and if F has a right (left) tail thinner than the normal tails, $\tau_{\rm R} < 1$ ($\tau_{\rm L} < 1$).

Table 1 presents the mean value, the standard deviation, the median, the skewness coefficient, the left-tail weight and the right-tail weight of the $SN(\alpha)$ distribution for several values of $\alpha > 0$. From the values of Table 1 we notice that when α increases from 0 to $+\infty$, the mean value, the median and the coefficient of skewness increase, but the variance decreases, as expected. The $SN(\alpha)$ distribution has a right-tail heavier than the normal tail, and a left-tail thinner than the normal tail. Moreover, the right tail-weight of the $SN(\alpha)$ quickly converges to 1.1585, the right tail-weight of the half-normal distribution, while the left tail-weight of the $SN(\alpha)$ converges more slowly to the left tail-weight of the half-normal distribution, 0.5393, a value very smaller than the tail-weight of the normal distribution. When α decreases from 0 to $-\infty$ we easily obtain the values of these parameters (coefficients) from the values of this table, taking into consideration that if the sign of α changes, the pdf is reflected on the opposite side of the vertical axis.

Table 1: Mean value (μ), standard deviation (σ), median (μ_e), skewness coefficient (β_1), left-tail weight (τ_L) and right-tail weight (τ_R) of the $SN(\alpha)$ distribution.

α	μ	σ	μ_e	β_1	τ_L	τ_R
0	0	1	0	0	1	1
0.3	0.2293	0.9734	0.2284	0.0056	0.9986	1.0017
0.5	0.3568	0.9342	0.3531	0.0239	0.9946	1.0077
1	0.5642	0.8256	0.5450	0.1369	0.9718	1.0457
2	0.7136	0.7005	0.6554	0.4538	0.9008	1.1284
3	0.7569	0.6535	0.6720	0.6670	0.8291	1.1540
5	0.7824	0.6228	0.6748	0.8510	0.7222	1.1584
10	0.7939	0.6080	0.6745	0.9556	0.6124	1.1585
$+\infty$	0.7979	0.6028	0.6745	0.9953	0.5393	1.1585

2.2. Inference

Regarding the estimation of the parameters in the location-scale skew-normal family of distributions, $SN(\lambda, \delta^2, \alpha)$, we are only able to obtain numerical maximum likelihood estimates (MLE), and thus, a closed form for their sampling distribution is not available.

Let $(Y_1, ..., Y_n)$ be a sample of size n from a $SN(\lambda, \delta^2, \alpha)$ distribution. The likelihood function is given by

$$L_{SN}(\lambda, \delta, \alpha) = \frac{2^n}{\delta^n} \prod_{i=1}^{n} \phi\left(\frac{y_i - \lambda}{\delta}\right) \prod_{i=1}^{n} \Phi\left(\alpha \frac{y_i - \lambda}{\delta}\right) \tag{2.2}$$

and the log-likelihood is given by

$$\ln L_{SN}(\lambda,\delta,\alpha) \;=\; n\ln 2 - n\ln\delta + \sum_{i=1}^{n}\ln\phi\left(\frac{y_i-\lambda}{\delta}\right) + \sum_{i=1}^{n}\ln\Phi\left(\alpha\,\frac{y_i-\lambda}{\delta}\right),$$

where $\ln(\cdot)$ denotes the natural logarithm function.

The MLE estimates of λ, δ and α, denoted $\widehat{\lambda}$, $\widehat{\delta}$ and $\widehat{\alpha}$, are the numerical solution of the system of equations

$$(2.3)\qquad \begin{cases} \delta^2 \;=\; \dfrac{1}{n}\displaystyle\sum_{i=1}^{n}(y_i-\lambda)^2\;, \\[2ex] \alpha\displaystyle\sum_{i=1}^{n}\frac{\phi\left(\alpha\,\frac{y_i-\lambda}{\delta}\right)}{\Phi\left(\alpha\,\frac{y_i-\lambda}{\delta}\right)} \;=\; \displaystyle\sum_{i=1}^{n}\frac{y_i-\lambda}{\delta}\;, \\[2ex] \displaystyle\sum_{i=1}^{n}\frac{\frac{y_i-\lambda}{\delta}\;\phi\left(\alpha\frac{y_i-\lambda}{\delta}\right)}{\Phi\left(\alpha\,\frac{y_i-\lambda}{\delta}\right)} \;=\; 0\;. \end{cases}$$

We may have some problems to obtain these estimates in the case of small-to-moderate values of the sample size n as well as for values of α close to zero. Note that if all the values of the sample are positive (negative), for fixed values of λ and δ, the log-likelihood function is an increasing (decreasing) function of α, producing therefore boundary estimates, and for $\alpha = 0$, the expected Fisher information matrix is singular.

Several authors have given important suggestions to find these estimates. For instance, for a fixed value of α, solve the last two equations of (2.3) for obtaining λ and δ, taking into account the first equation, and then, repeat these steps for a reasonable range of values of α. Another suggestion to get around these problems of estimation is to consider another re-parametrization for the skew-normal distributions $SN(\lambda,\delta^2,\alpha)$ in (1.1), in terms of the mean value μ, the standard deviation σ and the asymmetry coefficient β_1. For details in this topic see, for instance, Azzalini (1985), Azzalini and Capitanio (1999) and Azzalini and Regoli (2012), among others.

To decide between the use of a normal or a skew-normal distribution to fit the data, apart from the information given by the histogram associated to the data sample and the fitted pdf estimated by maximum likelihood, we can advance to the confirmatory phase with a likelihood ratio test.

To test the normal distribution against a skew-normal distribution, i.e., the hypotheses $H_0\colon X\sim SN(\lambda,\delta^2,\alpha=0)$ versus $H_1\colon X\sim SN(\lambda,\delta^2,\alpha\neq 0)$, the likelihood ratio statistic Λ is given by

$$\Lambda = \frac{L_{SN}\big(\widehat{\lambda},\widehat{\delta},\alpha=0\big)}{L_{SN}\big(\widehat{\lambda},\widehat{\delta},\widehat{\alpha}\big)} \,, \tag{2.4}$$

where $L_{SN}(\lambda,\delta,\alpha)$, given in (2.2), denotes the likelihood function for the $SN(\lambda,\delta^2,\alpha)$ distribution. Under the null hypothesis, $-2\log\Lambda$ is distributed as a chi-square distribution with 1 degree of freedom. For a large observed value of $-2\log\Lambda$, we reject the null hypothesis, i.e., there is a strong evidence that the $SN\big(\widehat{\lambda},\widehat{\delta}^2,\widehat{\alpha}\big)$ distribution presents a better fit than the normal $N(\widehat{\mu},\widehat{\sigma}^2)$ distribution to the data set under consideration.

2.3. Other stochastic results

Among other results valid for the skew-normal distribution, we shall refer the following ones:

Proposition 2.3. *If Z_1 and Z_2 are independent random variables with standard normal distribution, then $Z_1|_{Z_2\le\alpha Z_1} \sim SN(\alpha)$. Also,*

$$X := \begin{cases} Z_2 & \text{if } Z_1 < \alpha Z_2 \\ -Z_2 & \text{otherwise} \end{cases} \sim SN(\alpha)\,.$$

Proposition 2.3 allows us to write the following algorithm for the generation of random samples, $(Y_1,...,Y_n)$, of size n, from a $SN(\lambda,\delta^2,\alpha)$ distribution.

Algorithm 2.1. Repeat Steps 1.–4. for $i=1$ to n:

1. Generate two independent values, Z_1 and Z_2, from a $N(0,1)$ distribution;

2. Compute $T=\alpha\,Z_2$;

3. The value $X_i = \begin{cases} Z_2 & \text{if } Z_1 < T \\ -Z_2 & \text{otherwise} \end{cases}$ comes from a $SN(\alpha)$;

4. The value $Y_i = \lambda + \delta\,X_i$ comes from a $SN(\lambda,\delta^2,\alpha)$.

Figure 2 presents four histograms associated to samples of size one thousand generated from a $SN(\alpha)$ distribution with shape parameter $\alpha=0,1,2,3$, respectively, together with the pdf's of a normal and of a skew normal distribution fitted to the data by maximum likelihood. From Figure 2 we easily observe that as α increases the differences between the two estimated pdf's become larger, and the normal fit is not the most appropriate to describe the data. Note that, even in potential normal processes, real data are not exactly normal and usually exhibit some level of asymmetry. Thus, in practice, we advise the use of the skew-normal distribution to model the data.

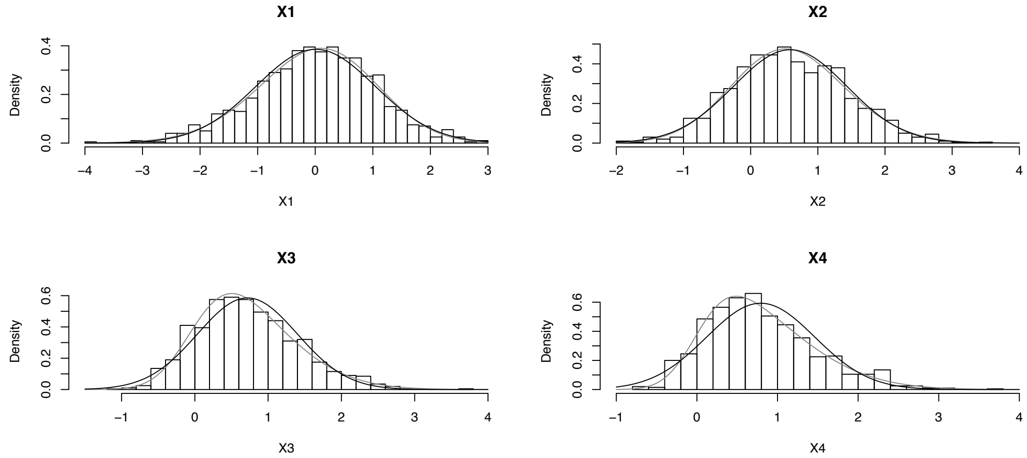

Figure 2: $X_1 \sim SN(0)$, $X_2 \sim SN(1)$, $X_3 \sim SN(2)$, $X_4 \sim SN(3)$. Histograms and estimated pdf's, $SN(\hat{\lambda}, \hat{\delta}, \hat{\alpha})$ and $N(\hat{\mu}, \hat{\sigma})$.

Another result with high relevance for applications, which allows us to design, in Section 4, control charts to monitor specific bivariate normal processes, is the one presented in Proposition 2.4.

Proposition 2.4. *Let (Z_1, Z_2) be a bivariate normal variable, with $E(Z_1) = E(Z_2) = 0$, $V(Z_1) = V(Z_2) = 1$ and $\operatorname{corr}(Z_1, Z_2) = \rho$. Let $T_m = \min(Z_1, Z_2)$ and $T_M = \max(Z_1, Z_2)$, where $\min(\cdot)$ and $\max(\cdot)$ denote the minimum and the maximum operators, respectively.*

i. *If $\rho = 1$, T_m and T_M have a $N(0,1)$ distribution.*

ii. *If $\rho = -1$, T_m and T_M have half-normal distributions, being $T_m \leq 0, \forall m$ and $T_M \geq 0, \forall M$.*

iii. *If $|\rho| \neq 1$, $T_m \sim SN(-\alpha)$ and $T_M \sim SN(\alpha)$, with $\alpha = \sqrt{\dfrac{1-\rho}{1+\rho}}$. In particular, if Z_1 and Z_2 are independent variables, $\rho = 0$, and then, $T_m \sim SN(-1)$ and $T_M \sim SN(1)$.*

3. CONTROL CHARTS BASED ON THE SKEW-NORMAL DISTRIBUTION

The most commonly used charts for monitoring industrial processes, or more precisely, a quality characteristic X at the targets μ_0 and σ_0, the desired mean value and standard deviation of X, respectively, are the Shewhart control charts with 3-sigma control limits. More precisely, the sample mean chart (M-chart), the sample standard deviation chart (S-chart) and the sample range chart (R-chart), which are usually developed under the assumptions of independent and normally distributed data. Additionally, the target values μ_0 and σ_0 are not usually fixed given values, and we have to estimate them, in order to obtain the control limits of the chart.

The ability of a control chart to detect process changes is usually measured by the expected number of samples taken before the chart signals, i.e., by its ARL (*average run length*), together with the *standard deviation of the run length* distribution, SDRL.

Whenever implementing a control chart, a practical advice is that 3-sigma control limits should be avoided whenever the distribution of the control statistic is very asymmetric. In such a case, it is preferable to fix the control limits of the chart at adequate probability quantiles of the control statistic distribution, in order to obtain a fixed ARL when the process is in-control, usually 200, 370.4, 500 or 1000, or equivalently, the desired FAR (*false alarm rate*), i.e., the probability that an observation is considered as out-of-control when the process is actually in-control, usually 0.005, 0.0027, 0.002 or 0.001. General details about Shewhart control charts can be found, for instance, in Montgomery (2005).

In the case of skew-normal processes we do not have explicit formulas for the MLE estimators of the location, scale and shape parameters, and thus, a closed-form for their sampling distribution is not available. The same happens for other statistics of interest, such as, the sample mean, the sample standard deviation, the sample range and the sample percentiles, among others. Thus, to monitor skew-normal processes, the bootstrap control charts are very useful, despite of the disadvantages of a highly time-consuming Phase I. Moreover, many papers, see for instance, Seppala *et al.* (1995), Liu and Tang (1996) and Jones and Woodall (1998), refer that for skewed distributions, bootstrap control charts have on average a better performance than the Shewhart control charts. Other details about the bootstrap methodology and bootstrap control charts can be found, for instance, in Efron and Tibshirani (1993), Bai and Choi (1995), Nichols and Padgett (2006) and Lio and Park (2008, 2010).

3.1. Bootstrap control charts for skew-normal processes

To construct a bootstrap control chart we only use the sample data to estimate the sampling distribution of the parameter estimator, and then, to obtain appropriate control limits. Thus, only the usual assumptions of Phase II of SPC are required: stable process and independent and identically distributed subgroup observations. The following Algorithm 3.1, similar to the ones proposed in Nichols and Padgett (2006) and Lio and Park (2008, 2010), can be used to implement bootstrap control charts for subgroup samples of size n, to monitor the process mean value and the process standard deviation of a skew-normal distribution, respectively. This algorithm can be easily modified in order to implement bootstrap control charts for other parameters of interest.

Algorithm 3.1.

Phase I: Estimation and computation of the control limits

1. From in-control and stable process, observe k, say 25 or 30, random samples of size n, assuming the observations are independent and come from a skew-normal distribution, $SN(\lambda, \delta^2, \alpha)$.

2. Compute the MLE estimates of λ, δ and α, using the pooled sample of size $k \times n$.

3. Generate a parametric bootstrap sample of size n, $(x_1^*, ..., x_n^*)$, from a skew-normal distribution and using the MLEs obtained in Step 2. as the distribution parameters.

4. Select the Step associated to the chart you want to implement:

- **i**. **Two-sided bootstrap M-chart** to monitor the process mean value μ: from the bootstrap subgroup sample obtained in Step 3., compute the sample mean, $\hat{\mu}^* = \overline{x}^*$.
- **ii**. **Upper one-sided bootstrap S-chart** to monitor the process standard deviation σ: from the bootstrap subgroup sample obtained in Step 3., compute the sample standard deviation, $\hat{\sigma}^* = s^*$.

5. Repeat Steps 3.–4., a large number of times, say $B = 10\,000$ times, obtaining B bootstrap estimates of the parameter of interest, in our case, the process mean value or the standard deviation.

6. Let γ be the desired false alarm rate (FAR) of the chart. Using the B bootstrap estimates obtained in Step 5.,

- **i**. Find the $100(\gamma/2)$th and $100(1-\gamma/2)$th quantiles of the distribution of $\hat{\mu}^*$, i.e., the lower control limit LCL and the upper control limit UCL for the bootstrap M-chart of FAR$=\gamma$, respectively.
- **ii**. Find the $100(1-\gamma)$th quantile of the distribution of $\hat{\sigma}^*$, i.e., the upper control limit UCL for the bootstrap S-chart of FAR$=\gamma$. The lower control limit LCL is placed at 0.

Phase II: Process monitoring

7. Take subgroup samples of size n from the process at regular time intervals. For each subgroup, compute the estimate $\overline{x}$ and s.

8. **Decision:**

   i. If $\overline{x}$ falls between LCL and UCL, the process is assumed to be in-control (targeting the nominal mean value); otherwise, i.e., if the estimate falls below the LCL or above the UCL, the chart signals that the process may be out-of-control.

   ii. If s falls below the UCL, the process is assumed to be in-control (targeting the nominal standard deviation); otherwise, the chart signals that the process may be out-of-control.

In order to get information about the robustness of the bootstrap control limits, we must repeat Steps 1.–6. of Algorithm 3.1 a large number of times, say $r = 1000$, and then, compute the average of the obtained control limits, UCL and LCL, and their associated variances. The simulations must be carried out with different subgroup sample sizes, n, and different levels of FAR, γ. From this simulation study one would expect that, when the subgroup sample size n increases, the control limits get closer together, and when FAR decreases, the limits become farther apart.

In this study, using Algorithm 3.1, we have implemented M and S bootstrap control charts for subgroups of size $n = 5$, to monitor the process mean value of a skew-normal process at a target μ_0, and the process standard deviation at a target σ_0. Without loss of generality we assume $\mu_0 = 0$, $\sigma_0 = 1$ and $\alpha = 0$. The main interest is to detect increases or decreases in μ and to detect increases in σ (and not decreases in σ). The FAR of the charts is equal to $\gamma = 0.0027$, which corresponds to an in-control ARL of approximately 370.4. In Phase I we have considered $k = 25$ subgroups of size $n = 5$.

The performance of these bootstrap control charts to detect changes in the process parameters is evaluated in terms of the ARL, for a few different magnitude changes. When the process changes from the in-control state to an out-of-control state we assume that $\mu = \mu_0 \rightarrow \mu_1 = \mu_0 + \delta\sigma_0$, $\delta \neq 0$ and/or $\sigma = \sigma_0 \rightarrow \sigma_1 = \theta\sigma_0$, $\theta > 1$. In this work we have repeated 30 times Steps 1.–6. of Algorithm 3.1, and then, we have chosen a pair of control limits that allow us to obtain an in-control ARL approximately equal to 370.4, discarding the most extreme upper and lower control limits. Our goal, although out of the scope of this paper, is to improve this algorithm in order to obtain more accurate control limits without replication.

Table 2 presents the ARL values of the bootstrap M-chart and S-chart, and the associated standard deviation SDRL. Indeed, as can be seen from Table 2, the bootstrap control charts present an interesting performance, even when we consider small changes. As the magnitude of the change increases, the ARL values decrease fast. Despite of the fact that, in SPC, the classical M and S control charts are much more popular, these charts are good competitors, even for the case of normal data if we have to estimate the target process values.

Table 2: ARL and SDRL of the bootstrap M and S charts for subgroups of size $n = 5$. In-control, $\mu = \mu_0$ $(\delta = 0)$ and $\sigma = \sigma_0$ $(\theta = 1)$; when the process is out-of-control we assume either $\mu \to \mu_1 = \delta \neq 0$ or $\sigma \to \sigma_1 = \theta > 1$.

M-chart $(\mu \to \mu_1)$			S-chart $(\sigma \to \sigma_1)$		
δ	ARL	SDRL	θ	ARL	SDRL
0.0	370.5	(371.8)	1.0	370.7	(369.0)
0.1	371.7	(377.2)	1.1	112.8	(112.3)
0.3	168.3	(169.7)	1.2	45.1	(44.4)
0.5	61.5	(61.2)	1.3	22.5	(22.0)
1.0	8.4	(7.8)	1.4	12.9	(12.2)
1.5	2.4	(1.8)	1.5	8.4	(7.9)
2.0	1.3	(0.6)	1.6	6.1	(5.5)
2.5	1.0	(0.2)	1.7	4.6	(4.1)
−0.1	261.9	(261.4)	1.8	3.7	(3.2)
−0.3	90.7	(89.9)	1.9	3.1	(2.5)
−0.5	33.4	(32.4)	2.0	2.6	(2.1)
−1.0	5.0	(4.6)	2.5	1.6	(1.0)
−1.5	1.8	(1.2)			
−2.0	1.1	(0.4)			
−2.5	1.0	(0.1)			

3.2. Control charts for bivariate normal processes

Let (X_1, X_2) be a bivariate normal process and, without loss of generality, assume that the quality characteristics X_1 and X_2 are standard normal variables, possibly correlated, denoting ρ the correlation coefficient. The result presented in Proposition 2.4 allows us to design control charts based on the statistics $T_m = \min(X_1, X_2)$ and $T_M = \max(X_1, X_2)$ to monitor this bivariate normal process.

These univariate statistics permit the implementation of control charts, here denoted T_m-chart and T_M-chart, to monitor simultaneously two related quality characteristics, alternatives to the multivariate control charts based on the Hotelling (1947) statistic and its variants.

Moreover, these charts can be used when in each time of sampling we only have available one observation from each variable of interest, X_1 and X_2, but can be extended to other situations. For instance, when the distributions of X_1 and X_2 have different parameters, replacing X_1 and X_2 by standardized data, and also when we have samples of size greater than one from each of the variables X_1 and X_2, replacing the observations of the samples by the standardized sample means.

First we have implemented a two-sided T_M chart to detect changes in μ, from $\mu_0 = 0$ to $\mu_1 = \mu_0 + \delta\,\sigma_0$, $\delta \neq 0$, assuming that the standard deviation is kept at $\sigma_0 = 1$. We have considered different magnitude changes, and apart from independent data we have also considered correlated data with different levels of positive and negative correlation. The obtained ARL values are presented in Table 3.

Table 3: ARL of the two-sided T_M-chart. $X_i \sim N(\mu, \sigma)$, $i = 1, 2$, $\text{corr}(X_1, X_2) = \rho$. In-control: $\mu = \mu_0$ $(\delta = 0)$ and $\sigma = \sigma_0 = 1$; when the process is out-of-control, we assume that only $\mu \to \mu_1 = \delta \neq 0$.

ρ δ	0.0	0.1	0.25	0.5	0.9	1.0	−0.25	−0.5
0.0	370.4	370.4	370.4	370.4	370.4	370.4	370.4	370.4
0.1	361.6	359.5	357.1	354.2	352.7	352.9	368.4	379.6
0.3	249.7	248.6	247.4	247.0	251.0	253.1	253.5	258.7
0.5	144.1	144.0	144.4	145.9	152.5	155.2	144.7	145.5
1.0	36.7	36.9	37.3	38.6	42.5	43.9	36.5	36.4
1.5	11.6	11.7	12.0	12.7	14.4	15.0	11.4	11.3
2.0	4.6	4.7	4.9	5.2	6.0	6.3	4.5	4.4
2.5	2.4	2.4	2.5	2.7	3.1	3.2	2.2	2.2
−0.1	330.8	334.7	339.6	345.9	352.1	352.9	318.2	298.2
−0.3	196.1	204.6	215.9	231.6	249.9	253.1	170.6	135.9
−0.5	100.8	107.9	117.9	132.6	151.5	155.2	80.6	56.8
−1.0	21.7	24.1	27.7	33.5	42.0	43.9	15.7	9.7
−1.5	6.7	7.5	8.8	10.9	14.2	15.0	4.8	3.1
−2.0	2.9	3.2	3.7	4.6	6.0	6.3	2.2	1.7
−2.5	1.7	1.9	2.1	2.4	3.1	3.2	1.4	1.2

From these values we observe that as the magnitude changes increases, the ARL decreases, as expected, and that reductions in μ are detected faster than increases. We easily observe that the level of correlation ρ does not have a great impact on the performance of the chart. However, if the quality characteristics, X_1 and X_2, are positively correlated, the ARL's become larger as the level of correlation increases, i.e., the chart becomes less efficient to detect the change.

Table 4: ARL of the upper one-sided T_M-chart. $X_i \sim N(\mu,\sigma)$, $i=1,2$, $\mathrm{corr}(X_1,X_2)=\rho$. In-control: $\mu=\mu_0$ $(\delta=0)$ and $\sigma=\sigma_0$ $(\theta=1)$; when the process is out-of-control, $\mu \to \mu_1=\delta>0$ and/or $\sigma\to\sigma_1=\theta>1$.

δ	θ \ ρ	0.0	0.1	0.25	0.5	0.9	1.0	−0.25	−0.5
0.0	1.0	370.4	370.4	370.4	370.4	370.4	370.4	370.4	370.4
	1.1	156.7	156.9	157.4	159.3	167.1	175.0	156.6	156.6
	1.5	22.2	22.4	22.8	23.8	27.6	31.4	22.0	22.0
	2.0	7.7	7.9	8.1	8.6	10.4	12.2	7.6	7.5
	2.5	4.6	4.7	4.9	5.2	6.4	7.5	4.5	4.4
0.1	1.0	268.0	268.1	268.4	269.3	272.3	273.4	268.0	268.0
	1.1	119.5	119.7	120.2	122.2	129.2	135.5	119.3	119.3
	1.5	19.0	19.2	19.5	20.5	23.8	27.1	18.8	18.8
	2.0	7.1	7.2	7.4	7.9	9.5	11.1	6.9	6.8
	2.5	4.3	4.4	4.6	4.9	6.0	7.1	4.2	4.1
0.3	1.0	144.4	144.5	145.0	146.6	151.4	153.1	144.2	144.2
	1.1	71.1	71.3	71.8	73.4	79.0	83.2	70.9	70.9
	1.5	14.2	14.3	14.6	15.4	18.0	20.4	14.0	13.9
	2.0	5.9	6.0	6.2	6.6	8.0	9.3	5.7	5.7
	2.5	3.8	3.9	4.1	4.4	5.3	6.2	3.7	3.6
0.5	1.0	80.7	80.9	81.4	82.9	87.4	89.0	80.0	80.5
	1.1	43.6	43.8	44.3	45.6	49.8	52.6	43.4	43.4
	1.5	10.7	10.8	11.1	11.7	13.8	15.6	10.5	10.5
	2.0	5.0	5.1	5.3	5.6	6.8	7.9	4.8	4.8
	2.5	3.4	3.5	3.6	3.9	4.7	5.5	3.3	3.2
1.0	1.0	22.2	22.4	22.7	23.6	26.0	26.8	22.0	22.0
	1.1	14.7	14.9	15.2	15.9	17.9	19.0	14.5	14.5
	1.5	5.7	5.8	6.0	6.4	7.6	8.5	5.6	5.5
	2.0	3.4	3.5	3.6	3.9	4.7	5.4	3.3	3.2
	2.5	2.6	2.7	2.8	3.0	3.6	4.2	2.5	2.4
1.5	1.0	7.7	7.8	8.1	8.5	9.6	10.0	7.6	7.5
	1.1	6.1	6.1	6.3	6.7	7.7	8.2	5.9	5.8
	1.5	3.4	3.5	3.6	3.9	4.6	5.1	3.3	3.2
	2.0	2.5	2.5	2.6	2.9	3.4	3.8	2.4	2.3
	2.5	2.1	2.2	2.2	2.4	2.9	3.3	2.0	1.9
2.0	1.0	3.4	3.5	3.6	3.9	4.4	4.6	3.3	3.2
	1.1	3.0	3.1	3.2	3.4	4.0	4.2	2.9	2.8
	1.5	2.3	2.3	2.4	2.6	3.0	3.3	2.1	2.1
	2.0	1.9	2.0	2.1	2.2	2.6	2.9	1.8	1.7
	2.5	1.8	1.8	1.9	2.0	2.4	2.7	1.7	1.6
2.5	1.0	1.9	2.0	2.0	2.2	2.5	2.6	1.8	1.7
	1.1	1.8	1.9	2.0	2.1	2.4	2.5	1.7	1.6
	1.5	1.7	1.7	1.8	1.9	2.2	2.4	1.6	1.5
	2.0	1.6	1.6	1.7	1.8	2.1	2.3	1.5	1.4
	2.5	1.5	1.5	1.6	1.7	2.0	2.2	1.4	1.3

On the other hand, the best performance of the chart is obtained when there is a decrease in the process mean value and the quality characteristics are negatively correlated. This control chart is ARL-biased, and maybe due to this fact, we have observed the chart is not appropriate to detect simultaneous changes in μ and σ. Then, we think sensible to implement an upper one-sided T_M-chart to detect changes in μ and/or σ.

From the ARL values presented in Table 4, we conclude that the upper one-sided T_M-chart presents an interesting performance to detect increases in one of the process' parameters, μ or σ, but also to detect simultaneous changes in these parameters. We observe again that the level of correlation, ρ, between the quality characteristics X_1 and X_2, has a small impact on the performance of the chart. Finally, the lower one-sided T_m-chart has a similar performance to detect changes from $\mu \to \mu_1 < 0$ and/or $\sigma \to \sigma_1 > 1$.

4. AN APPLICATION IN THE FIELD OF SPC

In this section we consider an application to real data from a cork stopper's process production. The objective is modeling and monitoring the data from this process, for which we know the corks must have the following characteristics:

Table 5: Technical specifications: cork stoppers caliber 45 mm × 24 mm.

Physical quality characteristic (mm)	Mean target	Tolerance interval
Length	45	45 ± 1
Diameter	24	24 ± 0.5

For this purpose we have collected from the process production a sample, of size $n = 1000$, of corks' lengths and diameters. First, we fitted a normal and a skew-normal distribution to the data set. Looking to the histograms obtained from the sample data, presented in Figure 3, both fits seem to be adequate, and the differences between the two pdf's are small.

Then, to test the underlying data distribution, we have used the Shapiro test of normality and the Kolmogorov–Smirnov (K-S) for testing the skew-normal distribution. Unexpectedly, although the fits seem to be similar, from these tests of goodness-of-fit the conclusions are different: the normality for the length's and diameter's data is rejected, for the usual levels of significance (5% and 1%), while

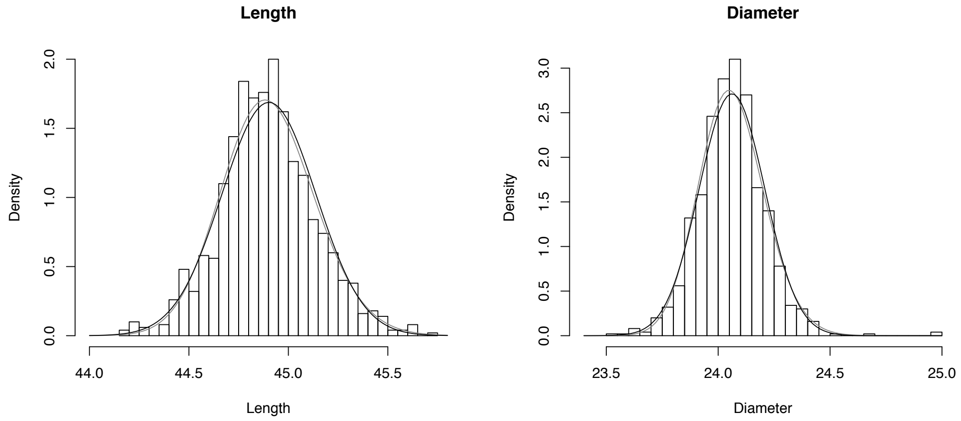

Figure 3: Histograms and estimated pdf's of the normal and skew-normal fit to the length and diameter data.

the skew-normal distribution is not rejected. The p-values for the Shapiro and K-S tests are presented in Table 6. Looking to the maximum likelihood estimates of some parameters of interest of the fitted distributions, presented in Table 7, we observe that there exist some differences between the estimates obtained for the mean value and the location, as well as between the estimates obtained for the standard deviation and the scale. Moreover, the data exhibit some skewness and the estimate of the shape parameter is not very close to zero, as it may happen in the case of normal data.

Table 6: P-value's of the Shapiro test of normality and of the Kolmogorov–Smirnov (K-S) for testing a skew-normal.

	Length	Diameter	Decision
Shapiro	0.0018	0.0052	Normality rejected*
K-S	0.2376	0.2923	The skew-normal distribution is not rejected*

* Conclusion for a level of significance of 5% and 1%.

Table 7: Maximum likelihood estimates of some parameters of interest of the fitted distributions.

Data	Location	Scale	Shape	Mean	Standard deviation	Skewness
Length	44.7329	0.2907	1.0720	44.9025	0.2361	0.1591
Diameter	23.9526	0.1830	1.1358	24.0622	0.1466	0.1795

To confirm the conclusions obtained by the previous tests of goodness-of-fit we have used the likelihood ratio test presented in subsection 2.2. As we obtained an observed value $-2\ln\Lambda_{\text{obs}} > 3.84$ (for length's and diameter's data), there is a strong evidence that the $SN\big(\widehat{\lambda}, \widehat{\delta}, \widehat{\alpha}\big)$ distribution presents a better fit than the normal $N(\widehat{\mu}, \widehat{\sigma}^2)$ distribution, for a level of significance of 5%.

Finally, based on Algorithm 3.1, we illustrate the implementation of the M and S bootstrap control charts for subgroups of size $n = 10$ to monitor the process mean value and the process standard deviation of the corks' diameter. The Phase I data set consists of $k = 25$ subgroups of size $n = 10$, and we have been led to the following control limits: $\text{LCL} = 23.936484$ and $\text{UCL} = 24.215071$ for the M-chart, and $\text{UCL} = 0.249708$ for the S-chart. From these subgroups we have also estimated the control limits of the corresponding Shewhart charts, assuming normality, here denoted by LCL_{sh} and UCL_{sh}, and the center line, CL. We obtained $\text{LCL}_{\text{sh}} = 23.947788$, $\text{UCL}_{\text{sh}} = 24.200532$ and $\text{LC} = 24.07416$ for the M-chart, and $\text{UCL}_{\text{sh}} = 0.223152$ and $\text{CL} = 0.129573$ for the S-chart.

In Figure 4 we picture the M and S bootstrap control charts together with the corresponding Shewhart charts with estimated control limits, for use in Phase II of process monitoring. We immediately observe that the bootstrap control limits, LCL and UCL, are set up farther apart than the control limits of the Shewhart M and S charts, LCL_{sh} and UCL_{sh}.

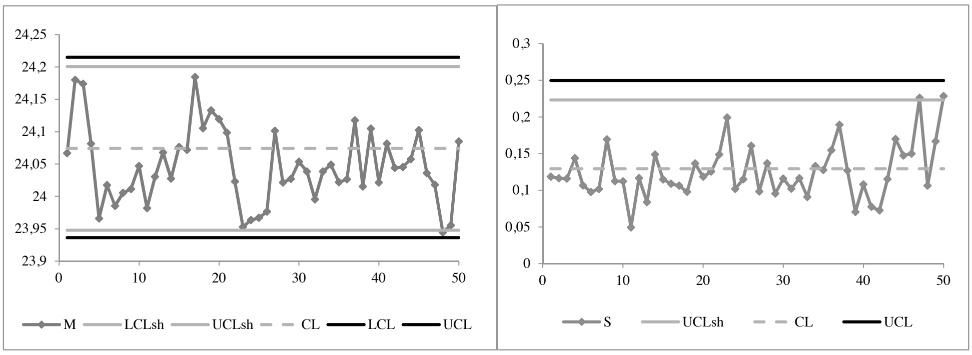

Figure 4: Bootstrap M and S charts together with the corresponding Shewhart charts with estimated control limits.

The Phase II data set used in this illustration consists of $m = 50$ subgroups of size $n = 10$, supposed to be in-control. We have computed the statistics $\overline{x}$ and s associated to these 50 subgroups, and we have plotted them in the charts (here denoted M and S). While the bootstrap charts do not signal changes in the process parameters, the Shewhart charts indicate that the process is out-of-control, due to changes in the process mean value and standard deviation.

5. SUMMARY AND RECOMMENDATIONS

Designing a control chart under the assumption of skew-normal data and with control limits estimated via bootstrapping adds a relevant contribution to the SPC literature in what concerns the implementation of robust control charts. The use of this family of distributions, that includes the Gaussian as a particular member, allows more flexibility to accommodate uncontrollable disturbances in the data, such as some level of asymmetry or non-normal tail behavior. Moreover, despite of the fact that, in SPC, the classical M and S control charts are much more popular, these charts are good competitors, even for the case of normal data if we have to estimate the target process values.

In order to integrate it within a quality process control system, we can suggest, for instance, an a priori analysis of the process data. A simple boxplot representation with the Phase I data subgroups can anticipate an underlying data distribution that exhibits some level of asymmetry, possibly with some outliers, and in this case, we suggest the use of the proposed bootstrap control charts instead of the traditional Shewhart-type charts implemented for normal data.

Among other issues not addressed in this paper, the proposed control charts should be compared to the existing parametric and nonparametric control charts. Also important is to study the effect of increasing the Phase I sample on the performance of the chart, as well as the determination of the minimum number m of subgroups in Phase I, the sample size n and the number of replicates bootstrap r we must consider in order to have charts with the same performance for the scenarios of known and unknown process parameters. Finally, an exhaustive and comparative study about the performance of control charts based on the skew-normal and on the normal distributions must be carried out to have an idea about the range of values of the shape parameter α of the skew-normal distribution for which the performance of the two charts differ significantly. This will help a practitioner to make a decision on which control chart is preferable to suit his needs.

ACKNOWLEDGMENTS

This research was partially supported by national funds through the Fundação Nacional para a Ciência e Tecnologia, Portugal — FCT, under the PEst-OE/MAT/UI0006/2011 project.

We would like to thank to the two anonymous referees the very helpful comments and suggestions for future research.

REFERENCES

[1] Abtahi, A.; Towhidi, M. and Behboodian, J. (2011). An appropriate empirical version of skew-normal density, *Statistical Papers*, **52**, 469–489.

[2] Azzalini, A. (1985). A Class of distributions which includes the normal Ones, *Scandinavian J. of Statistics*, **12**, 171–178.

[3] Azzalini, A. (1986). Further results on a class of distributions which includes the normal ones, *Statistica*, **XLVI**, 199–208.

[4] Azzalini, A. (2005). The skew-normal distribution and related multivariate families, *Scandinavian J. of Statistics*, **32**, 159–188.

[5] Azzalini, A. (2011). R package 'sn': The skew-normal and skew-t distributions (version 0.4-17). URL `http://azzalini.stat.unipd.it/SN`.

[6] Azzalini, A. and Capitanio, A. (1999). Statistical applications of the multivariate skew normal distributions, *J. R. Stat. Soc.*, series B, **61**, 579–602.

[7] Azzalini, A. and Regoli, G. (2012). Some properties of skew-symmetric distributions, *Annals of the Institute of Statistical Mathematics*, **64**, 857–879.

[8] Bai, D.S. and Choi, I.S. (1995). $\overline{X}$ and R control charts for skewed populations, *J. of Quality Technology*, **27**(2), 120–131.

[9] Chakraborti, S.; Human, S.W. and Graham, M.A. (2011). *Nonparametric (distribution-free) quality control charts.* In "Methods and Applications of Statistics: Engineering, Quality Control, and Physical Sciences" (N. Balakrishnan, Ed.), 298–329.

[10] Chakraborti, S.; Human, S.W. and Graham, M.A. (2009). Phase I statistical process control charts: an overview and some results, *Quality Engineering*, **21**(1), 52–62.

[11] Efron, B. and Tibshirani, R. (1993). *Introduction to the Bootstrap*, Chapman and Hall, New York.

[12] Fernandez, C. and Steel, M.F.J. (1998). On Bayesian modeling of fat tails and skewness, *J. Am. Stat. Assoc.*, **93**, 359–371.

[13] Hoaglin, D.M.; Mosteller, F. and Tukey, J.W. (1983). *Understanding Robust and Exploratory Data Analysis*, Wiley, New York.

[14] Hotelling, H. (1947). *Multivariate quality control illustrated by air testing of sample bombsights.* In "Selected Techniques of Statistical Analysis" (C. Eisenhart, M.W. Hastay and W.A. Wallis, Eds.), pp. 111–184, McGraw-Hill, New York.

[15] Human, S.W. and Chakraborti, S. (2010). A unified approach for Shewhart-type phase I control charts for the mean, *International Journal of Reliability, Quality and Safety Engineering*, **17**(3), 199–208.

[16] Jamalizadeb, A.; Arabpour, A.R. and Balakrishnan, N. (2011). A generalized skew two-piece skew normal distribution, *Statistical Papers*, **52**, 431–446.

[17] Jones, L.A. and Woodall, W.H. (1998). The performance of bootstrap control charts, *J. of Quality Technology*, **30**, 362–375.

[18] Lio, Y.L. and Park, C. (2008). A bootstrap control chart for Birnbaum–Saunders percentiles, *Qual. Reliab. Engng. Int.*, **24**, 585–600.

[19] Lio, Y.L. and Park, C. (2010). A bootstrap control chart for inverse Gaussian percentiles, *J. of Statistical Computation and Simulation*, **80**(3), 287–299.

[20] Liu, R.Y. and Tang, J. (1996). Control charts for dependent and independent measurements based on the bootstrap, *JASA*, **91**, 1694–1700.

[21] Montgomery, D.C. (2005). *Introduction to Statistical Quality Control*, Wiley, New York.

[22] Nichols, M.D. and Padgett, W.J. (2006). A bootstrap control chart for Weibull percentiles, *Qual. Reliab. Engng. Int.*, **22**, 141–151.

[23] O'Hagan, A. and Leonard, T. (1976). Bayes estimation subject to uncertainty about parameter constraints, *Biometrika*, **63**, 201–202.

[24] Owen, D.B. (1956). Tables for computing bivariate normal probabilities, *Ann. Math. Statist.*, **27**, 1075–1090.

[25] Seppala, T.; Moskowitz, H.; Plante, R. and Tang, J. (1995). Statistical process control via the subgroup bootstrap, *J. of Quality Technology*, **27**, 139–153.

REVSTAT – Statistical Journal
Volume 11, Number 1, March 2013, 105–119

IMPROVING SSA PREDICTIONS BY INVERSE DISTANCE WEIGHTING

Authors: Richard O. Awichi
– Uganda Martyrs University, Nkozi, Uganda
ichbinrao@gmail.com

Werner G. Müller
– Johannes Kepler University, Linz, Austria
werner.mueller@jku.at

Abstract:

- This paper proposes a method of utilizing spatial information to improve predictions in one dimensional time series analysis using singular spectrum analysis (SSA). It employs inverse distance weighting for spatial averaging and subsequently multivariate singular spectrum analysis (MSSA) for enhanced forecasts. The technique is exemplified on a data set for rainfall recordings from Upper Austria.

Key-Words:

- *singular spectrum analysis; inverse distance weighting; spatio-temporal predictions.*

AMS Subject Classification:

- 49A05, 78B26.

1. INTRODUCTION

Singular spectrum analysis (SSA) is a recently popularized tool for time series analysis, cf. [10]. The origins of SSA can be traced to [2, 4, 6]. More information about the history of SSA can be found in [22]. It is a model free approach to time series analysis and literally any time series with a notable structure can be analysed using SSA. Indeed it has a wide area of applications ranging from mathematics and physics [10], to economics and financial mathematics [13, 14], environmental sciences [15], social sciences [12], and medicine [7]. It is now implemented under various software platforms, here we use Rssa, see [9] and a program called CaterpilarSSA as can be downloaded from `http://www.gistatgroup.com/cat/programs.html`. The aim of SSA is twofold:

i) To make a decomposition of the original series into a sum of a small number of independent and interpretable components such as a slowly varying trend, oscillatory components and a structure less noise;

ii) To reconstruct the decomposed series so as to make predictions without the noise component.

MSSA is an extension of SSA and takes advantage of the (delay) embedding procedure to obtain a similar formulation as SSA, albeit with larger matrices for multidimensional time series. It has previously been successfully applied to the study of climate fields, see [18]. Here we will employ it to jointly model an original time series with a spatial average of which we believe will improve predictions by pooling spatially dependent information.

One of the simplest but effective ways of generating spatial averages is inverse distance weighting, which was first introduced, incidentally also for the analysis of rainfall data in [11]. It was subsequently propagated in [20] and became thereafter one of the most popular spatial interpolation techniques (cf. eg. [16]).

Section 2 is devoted to reviewing the basics of SSA. Section 3 discusses forecasting, while Section 4 briefly presents MSSA, an extension of the SSA techniques to multivariate data and introduces a method of incorporating spatial dependence to improve forecasts. The application is presented in Section 5 and conclusions appear in Section 6.

2. SINGULAR SPECTRUM ANALYSIS

Most classical time series models devised for analysis and forecasting are based on restrictive assumptions of normality, linearity and stationarity, cf. [3].

A number of time series are deterministic, linear and dynamical systems thus allowing linear models to be used for modelling and forecasting. However, many time series exhibit nonlinear behaviour and therefore would require a method that works well for both linear and nonlinear, stationary and nonstationary data sets. SSA is one such technique.

2.1. A brief review of SSA

The Basic SSA, as it is commonly referred to, has two main stages: Decomposition and Reconstruction; each of which consists of two steps as described below. The main concept in SSA is the aspect of separability of the original time series into signal and noise so that the analysis and forecasting can be done on signal in the absence of noise. Separability will be mentioned again later. In the following discussion, we follow the approach in [10, Chapter 1].

Let $F_N = \{f_1, f_2, \ldots, f_N\}$ be a real valued, nonzero (at least one $f_i \neq 0$) time series data of sufficient length N without missing values.

Stage 1: *Decomposition*

Step 1: Embedding

This (standard) time series procedure maps the one dimensional time series, F_N into multidimensional lagged vectors, $X_1 : \cdots : X_K$, where

$$X_i = (f_1, \ldots, f_{i+L-1})^T \in R^L , \qquad 1 \leq i \leq K \quad \text{and} \quad K = N - L + 1 \ .$$

The single most important parameter of embedding is the window length, L, an integer such that $2 < L < N$. This parameter should always be large enough to permit reasonable separability. It should not be greater the $N/2$ for optimum results. See [8] for more on the choice of parameters for SSA. The vectors X_i, called the lagged vectors or L lagged vectors (to emphasize their dimension) form the K columns of the trajectory matrix X, i.e. $X = [X_1 : \cdots : X_K]$.

Specifically X is given as follows:

$$X = \begin{pmatrix} f_1 & f_2 & f_3 & \cdots & f_K \\ f_2 & f_3 & f_4 & \cdots & f_{K+1} \\ f_3 & f_4 & f_5 & \cdots & f_{K+2} \\ \vdots & \ddots & \vdots & \ddots & \vdots \\ f_L & f_{L+1} & f_{L+2} & \cdots & f_N \end{pmatrix} .$$

The $L \times K$ matrix X is a Hankel matrix, i.e. the elements along the anti-diagonal, $i + j =$ constant are equal, for the i^{th} row and j^{th} column.

Step 2: Singular Value Decomposition, SVD

This decomposes the trajectory matrix X and represents it as a sum of elementary matrices (rank-one bi-orthogonal). This is done by:

i) Calculating the matrix $S = XX^T$.

ii) Obtaining eigenvalues, λ_i of S such that $\lambda_1 \geq \lambda_2 \geq \cdots \geq \lambda_L \geq 0$. Since S is positive definite, the eigenvalues are positive.

iii) For each λ_i, calculate U_i and V_i, the left and right singular vectors of X. The U_is are orthonormal system of eigenvectors corresponding to each λ_i such that $\langle U_i, U_j \rangle = 0$, $i \neq j$ (orthogonality) and $\|U_i\| = 1$ (unit norm property) and $V_i = X^T U_i / \sqrt{\lambda_i}$.

iv) Set $d = \max(i \colon \lambda_i > 0) = \operatorname{rank}(X)$. Then $X_i = \sqrt{\lambda_i}\, U_i V_i^T$ $(i = 1, \ldots, d)$, and the SVD of the trajectory matrix represents it as a sum of the X_i, i.e.:

$$\begin{aligned} X &= \sum_{i=1}^{d} X_i \\ &= X_1 + X_2 + \cdots + X_d \; . \end{aligned} \tag{2.1}$$

The collection $(\sqrt{\lambda_i}, U_i, V_i)$ is called the i^{th} eigentriple of X, $\sqrt{\lambda_i}$ are the singular values of X and the set $\{\sqrt{\lambda_i}\}_{i=1}^{d}$ is the spectrum of X.

The ratio $\lambda_i / \sum\limits_{i=1}^{d} \lambda_i$ is the characteristic contribution (or its share) of X_i to (2.1). The first eigenvalue has the largest contribution and the last has the smallest.

If all the eigenvalues have multiplicity one, then (2.1) is uniquely determined.

Stage 2: *Reconstruction*

Step 3: Grouping

This corresponds to splitting the elementary matrices X_i into several groups and summing the matrices within each group. If $I = i_1, \ldots, i_p$ be one such group, then the matrix X_I corresponding to the group I is defined as:

$$X_I = X_{i_1} + \cdots + X_{i_p} \; .$$

For m such groups (disjoint), then X will be given as:

$$X = X_{I_1} + \cdots + X_{I_m} \; . \tag{2.2}$$

Matrices X_{I_i} are called *resultant matrices* and the procedure of choosing the sets $I_1, \ldots, I_m$ is called the *eigentriple grouping*.

The contribution of component X_I in (2.2) is measured by the share of the corresponding eigenvalues, i.e. $\sum\limits_{i \in I} \lambda_i / \sum\limits_{i=1}^{d} \lambda_i$.

Step 4: Diagonal Averaging

This (last) step transfers each resultant matrix into a time series, which is an additive component of the initial (original) series, F_N. If z_{ij} stands for an element of a matrix Z, then the k^{th} term of the resulting series is obtained by averaging z_{ij} over all i, j such that $i + j = k + 2$ ([10, page 17, 24], [12, page 242]). This is diagonal averaging or Hankelization of the matrix Z. The result of the Hankelization of a matrix Z is the matrix $\mathcal{H}Z$. Diagonal averaging is a linear operation and maps the trajectory matrix of the initial series into the original series itself, i.e. it transfers each matrix I into a time series which is an additive component of the initial series F_N.

2.2. Separability

As mentioned earlier, the main concept in studying SSA properties is separability. This entails how well the components of the time series can be separated from each other to allow forecasting to be meaningfully done and also reliable construction of confidence bounds. Any time series may comprise trend (slowly varying component), periodic or quasi periodic components (like seasonal variations or harmonics generally) and noise. These may be generalized into signal and noise components. SSA decomposition of the series F_N can only be successful if the resulting additive components of the series are approximately separable from each other, [10, 12].

If a time series F_N can be split as $F_N = F_N^{(1)} + F_N^{(2)}$, then the matrix terms of the SVD step can be split into $X^{(1)}$ and $X^{(2)}$ respectively, i.e. $X = X^{(1)} + X^{(2)}$. This would imply that each row of $X^{(1)}$ is orthogonal to each row of $X^{(2)}$. Since rows (and columns) of the trajectory matrix X are themselves subseries of the initial series, the orthogonality condition of the rows of $X^{(1)}$ and $X^{(2)}$ is the condition of orthogonality of any subseries of length L and $K = N - L + 1$ of the series $F_N^{(1)}$ to any subseries of the same length, $F_N^{(2)}$. If this holds, then $F_N^{(1)}$ and $F_N^{(2)}$ are said to be weakly separable.

In geometrical terms, $F_N^{(1)}$ and $F_N^{(2)}$ are separable if and only if the subspace $\ell^{(L,1)}$ spanned by the columns of $X^{(1)}$ is orthogonal to the subspace $\ell^{(L,2)}$ spanned by the columns of $X^{(2)}$. One way to enhance separability of the series is auxiliary information about the series to help in choosing the window length, for example, if it is known that there is a seasonal component whose period is an integer, it is advisable to choose the window length which is a factor of the period, [10, page 44]. To choose eigentriples, one may use the graph of the logarithms of eigenvalues in which explicit plateau in the eigenvalue spectra prompts ordinal numbers of the eigentriple and a slowly decreasing sequence of singular values corresponds to noise components.

Another way to measure the separability between two series components, $F_N^{(1)}$ and $F_N^{(2)}$ (i.e. if $F_N = F_N^{(1)} + F_N^{(2)}$) is to calculate the weighted correlation or w-correlations between the two using the formula

$$\rho_{12}^{w} = \frac{\langle F_N^{(1)}, F_N^{(2)} \rangle_w}{\|F_N^{(1)}\|_w \, \|F_N^{(2)}\|_w} \ ,$$

where $\|F_N^{(i)}\|_w = \sqrt{\langle F_N^{(i)}, F_N^{(i)} \rangle_w}$, $i = 1, 2$, $\langle F_N^{(1)}, F_N^{(2)} \rangle_w = \sum\limits_{i=0}^{N-1} w_i f_i^{(1)} f_i^{(2)}$, and the weights w_i defined as follows:

Let $L^\star = \min(L, K)$ and $K^\star = \max(L, K)$. Then,

$$w_i = \begin{cases} i + 1 & \text{for} \ \ 0 \leqslant i \leqslant L^\star - 1 \ , \\ L^\star & \text{for} \ \ L^\star \leqslant i \leqslant K^\star \ , \\ N - i & \text{for} \ \ K^\star \leqslant i \leqslant N - 1 \ . \end{cases}$$

A natural hint for grouping is the matrix of the absolute values of the w-correlations corresponding to a full decomposition. If the absolute value of the w-correlation is small then the corresponding series are almost w-orthogonal and is said to be weakly separable. The series $F^{(1)}$ and $F^{(2)}$ are w-orthogonal if $\langle F_N^{(1)}, F_N^{(2)} \rangle_w = 0$, [10, 12].

Separability is analogous to independence of random variables whence the covariance and correlation between such random variables are zero, [5, Section 4.5].

3. FORECASTING WITH SSA

Details of SSA Forecasting can be found in [10, Chapter 2, 5] and in [19]. We have three basic conditions:

1) Time series has structure.

2) A mechanism identifying this structure is found.

3) A method of time series continuation, based on the identified structure is available.

In SSA, forecasting is done through application of linear recurrent formulae (LRF) or equations. The class of series governed by LRF is rather wide; it contains harmonics, polynomials and exponential series and is closed under term-by-term addition and multiplication, [12]. An infinite series is governed by some LRF if and only if it can be represented as a linear combination of products of exponential, polynomial and harmonic series. (The signal component of a separable time series is always a linear combination of these series.)

An important property of SSA decomposition is that the original series satisfies an LRF of the form $f_n = a_1 f_{n-1} + \cdots + a_d f_{n-d}$ for some dimension d; $a_1, \ldots, a_d$ are constants.

Thus for any N and L, there are at most d nonzero singular values in the SVD of the trajectory matrix X and so even if L and $K = N - L + 1$ are larger than d, we need at most d matrices X_i to reconstruct the series. If f_n satisfies the LRF above, it will always be represented as a sum of products of exponentials, polynomials and harmonics, [10].

Alternatively put, if $r < L$, (r = number of terms in the SVD step), then the series satisfies some LRF of some dimension $d \leqslant r$. This result also implies that if $\dim(\ell_r) < L$, then the series satisfies a natural LRF of dimension $L - 1$. Any such series satisfying an LRF can then be forecast for an arbitrary number of steps using the LRF.

The selection of the resultant matrices in the third step of Basic SSA algorithm implies selection of the r-dimensional space $\ell_r \in R^L$ spanned by the corresponding left singular vectors and if ℓ_r is non-vertical, it produces an appropriate LRF which can be used in forecasting.

An LRF that governs a series with the help of SSA may be found as follows. Let d be minimal dimension of all LRFs governing a time series F_N. If the window length L is greater than d and N is large enough, then the trajectory space of F_N is d dimensional. The trajectory space determines an LRF of dimension $L - 1$ that governs the time series. If this LRF is applied to the last terms of the series, a forecast of the series is obtained. The same idea works for an additive component $F_N^{(1)}$ of F_N. The assumption here is that $F_N^{(1)}$ is (strongly) separable from the residual $F_N^{(2)} = F_N - F_N^{(1)}$ for the selected window length L. Normally (strong) separability of the components of a series implies that each component satisfies some LRF, [10, Chapter 6]. If $F_N^{(2)}$ is noise, then forecasting is done for $F_N^{(1)}$. Thus using a selected set of eigentriples, estimation can be performed on $F_N^{(1)}$ and its trajectory space. The basic inputs for the SSA LRF for a series F_N include the window length L, N, linear space ℓ_v which is not a vertical space and the number M of points to forecast. The linear space is used to obtain an orthonormal basis $P_1, \ldots, P_r$ used in the forecasting process.

Forecasting is also closely linked to separability of the series as mentioned above. If $F_N = F_N^{(1)} + F_N^{(2)}$, then forecasting is done for the signal $F_N^{(1)}$ in the presence of the noise component $F_N^{(2)}$ which is given as $F_N^{(2)} = F_N - F_N^{(1)}$.

[10, pages 95–107] gives an account of the forecasting algorithm and properties of LRFs.

Construction of confidence bounds can be done by either the empirical method or the bootstrap technique. The empirical confidence intervals are constructed for the entire series, which is assumed to have the same structure in the future. Bootstrap bounds are obtained for the continuation of the signal, [10, 12].

4. MSSA WITH INVERSE DISTANCE WEIGHTING

Data mining is an automated search for knowledge hidden in large collections of data set attributes. In environmental science and other areas where space-time behaviour is an important focus of investigation, it is not uncommon to have attributes whose values change with space and time and quite often, due to spillovers or unobservable variables or omitted factors. This leads to spatial dependence that subsequently influence data analysis.

In light of spatial dependence, an inverse distance weighting technique, see [1, 20], is proposed as a means of incorporating spatial information to improve the prediction. We construct an additional explanatory variable by taking spatially weighted averages

$$\bar{y}_t = \sum_{i=1}^{n} w_i \, y_{it} \qquad \text{where} \quad w_i = \frac{1/d_i}{\sum\limits_{i=1}^{n} (1/d_i)} \; ,$$

with d_i denoting distances between the target location and the i^{th} measurement site.

Multivariate (or multichannel) Singular Spectrum Analysis (MSSA) is an extension of SSA to multidimensional data.

Assume that $y_j = \left(y_j^{(1)}, \ldots, y_j^{(m)}\right)$ is an m-variate time series, L the window length, $X^{(i)}$ $(i = 1, \ldots, m)$ the trajectory matrices of the one dimensional time series $\{y_j^{(i)}\}$ $(i = 1, \ldots, m)$, the trajectory matrix X of the multivariate series is given as $X = (X^{(1)}, \ldots, X^{(r)}, \ldots, X^{(m)})$; [10, 17]. Note that X is now an $L \times mK$ block Hankel matrix (there are m blocks of $X^{(i)}$ matrices).

The aims and techniques of MSSA are straightforward extensions to those of SSA and so are the algorithms. Hence we refrain from any further discussion regarding the theory of MSSA. For more details see [21, 17]. The advantage of MSSA over SSA, however, is that it automatically utilizes dependencies among the time series in the analysis. Consequently, the quality of MSSA forecasts are typically improved when the series are more strongly correlated.

The above pooling of the spatial information by inverse distance weighting leads to a new time series $\bar{y}_t$ that can be used as a kind of covariable to the Linz rainfall series to improve the predictions. We thus now employ a MSSA with the original Linz series complemented by the pooled one, i.e. $m = 2$ in this case. Of course this can be performed for all the time series, not only the Linz one and even jointly, but we will refrain from this for the sake of expository simplicity.

5. THE APPLICATION

The complete data set consisted of $N = 192$ monthly recordings of rainfall at several locations in Upper Austria for the period 1994 Jan to 2009 Dec (see Figure 1 for a depiction of the measurement locations with the solid dot indicating Linz). The data is provided by the Zentralanstalt für Meteorologie in Austria and is described in more detail in [15].

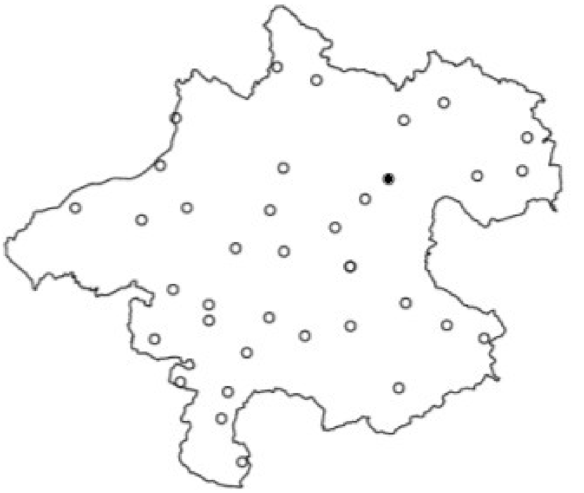

Figure 1: Upper-Austrian rainfall measurement network.
Empty circle indicate measurement locations, solid circle Linz.

The time series graph Figure 2 shows the general behaviour of the logarithm of Linz rainfall series and the reconstructed series for the period above. Since it is annual data, it provides auxiliary information for the choice of the window length as a factor of the period, 12 monthlies, hence the choice of $L = 96 = N/2$ as the standard window length for the analysis. It can be inferred from the figure that the grouping employed yielded a reconstructed series fairly close to the original hence rather reliable in-sample predictions.

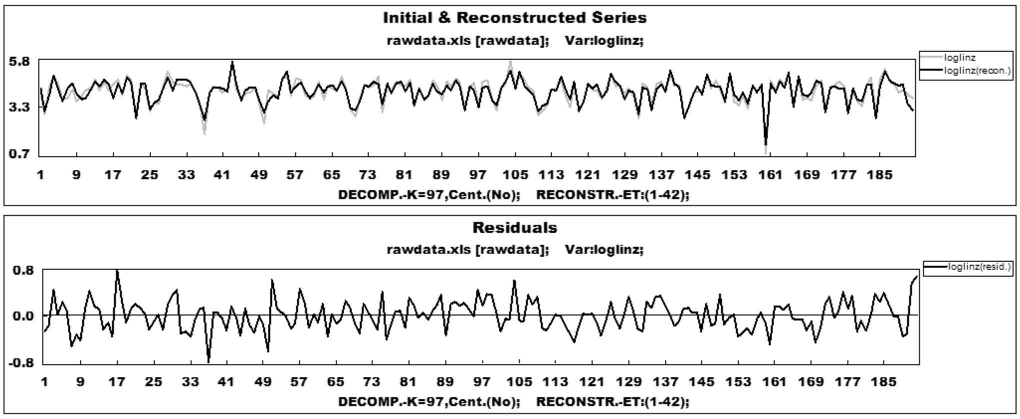

Figure 2: Initial (grey) and SSA reconstructed (black) series for Linz monthly rainfall data in logs; residuals below.

The plot in Figure 3 gives the eigenvalue graph. This graph is a plot of logarithms of the first 42 eigenvalues used in the reconstruction stage. As mentioned earlier, it shows the plateau for ordinal numbers in the eigentriple grouping. The remaining eigenvalues constitute the noise series and have not been included here. This graph shows a high percentage contribution of the first eigenvalue with a plateau for the second and third eigenvalues implying a particular type of signal. The other eigenvalues are gradually and slowly decreasing implying a strong tendency to noise after the 42$^{\text{nd}}$ eigenvalue.

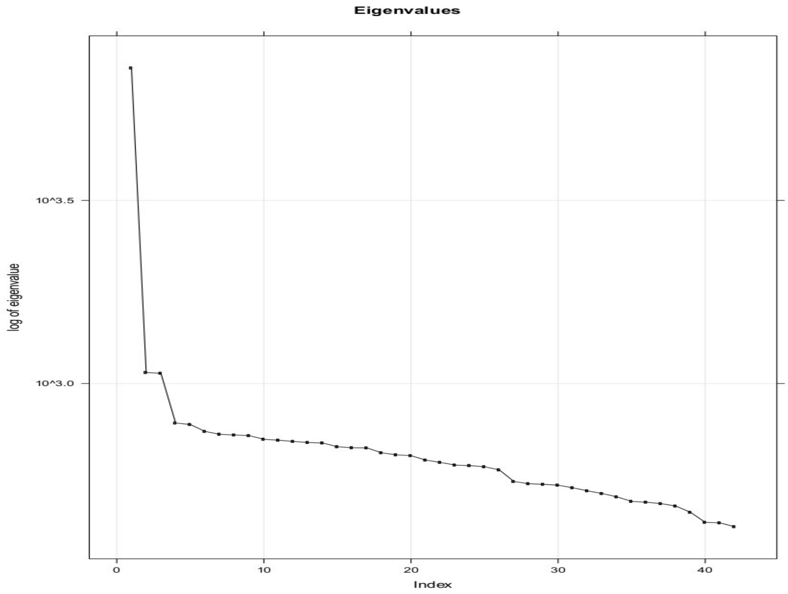

Figure 3: Eigenvalue graph for the first 42 eigenvalues used in the reconstruction stage of MSSA.

The graph in Figure 4 shows the w-correlations for the reconstructed components on a 20 grade grey scale from white to black corresponding to absolute values of correlations from 0 to 1, see [12, 10]. It shows the different eigenvalue groupings, even for the eigenvalues corresponding to the noise. This graph further illustrates the results of the grouping step and confirms the separation of signal from the noise for the original series as it clearly marks off the lags below 42. Furthermore some other possible eigentriple groupings were tried but the predictions were not better than for this particular grouping.

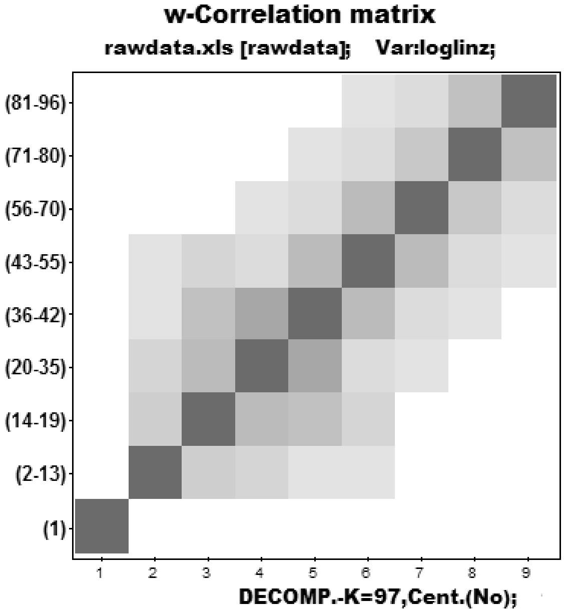

Figure 4: Matrix of w-correlations from the reconstructed components (1–42) and error (43–96) in the MSSA.

The following graphs in Figure 5 show the time series for the spatially pooled series and its effect on the Linz data series for the MSSA analysis. For the MSSA analysis we used two series, the Linz data and the inverse distance weighted average by employing the Euclidean distances d_i between Linz and each of the 36 other locations. Thus the nearer the locations to Linz, the stronger the weighting and vice versa. For missing values in the data, a new weight is calculated by excluding the corresponding distance measure from the w_is.

The in-sample SSA prediction was done with solely the Linz data to obtain the SSA prediction of Figure 1. Its root mean square error ($RMSE_{SSA}$) was found to be 0.247. The weighted average, using the inverse distance technique, was then included as a second series to study its effects, due to spatial spillover, on the Linz data for the MSSA prediction. This is shown in Figure 5. Its $RMSE_{MSSA}$ was found to be 0.245 and slightly less than $RMSE_{SSA}$. This indicates that the suggested technique of including spatial dependence in the SSA analysis may actually improve the forecasts. However, our results from other groupings show a less clear picture, particularly if not the standard window length of $L = N/2$ was used, and in further work, we want to investigate the capabilities of MSSA performing ensemble spatio-temporal predictions for the whole network of stations.

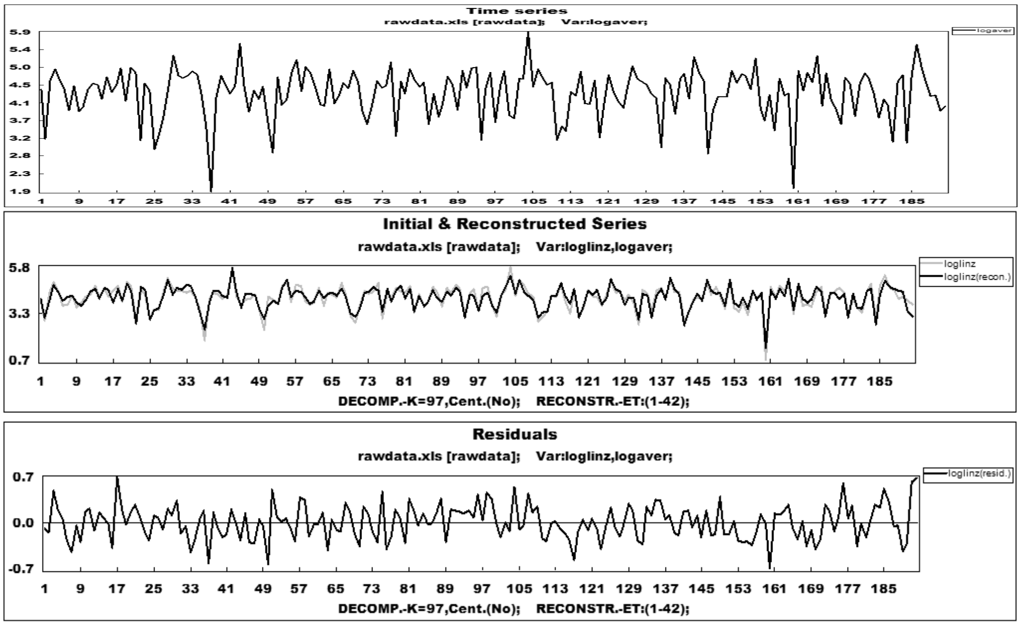

Figure 5: Time series for the inversely distance weighted data. Initial (black) and MSSA reconstructed (grey) series for Linz monthly rainfall data in logs; residuals below.

6. CONCLUSION

This short presentation illustrates the basic capabilities of SSA in separating the components of a time series and in forecasting without any assumptions about the time series data. It brings out the key advantage of the methodology of SSA in applied statistics: that of inference and prediction without specifying any particular model structure. Its extension to multidimensional data analysis, the MSSA is yet another elegant procedure to handle multidimensional data analysis without necessarily pre-specifying dependence structures. The suggested method of exploiting spatial dependence within the concept of MSSA is promising, particularly for the in-sample imputation of missing data. As mentioned earlier, we require further studies and refinements for assessing the capabilities of the technique for the out-of-sample predictions.

ACKNOWLEDGMENTS

We are grateful to the two anonymous referees for their attentive and detailed remarks which helped to considerably improve the paper.

REFERENCES

[1] Bakkali, S. and Amrani, M. (2008). About the use of spatial interpolation methods to denoising Moroccan resistivity data phosphate ”disturbances” map, *Acta Montanistica Slovaca*, **13**, 216–222.

[2] Basilevsky, A. and Hum, D.P.J. (1979). Karhunen–Loeve analysis of historical time series with an application to plantation births in Jamaica, *Journal of American Statistical Association*, **74**, 284–290.

[3] Brockwell, P.J. and Davis, R.A. (2002). *Introduction to Time Series and Forecasting*, Springer, New York.

[4] Broomhead, D.S. and King, G.P. (1986). Extracting qualitative dynamics from experimental data, *Physica D*, **20**, 217–236.

[5] Casella, G. and Berger, R.L. (2002). *Statistical Inference*, Second Edition, Duxbury / Thomson Learning, Australia, USA, Canada.

[6] Elsner, J.B. and Tsonis, A.A. (1996). *Singular Spectrum Analysis: A New Tool in Time Series Analysis*, Plenum.

[7] Ghodsi, M.; Hassani, H. and Sanei, S. (2010). Extracting fetal heart signal from noisy maternal ECG by multivariate singular spectrum analysis, *Statistics and Its Interface*, **3**, 399–411.

[8] Golyandina, N. (2010). On the choice of parameters in singular spectrum analysis and related subspace-based methods, *Statistics and Its Interface* **3**, 259–279.

[9] Golyandina, N. and Korobeynikov, A. (2012). Basic singular spectrum analysis and forecasting with R, *arXiv:1206.6910.*

[10] Golyandina, N.; Nekrutkin, V. and Zhigljavsky, A. (2001). *Analysis of Time Series Structure: SSA and Related Techniques*, Chapman & Hall; CRC, New York, London.

[11] Horton, R.E. (1923). Rainfall interpolation, *Monthly Weather Review*, **51**(6), 291–304.

[12] Hassani, H. (2007). Singular spectrum analysis: methodology and comparison, *Journal of Data Science*, **5**, 239–257.

[13] Hassani, H. and Thomakos, D. (2010). A Review on singular spectrum analysis for economic and financial time series, *Statistics and Its Interface*, **3**, 377–397.

[14] Kapl, M. and Müller, W.G. (2010). Prediction of steel prices: a comparison between a conventional regression model and MSSA, *Statistics and Its Interface*, **3**, 369–275.

[15] Mateu, J. and Müller, W.G. (Eds.) (2012). *Spatio-temporal Design: Advances in Efficient Data Acquisition; (Statistics in Practice)*, Wiley.

[16] Okabe, A. and Sugihara, K. (2012). *Spatial Analysis Along Networks: Statistical and Computational Methods; (Statistics in Practice)*, Wiley.

[17] Patterson, K.; Hassani, H.; Heravi, S. and Zhigljavsky, A. (2011). Multivariate singular spectrum analysis for forecasting revisions to real-time data, *Journal of Applied Statistics*, **38**(10), 2183–2211.

[18] Raynaud, S.; Yiou, P.; Kleeman, R. and Speich, S. (2005). Using MSSA to determine explicitly the oscillatory dynamics of weakly nonlinear climate systems, *Journal of Nonlinear Processes in Geophysics*, **12**, 807–815.

[19] Rodrigues, P.C. and de Carvalho, M. (2012). Spectral modeling of time series with missing data, *Applied Mathematical Modelling*, `http://dx.doi.org/10.1016/j.apm.2012.09.040`

[20] Shepard, D. (1968). A two-dimensional interpolation function for irregularly-spaced data, *Proceedings of the 1968 23*rd *ACM national conference*, ACM '68, ACM, New York, NY, USA, pp. 517–524.

[21] Hassani, H.; Heravi, S. and Zhigljavsky, A. (2009). Forecasting european industrial production with multivariate singular spectrum analysis, *International Journal of Forecasting*, **25**(1), 103–118.

[22] Zhigljavsky, A. (2010). Singular spectrum analysis for time series, *Statistics and Its Interface*, **3**, 255–258.

REVSTAT – Statistical Journal

Background

Statistical Institute of Portugal (INE, I.P.), well aware of how vital a statistical culture is in understanding most phenomena in the present-day world, and of its responsibility in disseminating statistical knowledge, started the publication of the scientific statistical journal *Revista de Estatística*, in Portuguese, publishing three times a year papers containing original research results, and application studies, namely in the economic, social and demographic fields.

In 1998 it was decided to publish papers also in English. This step has been taken to achieve a larger diffusion, and to encourage foreign contributors to submit their work.

At the time, the Editorial Board was mainly composed by Portuguese university professors, being now composed by national and international university professors, and this has been the first step aimed at changing the character of *Revista de Estatística* from a national to an international scientific journal.

In 2001, the *Revista de Estatística* published three volumes special issue containing extended abstracts of the invited contributed papers presented at the 23rd European Meeting of Statisticians.

The name of the Journal has been changed to REVSTAT – STATISTICAL JOURNAL, published in English, with a prestigious international editorial board, hoping to become one more place where scientists may feel proud of publishing their research results.

— The editorial policy will focus on publishing research articles at the highest level in the domains of Probability and Statistics with emphasis on the originality and importance of the research.

— All research articles will be refereed by at least two persons, one from the Editorial Board and another, external.

— The only working language allowed will be English.

— Three volumes are scheduled for publication, one in April, one in June and the other in November.

— On average, four articles will be published per issue.

Aims and Scope

The aim of REVSTAT is to publish articles of high scientific content, in English, developing innovative statistical scientific methods and introducing original research, grounded in substantive problems.

REVSTAT covers all branches of Probability and Statistics. Surveys of important areas of research in the field are also welcome.

Abstract / indexed in

REVSTAT is expected to be abstracted/indexed at least in *Current Index to Statistics*, *Statistical Theory and Method Abstracts* and *Zentralblatt für Mathematik*.

Instructions to Authors, special-issue editors and publishers

Papers may be submitted in two different ways:

— By sending a paper copy to the Executive Editor and one copy to one of the two Editors or Associate Editors whose opinion the author(s) would like to be taken into account, together with a postscript or a PDF file of the paper to the e-mail: revstat@fc.ul.pt.

— By sending a paper copy to the Executive Editor, together with a postscript or a PDF file of the paper to the e-mail: revstat@fc.ul.pt.

Submission of a paper means that it contains original work that has not been nor is about to be published elsewhere in any form.

Submitted manuscripts (text, tables and figures) should be typed only in black, on one side, in double spacing, with a left margin of at least 3 cm and not have more than 30 pages.

The first page should include the name, affiliation and address of the author(s) and a short abstract with the maximum of 100 words, followed by the key words up to the limit of 6, and the AMS 2000 subject classification.

Authors are obliged to write the final version of accepted papers using LaTeX, in the REVSTAT style.

This style (REVSTAT.sty), and examples file (REVSTAT.tex), which may be download to *PC Windows System* (Zip format), *Mackintosh*, *Linux* and *Solaris Systems* (StuffIt format), and *Mackintosh System* (BinHex Format), are available in the REVSTAT link of the National Statistical Institute's Website: http://www.ine.pt/revstat/inicio.html

Additional information for the authors may be obtained in the above link.

Accepted papers

Authors of accepted papers are requested to provide the LaTeX files and also a postscript (PS) or an acrobat (PDF) file of the paper to the Secretary of REVSTAT: liliana.martins@ine.pt.

Such e-mail message should include the author(s)'s name, mentioning that it has been accepted by REVSTAT.

The authors should also mention if encapsulated postscript figure files were included, and submit electronics figures separately in .tiff, .gif, .eps or .ps format. Figures must be a minimum of 300 dpi.

Also send always the final paper version to:

Maria José Carrilho
Executive Editor, REVSTAT – STATISTICAL JOURNAL
Instituto Nacional de Estatística, I.P.
Av. António José de Almeida
1000-043 LISBOA
PORTUGAL

Copyright

Upon acceptance of an article, the author(s) will be asked to transfer copyright of the article to the publisher, the INE, I.P., in order to ensure the widest possible dissemination of information, namely through the Statistics Portugal's website (http://www.ine.pt).

After assigning the transfer copyright form, authors may use their own material in other publications provided that the REVSTAT is acknowledged as the original place of publication. The Executive Editor of the Journal must be notified in writing in advance.